WEAR OF PARTICULAR AGRICULTURAL TRACTOR TIRES FOR DIFFERENT FIELD OPERATIONS IN AFRICA

Joseph Jerry Quaye

Thesis submitted to the University of Ottawa
in partial fulfillment of the requirements for the
Doctor of Philosophy in Mechanical Engineering

Ottawa-Carleton Institute for Mechanical and Aerospace Engineering
Faculty of Engineering
University of Ottawa

ABSTRACT

The overall objective of this study was to analyze the wear rate of tractor R-1 radial tires under specific operating conditions. The specific objectives were to examine the wear rate of the tires (a) when operating under different soil conditions and (b) different field operations, (c) to develop predictive models for the wear rate for both the front and rear tires under specific operating conditions, and (d) to validate the predictive models using measured values.

A Massey Ferguson 385 four-wheel drive (4WD) tractor with 56 kW engine power and 49 kW power take-off (PTO) was used to plow, harrow, and plant three different agricultural fields (Field 1, Field 2, Field 3). Each tire of the tractor was divided into four sections. On each section, three data points were positioned on each lug (tread). A Fowler digital gauge was used to measure the height of the tire lug at each data point before and after every operation. Baseline data was collected on each tire and analyzed, and a predictive model of the wear rate was developed and validated for each tire.

This experiment showed that a tire's wear rate increases as draft force, wheel slip, and soil moisture increase, and decreases as soil bulk density and tractor speed increase.

Also, the tires tended to wear faster on sandy soil compared with loam and clay soils. Additionally, the tires on the right side of the tractor wore faster than those on the left. For example, on Field 1, the rear right tire had a 5.46% higher wear rate than the rear left tire, while the wear on the front right tire exceeded that of the front left tire by 5.40%. The analysis of the predicted wear rate from the developed models versus the actual measurements showed that (a) the front left tire model has a high positive correlation of 0.84 ($r = 0.84$) and a coefficient of 0.77 ($r^2 = 0.77$), (b) the front right tire model shows an r of 0.83 and an r^2 of 0.77, (c) the rear left tire model has an r of 0.71 and an r^2 of 0.51, and (d) the rear right tire model has a correlation of

0.75 and a coefficient of 0.56. The study also estimated that to maintain uniform tire wear for a Massey Ferguson 385 4WD tractor operating within the context of this study, the two front tires should be swapped approximately every 1,475 ha, and the two rear tires should be swapped after about 1,105 ha. This paper further estimates that the maximum surface area that tires can cover before needing replacement is between 2,719 and 3,221 ha for the front tires, and 1,716 and 3,100 ha for the rear tires.

ACKNOWLEDGEMENTS

I offer my acknowledgment and gratitude first to Almighty God, who has brought me this far. My studies at the University of Ottawa serve not only academic purposes but also aim to fulfill God's divine assignment for me in Ottawa. I received immense support and guidance from many individuals during this research work.

I express my heartfelt appreciation to Dr. Claude Laguë (Professor Emeritus, School of Engineering Design and Teaching Innovation, Faculty of Engineering, University of Ottawa) for supervising this work. His relationship with students, thoroughness, understanding, professionalism, and sense of humor throughout my PhD program have not only shaped this thesis but also redefined my life and future endeavors.

I am grateful to Dr. Michel Nganbe (Professor, Department of Mechanical Engineering, Faculty of Engineering, University of Ottawa), Dr. Xin Wang (Professor, Department of Mechanical and Aerospace Engineering, Carleton University), Dr. Roland Bonffanais (Associate Professor, Department of Mechanical Engineering, Faculty of Engineering, University of Ottawa), and Dr. Patrick Dumond (Professor, School of Engineering Design and Teaching Innovation, Faculty of Engineering, University of Ottawa) for serving as my Thesis Advisory Committee members and providing valuable feedback on my thesis.

Many thanks go to Dr. Alberta N.A. Aryee (Associate Professor at Delaware State University), Dr. Enock Doudu (Senior Lecturer at Kentan Appiah-Minka University), and Dr. Adam Tettey Larbie (Chief Engineer, CFAO Ghana Limited) for reviewing and sharing their suggestions to improve this research work.

My appreciation goes to Mr. Maxwell Akandem, the owner of Akandem Farms Limited, Mr. Solomon, the farm manager, and the entire staff for their collaboration in carrying out this research. Their support and assistance were awesome.

I am grateful to the technicians at the engineering workshop of the University of Ottawa for helping with the fabrication of the tools essential to the experiments conducted for my study. I also appreciate the lab technicians at the University of Ghana Earth Science Laboratory and the University of Ottawa Geotechnical Laboratory for assisting me with some experiments. To my colleagues in the department, especially Kazem Alambeigi and Payam Parvizi, I am very thankful.

I sincerely thank the Moderator, the Clerk of the General Assembly, and the entire leadership of the Presbyterian Church of Ghana (PCG) for granting me the opportunity to pursue further studies. The PCG has consistently supported me throughout my PhD program. I am also thankful to the leadership and membership of the United Ghana Christian Church in Atlanta, Georgia, for their wonderful help and support during my studies. Additionally, I thank my new Christian families (PCG, Ottawa, and PCG, Montreal).

I sincerely appreciate my wife, Thywill, and our children, Josephine, Joel, and Jeromy, for their endless love, care, support, and great sacrifice throughout this program. I appreciate my parents, my siblings, and all my friends for their help.

DEDICATION

I dedicate this work to my wife, Thywill, my children, Josephine, Joel, and Jeromy, and my parents, Nii Tan II and Gladys Norkor Quaye.

TABLE OF CONTENTS

LIST OF TABLES

LIST OF FIGURES

NOMENCLATURE

ABBREVIATIONS

2WD	Two-wheel drive
4WD	Four-wheel drive
ANOVA	Analysis of variance
B_a	Ballast
CI	Confidence interval
II	Inner area of the inner tire lug
IO	Inner area of the outer tire lug
MI	Middle area of the inner tire lug
MO	Middle area of the outer tire lug
MR	Motion resistance
PTO	Power take-off
SI	Side of the inner tire lug
SO	Side of the outer tire lug

LIST OF SYMBOLS

A, B, and C	Specific parameters of the tractor/implement
A_c	Contact area between the tire and the soil (m^2)
A_1	Mean area of contact location (m^2)
C_s	Soil cohesion (N/m^2)
D	Implement draft force (N)
D_s	Specific draft force (N/cm)
d	Distance traveled by the tractor during field operation (m)
F	Dimensionless soil texture adjustment parameter (dimensionless)
$F_{adhesion}$	Adhesion force (N)
$F_{hysteresis}$	Deformation force (N)
F_i	Resistive adhesive force (N)
F_{max}	Maximum shearing force (N)
f	Energy release rate for junction friction (J/s)
GT	Gross traction (N)
H_L	Lug height (mm)
H_{La}	Lug height after the field operation (mm)
H_{Lb}	Lug height before the field operation (mm)
H_r	Replacement lug height (mm)
H_T	Total lug height (mm)
ID	Implement draft resultant force (N)

i	Slip (%)
K	Wear coefficient (g/m^2)
M	Total number of macroscopic sites (dimensionless)
M_c	Moisture content of the soil (%)
M_{ds}	Mass of dried soil (g)
M_{ws}	Mass of wet soil (g)
$\dot{M}$	The total number of asperities where each load (W) is applied (dimensionless)
N	Number of discs (dimensionless)
NT	Net traction (N)
$\dot{P}$	Mean pressure with speed over each asperity (N/m^2)
R	Soil reaction force (N)
R_{d1}	Distance traveled when the tractor is not engaged in any field operation (m)
R_{d2}	Distance traveled when the tractor is engaged in any field operation (m)
R_f	Soil reaction force on the front axle (N)
R_n	Soil reaction force for radial (N)
R_r	Soil reaction force on the rear axle (N)
R_t	Soil reaction force tangential to the soil surface (N)
r	Tire normal radius (mm)
r_0	Rolling radius at a specific zero condition (mm)
r_t	Torque radius (mm)
S	Shear strength (N/m^2)
SW_r	Static load on the front axle (N)
s	Tractor field speed (km/h)
T	Axle torque applied to the tire (Nm)
T	Tillage depth (cm)
V	Forward velocity (m/s)
v_a	Actual forward velocity (m/s)
v_t	Theoretical velocity (m/s)
W	Vertical dynamic load (N)
W_L	Amount of lug wear (mm)
W_s	Measured wear rate (mm/km)
W_p	Predicted wear rate (mm/km)
W_r	Amount of wear rate (mm/km)
W_{rp}	Wear rates for plowing (mm/km)
W_{rh}	Wear rate for harrowing (mm/km)
W_{rl}	Wear rate for planting (mm/km)
$W_{tractor}$	Total tractor weight (N)
w_i	Width of the attached implement (m)

w_p	Plow width (m)
w_t	Tire width (m)
ω	Wheel angular velocity (rad/s)
X_1	Distance between the center line of the rear axle and the center of gravity of the tractor (m)
X_2	Wheelbase of the tractor, i.e., the distance between the center line of the front and rear axles (m)
X_3	Perpendicular distance from the line of action of the implement draft resultant force to the point of action of the rear axle (m)
X_4	Height of the hitch point above the level of the application of the rear soil reaction (m)
X_5	Horizontal distance between the hitch and the center line of the rear axle (m)
x_h	Tractor distance traveled during harrowing (m)
x_l	Tractor distance traveled during planting (m)
x_p	Tractor distance traveled during plowing (m)
α	Angle of ID with the horizontal plane (°)
α_i	Angle of slip (°)
ρ	Density of the tread rubber compound (kg/m^3)
ρ_b	Soil bulk density (g/cm^3)
ε	Minimum wearable height of the tire lug before needing to replace the tire (mm)
σ	Tire wear per unit area (mm/m^2)
Ψ	Rate of motion resistance (N)
$\emptyset$	Angle of internal friction (°)
μ	Coulomb friction coefficient (dimensionless)
μ_{nt}	Net traction ratio (dimensionless)
μ_{gt}	Gross traction ratio (dimensionless)
$\mu_{adhesion}$	Coulomb friction coefficient for adhesion (dimensionless)
$\mu_{hysteresis}$	Coulomb friction coefficient for adhesion for deformation (dimensionless)
γ_1 *and* γ_2	Surface energies for the contacting bodies (J)

CHAPTER 1: OVERVIEW

1.1 Context and Motivation

Meeting the growing global demand for food is becoming an increasingly concerning issue, given that the world's population is expected to reach 10 billion people by 2050 (Renius, 2020). However, the agriculture labor force is in a constant state of decline as more and more arable lands are being used for non-agricultural purposes. For example, between 1986 and 2022 in the Adam Rural District in Ethiopia, the use of land for non-agricultural purposes increased by 59.88%, while use for agricultural purposes declined by 39.75% (Dadi et al., 2023).

Consistent improvement in agricultural mechanization is becoming the main pillar for mitigating the challenge of feeding the world, both now and in the future. Srivastava et al. (2006) reported that in 1900, agriculture employed two-thirds of the American population; by 2006, however, only 3% of the U.S. population was engaged in farming, due largely to farm mechanization. That report further notes that the use of tractors and other equipment has transformed American farming from a subsistence-based sector to a leading industry.

The use of machinery in agriculture served as the first technological approach to improving farming methods (e.g., greenhouses, intelligent farming), increasing food production and maximizing the use of agricultural land. End-to-end farm mechanization—from field preparation to harvest—ensures that field operations such as planting and harvesting are performed in a timely manner while also improving crop quality, labor efficiency, and farm productivity. Generally, the use of agricultural machinery both increases food production and improves the agricultural raw materials needed to feed agro-processing industries (Dorvlo, 2015). In recent times, due to technological advancements in the machines and equipment used for field operations in agriculture have brought about tremendous change in the areas of tilling of the soil, planting of the seeds, tending and growing crops, harvesting mature crops, and threshing of harvested crops, among other operations. These field operations depend heavily on tractors and the implements they are equipped with.

In crop production, agricultural tractors are important to both on-field and off-field operations (Figure 1.1). Their versatility and ability to move and operate farm implements make agricultural tractors indispensable to field operations.

Figure 1.1. An agricultural tractor (Copyright 2025 by Deere and Company).

The use of tractors and implements such as plows, harrows, planters, and crop harvesting equipment during field operations (e.g., tillage, planting, applying chemicals, harvesting) is essential to modern mechanized farming systems (Verma, 2006). As a self-propelled prime mover with different interfaces to allow connections to various farm equipment, tractors are multi-purpose machines, making them an integrated—and integral—unit in the agricultural production scheme. Despite recent global economic difficulties, farm tractor sales increased by approximately 17% in the U.S. and 10% in Canada between 2019 and 2020, making purchases of agricultural tractors the largest share of farm equipment sales (Association of Equipment Manufacturers, 2022).

In addition to the growing demand for food, the increase in the cost of maintaining agricultural machinery poses a significant challenge to modern agriculture. Given that new technological developments in farm mechanization are often accompanied by increased operational demands, tractors must be reliable and durable. This makes farm machinery repairs and maintenance critical to optimal performance. Kichler et al. (2011) note that equipment performance and in-field efficiency are the two variables that need to be improved to reduce the consumption of fuel and the cost of crop production. A key tractor component that needs to be managed effectively to ensure optimum utilization of power, proper soil management, and safe farm operations is the tractor tire. Generally, tractor tires are used on various agricultural soils, including dry or wet and firm or soft (Brassart, 1994). Occasionally, these tires are also used on paved roads when tractors are moved from one field to another.

Among the many functions that the tractor tires perform, the most important is providing traction. This key function is largely affected by parameters relating to the soil and the tire. Hence, good tire maintenance and timely replacement are necessary to maximize traction and minimize energy losses. The three types of losses that occur during tractor maneuvering on agricultural soil are transmission, motion resistance, and slip (Botta et al., 2012). Although excessive tire wear can significantly increase transmission losses, it has a greater impact on slip losses and motion resistance, which are the main reasons for the loss of power at the drawbar (the bar at the rear of the tractor to which an implement is connected). The direct consequences of increased motion resistance and slip are higher fuel consumption and greater soil compaction (Pohrt, 2019). These energy losses, which result from both soil and tire deformation, are termed motion resistance. Botta et al. (2012) note that tire wear, which occurs as a result of high wheel slip, is a key factor that increases soil compaction, which is undesirable when using agricultural tractors because compacted soil can restrict root growth and reduce water infiltration. Therefore, this study intends to assess the wear rate of agricultural tractor tires at different field operation thresholds.

1.2 Significance of the Study

To ensure maximum operation and extend the lifespan of a machine, the condition of the operator (e.g., fatigue level), the environment in which the machine is used, and the machine's condition must be monitored and evaluated. These factors work together to maximize the output efficiency of farm machines and boost productivity in farm mechanization.

Due to the seasonal nature of farming, ensuring that farm machinery is ready for each season is essential for a profitable farming period. Therefore, effective maintenance planning is needed to ensure farm machines operate efficiently and on schedule. Tractors are vital machinery in farm mechanization, as they undertake multiple field and non-field operations. Thus, they must be maintained before, during, and after each farming season to maximize their operational efficiency, extend their service life, and mitigate safety hazards. During field operations, the tire is a vital part of the tractor that requires both proper maintenance and a replacement plan.

The tire aids the tractor in providing the necessary traction for movement. The nature of the two contacting surfaces (the soil and the tire) greatly influences the traction necessary for tractor movement. As the tire and the contacting surface (both deformable) come into contact during operation, a certain amount of slip-induced wear occurs as the pull develops. A tractor tire wears down over time. As the wear increases (Figure 1.2[b]), the friction coefficient between the tire and the soil (contact surface) is reduced, resulting in a loss of traction and an increase in the potential for wheel slippage.

(a) Unworn (b) Worn

Figure 1.2. Closeup of the lugs on an unworn versus a worn tractor tire (Copyright 2025 by Alamy Limited).

Excessive wheel slippage is one of the major reasons for reducing the drawbar pull efficiency of the tractor. Because of their numerous advantages, most farmers prefer four-wheel drive (4WD) tractors over two-wheel drive (2WD) configurations. Some of these advantages include improved traction efficiency and reduced wheel slippage, especially for draft-intensive field operations such as tillage work. Using a 4WD tractor, traction is generated in both the front and rear wheels; therefore, the amount of wear on any tire will influence the total tractive force that is available to move the tractor and pull any attached implement. The wear that occurs on the tractor's front and rear tires during different field operations and under different field (soil) conditions is the focus of this study.

1.3 Study Objectives

The main objective of this research is to study the rate of wear of R-1 radial tractor tires under specific operational conditions. The specific objectives are:

a) To examine tire wear rates under different field (soil) conditions in which the tires operate.

b) To analyze tire wear rates for different field operations.

c) To develop models for the prediction of the wear rate for both the front and the rear tires under specific operating conditions.

d) To validate the prediction models using the actual data collected during the study.

1.4 Originality and Novelty of the Study

Extensive studies have been conducted on tire-contact surface interaction (Chang et al., 2021; Ivanov, 2016; Lepine & Cebon, 2018; Li et al., 2012a). These works have led to the creation of theoretical and empirical models that consider variables such as slip, static and dynamic tractor loads, and friction to assess tractive effectiveness and fuel consumption. As discussed in Chapter 2, Le Maître et al. (1998) predicted tire tread life and evaluated tire performance by measuring the rate of tire wear. However, most of these studies focus on the interaction between agricultural tires and paved surfaces; research on tractor tires and soil interaction is limited.

A study conducted by Dorvlo et al. (2014) measured the rate of rear-tire wear to determine the lifespan and depreciation of rear tractor tires by using a 2WD tractor to plow 11.7 ha of farmland. Given the advantages of 4WD over 2WD tractors, most modern farmers prefer using 4WD tractors for tillage work.

Notably, the Dorvlo et al. (2014) study focused only on plowing, which is not the only field operation a tractor is used for. Therefore, it is inappropriate to use the wear rate resulting from plowing to predict the lifespan and/or depreciation of the rear tires only. Since most tillage work is done using 4WD tractors, it is important to study the wear rate on both the front and rear tires.

The outcomes from this study on tire wear will:

- enable tractor users to determine the point at which a significant wear rate during tire usage will call for tire replacement, as recommended by the tire manufacturer;
- enable the tractor user to have a fair knowledge of which field operation causes a high tire wear rate; and
- provide proper knowledge for effective planned maintenance.

1.5 THESIS OUTLINE

The structure of this thesis is as follows:

- Chapter 1 provides an overview of the research. It outlines the context of, motivation for, significance of, and objectives of the study. It also discusses the originality of this research.
- Chapter 2 reviews the relevant literature on agricultural tractor tires, soil-tire interactions, and tire wear.
- Chapter 3 summarizes the materials and methods used for this research.
- Chapter 4 presents the results and the discussions of the experiment and the developed tire wear prediction model.
- Chapter 5 presents a research summary and conclusions and offers recommendations for future research.

CHAPTER 2: BACKGROUND AND LITERATURE REVIEW

2.1 INTRODUCTION

Agricultural tractor tires operate under a varied range of external conditions: different types of soil, various types of field operations, and different seasonal conditions (e.g., temperature and rainfall) (Lupker et al., 2002; Sabbioni et al., 2011). In agricultural field operations, tractor tires are expected to provide high tractive forces and tractive effectiveness under different load conditions, soil conditions (Lyasko, 2010), and tillage practices (Chen et al., 2005) to generate the required drawbar pull (Jenane & Bashford, 2000). Additionally, soil compaction caused by tires as they pass over the soil surface during field operations is also a factor in optimizing tire function. Traffic-induced soil compaction must be minimized in the case of random or uncontrolled traffic of tractors and other agricultural machines in agricultural fields. However, soil compaction can be desirable under controlled traffic conditions (e.g., no crops grown in traffic lanes and no traffic on fields and crops outside traffic lanes) when agricultural field operations are completed.

The conditions under which a tire operates influence, directly and indirectly, a tire's tread wear. Lupker et al. (2002) notes that in modeling the treadwear of a tire, one must consider a two-part sequence. The first part is the determination and selection of the operation and vehicle conditions. This depends on forces, slip (Braghin et al., 2006), the moment transfer in the tire contact area, and the tire-soil contact area (S. Persson, 2009; Wulfsohn, 2009). Second, the tire load for specific operational conditions is determined to model the friction and behavior of the tread wear of the tire contact area (Lupker et al., 2002). Agricultural tire wear depends on several factors, such as the type of tires, soil type, and the effect of traction. The following paragraphs discuss the impact of these factors on agricultural tire wear.

2.2 AGRICULTURE TRACTOR TIRES

These tires are designed to reflect the conditions under which they will operate. Generally, agricultural tires are designed either for on-road or off-road purposes. Industrial tractor tires are designed for heavy vehicles that usually operate on hard surfaces, such as concrete or asphalt. However, this is not the case for non-agricultural off-road operations (such as mining activities), for which tires must operate on deformable and highly variable surfaces. Agricultural tractor tires are designed to work on soft and deformable surfaces (soil). For that reason, the design of agricultural tire tread patterns may involve several considerations (Bauer Built Tire and Service, 2022). The quality of the tire depends on a basic rubber compound and the manufacturing process (Wennekes, 2008). The materials that make up tire compounds can be categorized into five groups:

1. **Rubber**: This is the basic material for tires, which can include natural and synthetic polymers (Tire Works Total Car Care, n.d.). Natural rubber comes from the sap of the *Hevea brasiliensis* tree (natural latex). It gives the tires high elasticity, impermeability, and supports a good reaction to vulcanization (a process that strengthens and hardens rubber, also known as curing) (Tractor Tyre Expert, 2021a). Butadiene rubber and styrene butadiene rubber are the main synthetic polymers used in tire manufacturing. These polymers greatly define the physical and chemical properties of the tire. Halobutyl rubber is used so that the inner liner of the tire will be impermeable (Tire Works Total Car Care, n.d.).
2. **Anti-wear materials**: These typically represent 30% of the total mass of the tire (Tire Works Total Car Care, n.d.). Reuvekamp (2003) notes that these materials are fillers such as carbon black and amorphous precipitated silica. They reinforce the tire to increase wear resistance, reduce rolling resistance, and ensure better traction. Varying the amount of carbon black

affects the tire’s shear modulus (rigidity and resistance to deformation) and hardness (Reuvekamp, 2003; Vilgis et al., 2009).

3. **Processing aids**: This involves adding relatively small plasticizers and softeners to facilitate the homogeneity of the tire’s end compound.
4. **Chemical protective additives**: These serve two functions. Antioxidant, accelerant, and retardant materials that enhance the physical and chemical properties of the tire help prevent the tire rubber from breaking when it is exposed to high temperatures and oxygen, while antiozonants minimize the impact of ozone on the tire’s surface.
5. **Curatives**: Elements such as sulfur and zinc oxide are used to transform rubber into a solid material during tire curing. During vulcanization, a crosslink in the rubber matrix is formed to reduce the vulcanization time. The number of molecular crosslinks introduced during vulcanization affects the shear modulus and the hardness of the tire. Various types of fibers are available to reinforce layers and overlap the rubber.

2.2.1 Components of a tractor tire

The different components in the construction of agricultural tires have a great impact on tire performance. Each component, as shown in Figure 2.1, has a specific role in ensuring the firmness of the tire so as to achieve top performance during field operations.

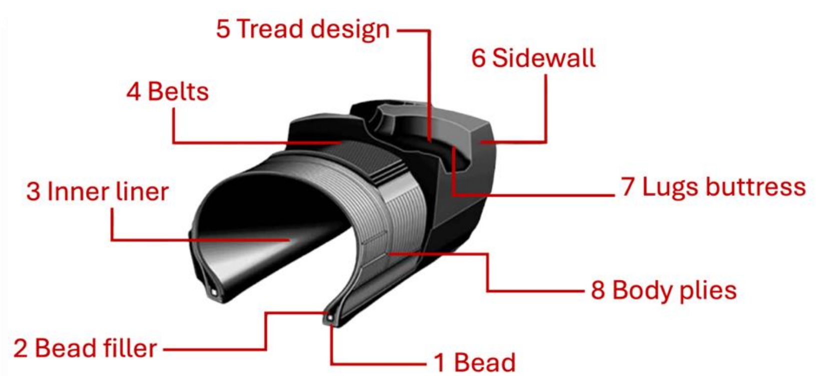

Figure 2.1. Components of a tractor tire (Copyright 2022 by Bridgestone American Tire Operations).

1. **Bead**: The bead holds the tire on the rim to ensure the tire stays seated on the wheel.
2. **Bead filler**: This is incorporated within the bead configuration and the sidewall area to maximize the stability, steering response, and case durability of the tire (Bridgestone, n.d.-b).
3. **Inner liner**: This is a synthetic rubber with a similar function to an inner tube. It insulates the tube and prevents air and moisture penetration.
4. **Belts**: These are steel cords in the tire that enable the tire to maintain its shape. They are configured in layers in the rubber to give strength and stability.
5. **Tread design**: This interacts with the contact surface to provide traction. Tread designs vary between tires to maximize traction and resist wear, abrasion, and heat.
6. **Sidewall**: The sidewall is made of flexible rubber, which protects the side of the tire and provides lateral stability. The flex of the sidewall is a key function in choosing the right tire for the right job (Bridgestone, n.d.-b).
7. **Lugs buttress**: Lug buttress, together with lug depth, offers tread stability.
8. **Body plies**: The textile cords (running radially in this case; refer to 2.2.2) sets the tire strength and load capacity.

2.2.2 Tire design

Tires can have one of two designs: bias ply (also called diagonal ply) and radial ply (Renius, 2020) (Figure 2.2). Both types of tires can be used with or without an innertube.

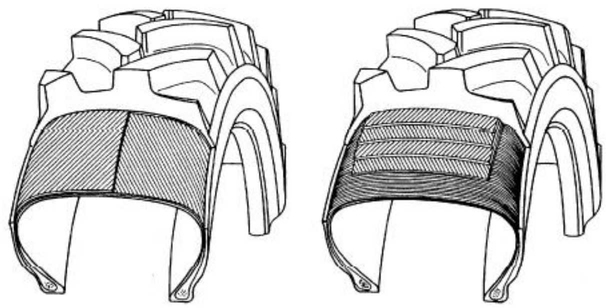

Figure 2.2. Basic design of bias ply and radial ply-tires (Renius, 2020).

2.2.2.1 Radial ply tire

The textile cord in the radial tire is aligned in a radial direction at 90° angles at the crown (Gent & Walter, 2006; Wennekes, 2008). Yahya (1985) indicates that the circumference of the tire directly under the tread is made of multi-layer belts with cords of high modulus of elasticity (a material that resists elastic deformation). The construction of a radial tire consists of two parts: (1) the casing, which is made of cable layers coated with rubber steel that arcs from bead to bead; and (2) the steel belts beneath the tread that make the crown rigid to resist cuts and punctures (Goodyear Tire and Rubber Co., 2004).

2.2.2.2 Bias ply tire (conventional tire)

The cord of the bias ply tire body runs diagonally from bead to bead. The angle of the ply cord of the body to the tread center line is less than 90º running from one bead to another (Gent & Walter, 2006) and is typically opposing angles of 45º (Bridgestone, n.d.-a). The construction of a bias ply tire is simple and easier to manufacture. This makes the cost of manufacturing more effective compared with radial ply tires (Bridgestone, n.d.-b). However, shear normally occurs between the body ply cords. This generates heat and gives poor wear characteristics (Gent & Walter, 2006). The disadvantages of bias ply tires, such as low traction, rapid wear, and higher fuel consumption, are the result of the required flexibility of the tire sidewall and the all-sided reinforcement (Wennekes, 2008).

2.2.2.3 Comparison between radial and bias ply tire

The market share of radial tires continues to increase because they ensure prolonged tread wear and a smoother ride and offer 80% more resistance to cuts and penetration in the tread area (Goodyear Tire and Rubber Co., 2004). According to Enyart (2008), the entire tire world saw a dramatic change with the introduction of radial tire design. He argues that most farmers in North America are well versed in radial tire advancement, and have radial tires installed on their field tractors due to three key reasons: reduced soil compaction, which improves root development, nutrient uptake, and increases crop yield; improved traction, which results in better tractive efficiency and a reduction in fuel consumption; and improved ride, which reduces operator fatigue. Goodyear Tire and Rubber Co. (2004) indicated that radial tire usage continues to dominate in heavy off-road equipment.

The values of the coefficient of net traction (k) are 10% to 12% higher for agricultural radial ply tires used on different types of soil for off-road applications (Figure 2.3[a]) (Renius, 2020) compared with corresponding values for bias ply tires (Figure 2.3[b]) (Söhne, 1968). The radial tire has a flexible tire wall, which enables a greater soil contact area that generates good tractive forces that are applied by the soil to the tractor tires. This results in lower contact pressure (Jarrett, 1995), greater net traction, lower rolling resistance, higher tractive efficiency, and longer lifespan. Nearly 50 years after the commercial introduction of radial tires, radials have outperformed bias ply tires in most instances (Bridgestone, n.d.-a). However, the complexity of the construction of radial ply tires increases tire material and manufacturing costs (Gent & Walter, 2006).

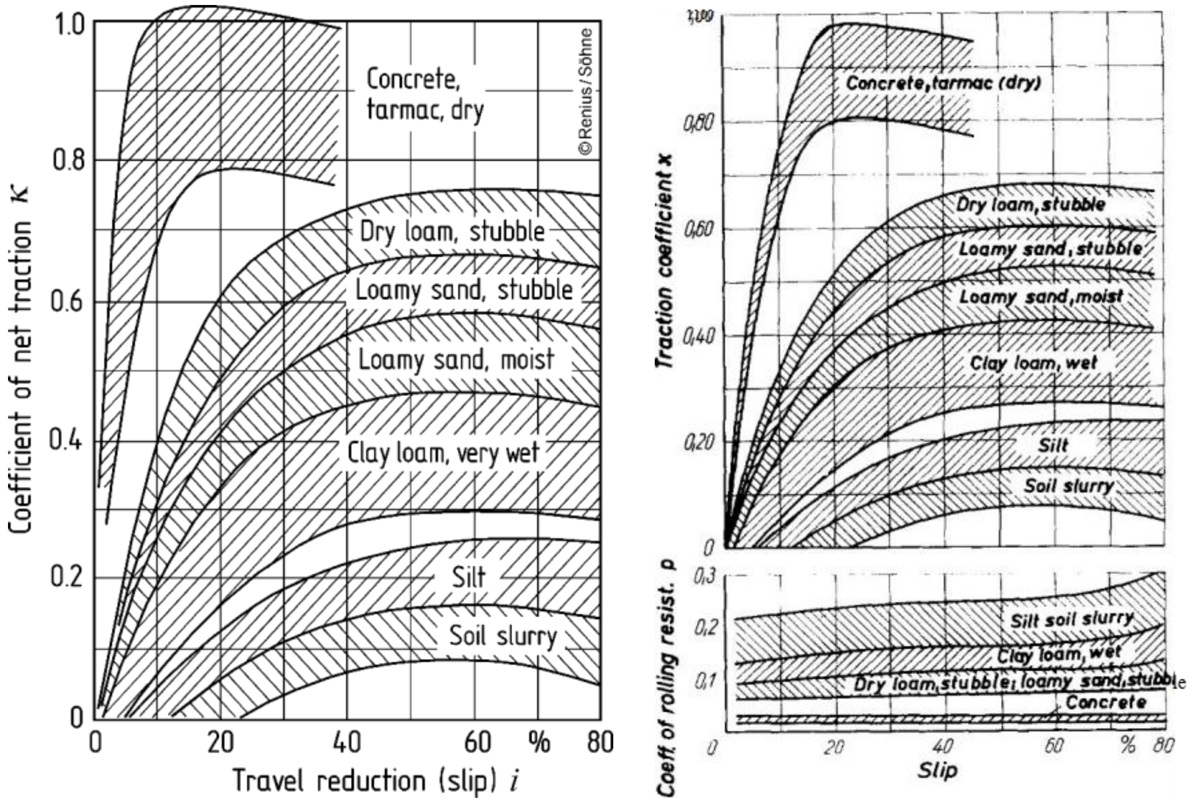

(a) Radial ply **(b) Bias ply**

Figure 2.3. Net traction coefficient for a radial ply (Renius, 2020) versus bias ply tire (Söhne, 1968).

2.2.3 Tire designation and parameters

Agricultural tractor tires have a standard coding system, described by an alphanumeric code that indicates the tire's functionality. These standards for tires, rims, and their auxiliary components, like tubes and valves, are established and promulgated by the Tire and Rim Association. Figure 2.4 shows an example of an agricultural tractor tire code in inches as it would appear on the side wall of a tire.

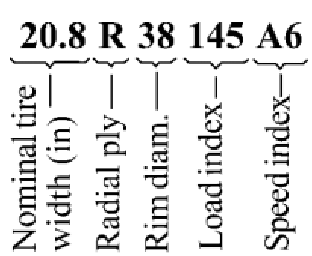

Figure 2.4. Tire code for an agricultural tractor. Rim diameter is in inches (Renius, 2020).

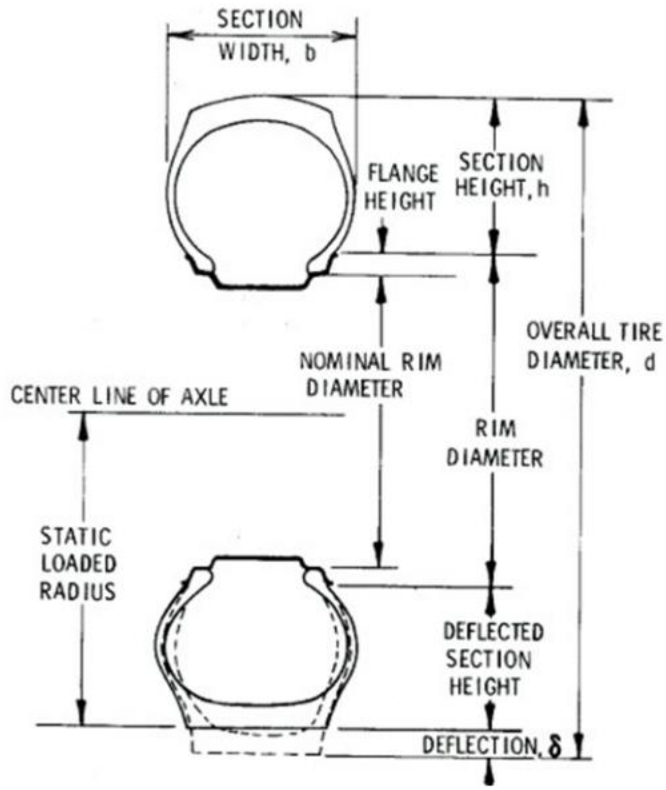

Figure 2.5. Parameters of a tractor tire (Srivastava et al., 2006).

2.2.3 Key parameter definitions

- **Section width**: This is the first number in a tire code, which is shown in Figure 2.4 as 20.8 inches (528.32 mm).
- **Overall tire diameter**: This is an important metric to get the radius of the tire (Wulfsohn, 2009). The data handbook supplied by the tire manufacturer provides the (unloaded) overall tire diameter.
- **Static loaded radius**: This is the distance from the contact surface to the wheel axle (Figure 2.5). It is provided by the manufacturer.
- **Tire deflection**: This is obtained on a hard surface by dividing the (unloaded) overall diameter of the tire by two, minus the static loaded radius.
- **Tire load index:** The amount of weight the tire can support (Figure 2.4).

- **Rim diameter**: This is the second number in a tire code, which is shown in Figure 2.4 as 38 inches (965.2 mm).
- **Section height**: This is the total diameter of the (unloaded) tire minus the diameter of the tire rim divided by two.

2.2.4 Mechanical properties of tractor tires

The rubber compound is the basic material for manufacturing tractor tires (Tire Works Total Car Care, n.d.; Wennekes, 2008). The mechanical properties of any rubber compound depend on the vulcanization process, the chemical reaction of vulcanization, and the manufacturing process. During the vulcanization process, crosslinks are set between the long-chain polymer molecules. This forms a three-dimensional permanent network, transforming the soft material into a solid elastic material.

At a constant temperature, a series of vulcanization tests is done at different times to show how the cure (vulcanization) affects the mechanical properties of the rubber compound. Varying the temperature helps to achieve the desired mechanical properties of the rubber compounds (Callister, 2006). As the temperature increases, the rubber compound passes through multiple transition stages, exhibiting various elastomeric properties like the static modulus of an elastomer with a phase changing from a glassy region to a viscoelastic or flow region (Clark, 1971). Agricultural tractor tires have the following mechanical properties: tensile strength ranging from 17.24 to 27.58 MPa, a static modulus of 300% in the range of 6.9 to 11.7 MPa, a breaking elongation in the range of 400% to 600% (S. K. Clark, 1971), and a 0.5 Poison ratio (Gent, 2012). To obtain these properties, the stress-strain curve in Figure 2.6 is used during the manufacturing of the tire compound to adjust the cure rate and ensure that the required range of static modulus, tensile strength, and breaking elongation is attained.

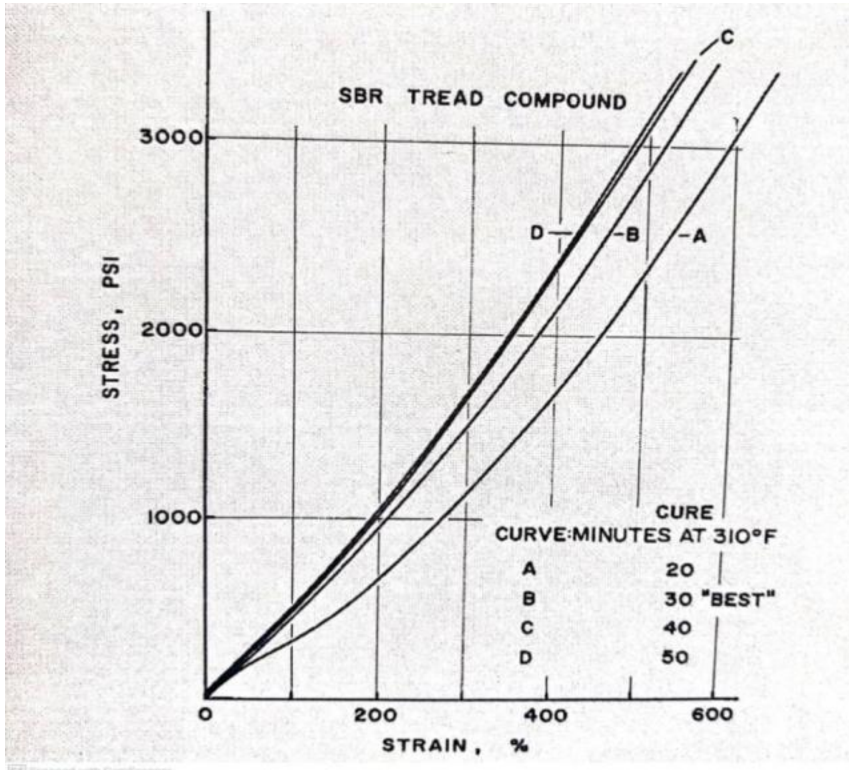

Figure 2.6. Stress-strain curves with cure of a rubber tire (Clark, 1971).

Measuring the hardness of a rubber tread compound involves indenting the compound with a rigid indenter of a specific shape or size under a particular localized condition (Gent, 2012). The hardness can be tested either by using the Shore A Durometer scale, which uses a truncated conical indicator, or an Internal Rubber Hardness (IRHD) scale, which uses a spherical indenter (Gent, 2012). The indentation is indicated on a non-linear scale from 0 to 100 on the IRHD (Gent & Walter, 2006). A rubber tread compound with a Shore A hardness of 50 to 65 units indicates a soft to medium-hard rubber. The measured hardness correlates with the elastic shear modulus (G) (Briscoe & Sebastian, 1993; Gent & Walter, 2006). The shear modulus of elasticity is approximately equal to the tensile modulus divided by three. The rubber compound used in the tire is inelastic for the tire to have good traction, wear resistance, and durability. Gent and Walter (2006) note that adding 30% or more of carbon black or silicon powder to all tire compound components, treads, and sidewalls makes them stiffer. This makes the tire stronger and more resilient to abrasion at three times the rate of an unfilled compound.

The stress-strain hysteresis loop in Figure 2.7 shows the viscoelasticity of the composite for accuracy in analyzing the structure of a tire. This causes the tire to exhibit some shock-damping characteristics.

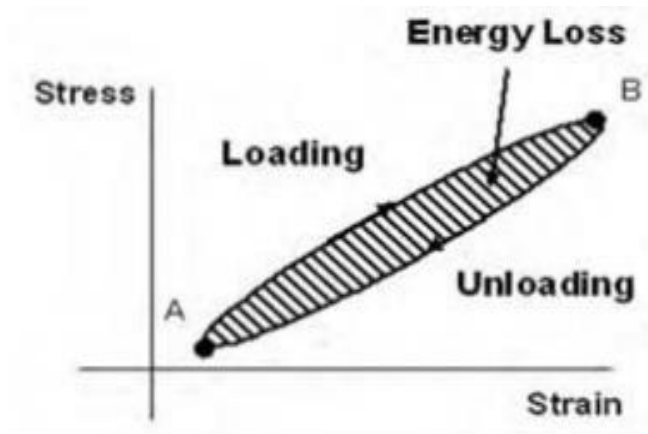

Figure 2.7. The stress-strain hysteresis loop (Gent & Walter, 2006).

The region between the loading and unloading curves represents the mechanical energy loss due to rolling resistance in the form of heat, which affects the tire's temperature.

2.3 TIRE-SOIL INTERACTION

The main purpose of tractor tires is to apply tractive forces on agricultural soils that are deformable (Carroll et al., 2006; Upadhyaya et al., 2009). By shearing the soil, the tractive tire develops a traction force on the deformable soil surface (Carroll et al., 2006) as shown in Figure 2.8, where R is the soil reaction force, R_n and R_t are the radial and tangential components of R**,** T is the axle torque applied to the tire, NT is the net traction, V represents the vehicle forward velocity, ω is the wheel angular velocity, W is the vertical dynamic load, Ψ is the angle of motion resistance of the tire, and r_t is the torque radius.

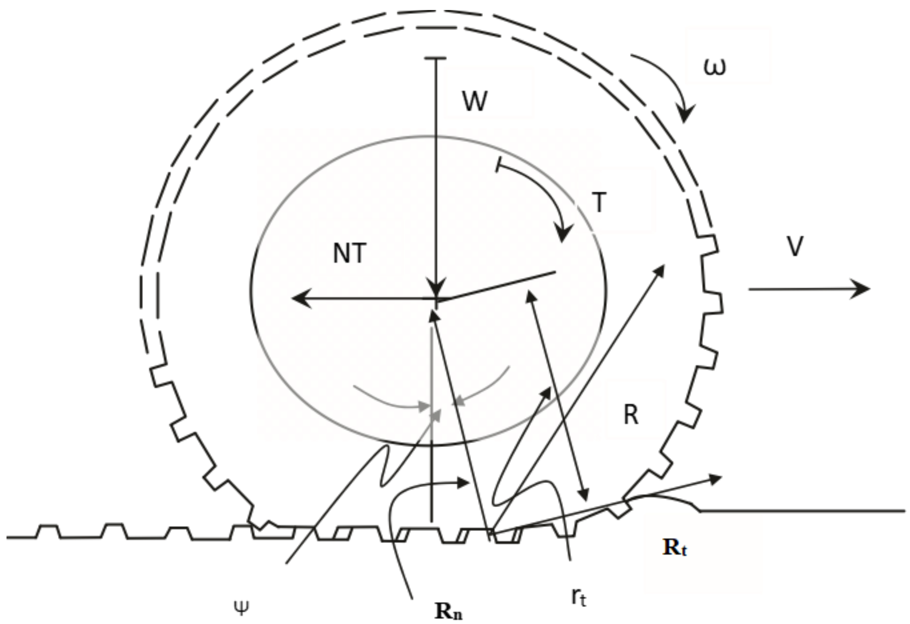

Figure 2.8. Forces and torque for a tractor tire on deformable soil (S. Persson, 2009).

In analyzing the traction of a wheel on a deformable surface, Macmillan (2002) proposed considering the following key factors:

- **Static-vertical load**: This is the total force that is normal for the supporting surface, and with reference to the plane when there is traction or torque.
- **Static-loaded radius**: This is the radius between the wheel center and the tread contact surface at a reference load and pressure. It is provided in the tire data by the manufacturer.
- **Dynamic load**: The total load exerted by the wheel, which is normal to the supporting surface when the tractor wheel is in operation.
- **Input torque**: The mechanical torque provided by the tractor's engine and transmission and applied to the drive axle(s).
- **Traction force**: This is the horizontal reaction generated by the soil on the driving wheel(s). It reacts equally to the horizontal force caused by the driving wheel(s).

- **Rolling resistance:** This is influenced by the tire design and soil conditions (Gharibkhani et al., 2012), and both the tire and the soil deformable contacts (Gharibkhani, 2014). It is the force that opposes the motion of the wheel as it moves on the soil.
- **Rolling radius**: The distance traveled per revolution (C_R) divided by 2π under some defined zero conditions, like zero net traction (Macmillan, 2002). It is key to determining the angular and forward velocities of the wheel.
- **Net traction**: The force developed by the wheel and transferred to the vehicle.
- **Net traction ratio (μ_{nt})**: The net traction divided by the dynamic load.
- **Zero condition**: A natural situation where the rear speed traveled by the tractor is equal to the linear speed of the surface of the wheel (Macmillan, 2002).
- **Torque force**: This is the required force to roll the tractor wheel freely on the contacting surface and react equally to the rolling resistance.
- **Gross traction (GT):** The torque input (T) divided by the rolling radius at a specific zero condition (r_0).

$$GT = \left(\frac{T}{r_0}\right) \tag{1}$$

- **GT ratio:** This is the ratio of GT to dynamic load (W).

$$\left(\mu_{gt}\right) = \frac{GT}{W} \tag{2}$$

- **Motion resistance (MR)**: This is given by the tire's GT minus net traction.

$$MR = GT - NT \tag{3}$$

- **Input power**: The product of input torque (T) and the wheel angular velocity (ω).

  Wheel input power = Tω (4)

- **Output power**: The net traction (NT) multiplied by the actual forward speed (V_a).

- **Weight transfer**: The difference between the normal forces on the tractor wheel under operating conditions and under static conditions.
- **Travel ratio**: Ratio of speed when generating output to the operating speed under the specific zero conditions.

$$Travel\ ratio = \frac{actual\ forward\ velocity\ (v_a)}{theoretical\ velocity\ (v_t)} \qquad (5)$$

- **Slip (*i*)**: This measures the relative movement that occurs when the wheel comes into contact with the supporting surface.

$$i = \frac{R_{d1} - R_{d2}}{R_{d1}} \times 100 \qquad (6)$$

- **Ballast (B_a)**: This is the addition or removal of weight on the total load of the tractor to improve traction.

2.3.1 Traction

Tractive device: Traction is a key fact affecting tractor performance. Therefore, an agricultural tractor tire must provide sufficient tractive ability for self-propulsion and propulsion of other farm implements, whether on a hard surface or on deformable terrain. The complex behavior of soil as an engineering material means that the understanding of the interaction between the tractor and transport devices and the deformable terrain on which they operate is yet to be fully developed (Upadhyaya et al., 2009). However, both theoretical and experimental work has been done in analyzing traction (Mohsenimanesh et al., 2009), improving traction (Jenane & Bashford, 2000), and predicting the tractive effectiveness of a pneumatic rubber tire on deformable soil (Brassart, 1994; Garciano et al., 2010; Lupker et al., 2002).

The effect of traction on agricultural equipment depends on the tractive device being used. Figures 2.9 to 2.11 show the three categories of wheeled agricultural tractors that farmers generally use. Renius (2020) notes that agricultural tractors can generate traction power through the following configurations: (1) a conventional rear-wheel drive (2WD) tractor, as shown in Figure 2.9; (2) a 4WD tractor with small front and large rear wheels (Figure 2.10[a]) or four equally sized wheels (Figure 2.10[b]); and a 4WD tandem (articulated) tractor (Figure 2.10[c]).

Different types of agricultural track tractors are shown in Figure 2.11. The tracks can be made of either steel (similar to those used by many construction and roadwork machines) or rubber. In the case of agricultural tracked tractors, rubber tracks are preferred because they allow for higher operating speeds as well as operation on paved surfaces. These tractors come in three different configurations: (1) two equally sized tracks (Figure 2.11[a]); (2) four equally sized half-tracks (two on each axle; Figure 2.11[b]); and (3) two pairs of half-tracks, with a smaller track on the front axle and a larger one on the rear axle (Figure 2.11[c]). A 2WD tractor transmits torque through the rear axle while, in a 4WD tractor, torque is transmitted to both the front and rear axles. Four-wheel drive tractors can be classified into two groups. First, in a front wheel–assisted 4WD tractor, the front wheels assist the rear wheels (the front tires are smaller than the rear tires) and the front-wheel drive can be disengaged. Second, the true 4WD tractor, which can be either articulated or have a fixed frame. Articulated tractors are hinged in the middle and steered using a powerful hydraulic system (Jerry, 2002). A fixed frame (non-articulated) 4WD tractor has the ability to be steered using the front wheels only or by the wheels on both the front and rear axles. Comparisons of 2WD and 4WD tractors have been widely done (Renius, 2020b) and have shown the advantages that make 4WD tractors preferable. In a 4WD tractor, the entire weight of the vehicle is utilized as a load on the driven axle. Also, because 4WD tractors have equally sized wheels, the front wheels compact the soil which, when done under controlled traffic conditions, reduces the total rolling resistance and results in a better transmission of power by the rear wheels (Söhne, 1968).

Figure 2.9. Two-wheel drive tractor (Copyright 2025 by Deere and Company).

(a) (b) (c)

Figure 2.10. Types of four-wheel drive tractor (Copyright 2025 by Deere and Company).

Note. Image (a) is of a tractor with small front wheels and large rear wheels; image (b) shows a tractor with wheels of equal size; image (c) is a tandem tractor.

(a) (b) (c)

Figure 2.11. Types of track tractors (Copyright 2025 by Deere and Company).

Note. Image (a) shows a tractor with two equally sized full tracks; image (b) is a tractor with four equally sized half-tracks, and image (c) is a tractor with two pairs of differently sized half-tracks.

2.3.3 Tractive force analysis

The tractor tires transmit the power from the tractor to the ground to generate a tractive force. The basic model for determining the tractive force on a deformable soil is the Mohr-Coulomb equation (Carroll et al., 2006):

$$F_{max} = A_c C_s + W \tan\emptyset \quad (7)$$

Where

F_{max} = maximum shearing force (N)

A_c = the tire and the soil area of contact (m^2)

$\emptyset$ = angle of internal friction (^{0})

C_s = soil cohesion (N/m^2).

The basic force components applied by the tractive device can be represented by a) dynamic load, which is perpendicular to the direction of travel, and b) the pull or net tractive force (S. Persson, 2009).

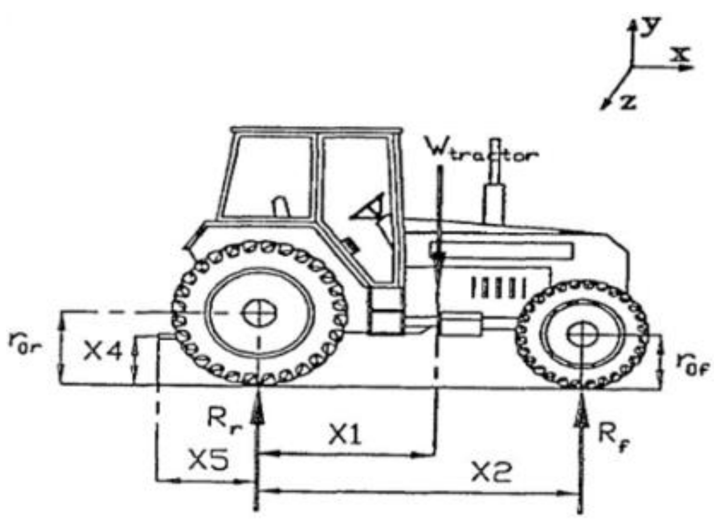

Figure 2.12. Forces acting on a tractor at equilibrium (Brassart, 1994).

From Figure 2.12, considering the static equilibrium for a stationary 4WD tractor,

$R_r \ = SW_r$

$R_f \ = SW_t$

But

$$R_r \ + \ R_f \ = \ W_{tractor} \tag{8}$$

Hence,

$$X_2 R_f - \ X_2 W_{tractor} = 0 \tag{9}$$

Where

R_r = the rear axle reaction force by the soil (N)

R_f = the front axle reaction force by the soil (N)

SW_r = the rear axle static load (N)

SW_f = the front axle static load (N)

$W_{tractor}$ = total tractor weight (N) and

X_2 is the wheelbase of the tractor distance between the center line (m) of the front and rear axles.

X_1 is the horizontal difference between the center line of the rear axle and the tractor's center of gravity (m)

$$X_1 \ = \ \frac{X_2 R_f}{X_2 W_{tractor}} \tag{10}$$

For the force under the dynamic equation of a tractor under steady-state conditions,

$$W_f \ = \ \frac{W_{tractor} X_1 - \mathrm{ID} X_3}{X_2} \tag{11}$$

$$W_r = \ W_{tractor} + ID \ Sin \ (\alpha) \ W_f \tag{12}$$

Where

ID = implement draft force (kN)

α = the angle the implement draft makes with the horizontal plane (°)

X_3 is the perpendicular distance between the ID action line to the point of action of the rear axle, given as

$$X_3 \approx X_4 Cos(\alpha) + X_5 Sin(\alpha) \tag{13}$$

Where X_4 is the height of the hitch point above the level of the application of the rear soil reaction (or above the drawbar) and X_5 is the horizontal distance between the hitch point and the center line of the rear axle.

2.4 Tire Wear

2.4.1 Mechanisms of tire wear

As the tractor tires roll along the contacting soil surface, the shearing force between the tires and the soil causes the rubber to wear. Therefore, tractor tire wear is the progressive loss of the tire tread. The basic mechanisms of tire wear are friction, abrasion, and fatigue.

2.4.1.1 Friction

The friction between the soil and the tire enables the tractor to move, negotiate curves, and stop. The traction tire has a high coefficient of internal friction and low permeability to gases (Gent & Walter, 2006). The Coulomb friction coefficient (μ) is used to characterize the frictional resistance between two surfaces.

$$\mu = \frac{Frictional\ force}{Normal\ force} \tag{14}$$

Friction is the most commonly used variable of soil property that relates to traction. Using the Coulomb equation (Equation 9) to express the horizontal force of traction on the given soil, the coefficient of friction of the soil is a key parameter because most agricultural soils are neither purely cohesive nor purely frictional but exhibit both cohesion and friction characteristics, as shown in Figure 2.13 (Brassart, 1994; Carroll et al., 2006).

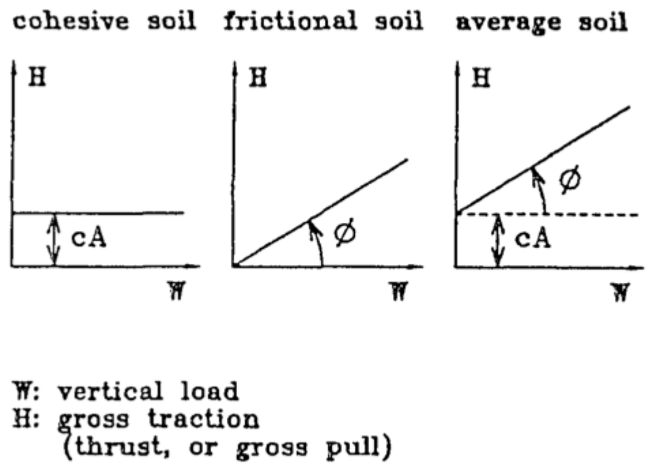

Figure 2.13. Soil cohesive and friction characteristics (Brassart, 1994).

2.4.1.1.1 Friction model

Significant progress has been made in modeling the friction behavior of rubbers on rough and self-affine surfaces (Heinrich & Klüppel, 2008; Le Gal et al., 2005; B. Persson et al., 2004). Vieira et al. (2015) indicate that over the years, the Moore formulation model of mathematically independent components (hysteresis and adhesion) of rubber-pavement contact interaction has been widely used when analyzing the friction behavior of rubber-pavement contact surfaces. The two forces at the contact surfaces that cause failure in the friction mechanism of elastomers are:

(1) adhesion forces due to the interaction of surface molecules at the interface; and

(2) deformation forces, due to a delay in the recovery of the elastomer after the indention of a particular asperity, which results in hysteresis friction. A delay in the viscoelastic response of the

rubber materials and the sliding interface of the contact area results in energy dissipation, which gives rise to a substantial temperature increase at the sliding surface and with the sliding bodies.

$$F = F_{adhesion} + F_{hysteresis} \tag{15}$$

Dividing Equation 15 by the load (W),

$$\mu = \mu_{adhesion} + \mu_{hysteresis} \tag{16}$$

$$\mu_{adhesion} = \frac{F_{adhesion}}{W} = \sum_{i=1}^{M} {F_i}/{W} \tag{17}$$

$$= \frac{MA_1S}{W} \tag{18}$$

Where

M = total number of macroscopic sites

A_1 = mean area of contact location (m^2)

S = shear strength (N/m^2)

F_i = resistive adhesive force (N)

But

A_1 in hysteresis friction $= \frac{W}{\dot{M}\dot{P}}$

$\dot{M}$ is the total number of asperities where each load (W) is applied.

$\dot{P}$ is the mean pressure with speed over each asperity (N/m^2).

Beyond Moore's friction model, more complex friction models have been developed for tires on hard surfaces (Heinrich & Klüppel, 2008; Le Gal et al., 2005; B. Persson et al., 2004) and deformable surfaces(Garciano et al., 2010; Lyasko, 2010; Upadhyaya et al., 2009). Vieira et al. (2015) evaluated the friction mechanism of tire-pavement contact and tire-sandpaper contact interactions. Their study modeled adhesion friction by estimating the geometric mean of the surface energies of the contacting surfaces.

$$F_{adhesion\ 1,2} = 2f\sqrt{\gamma_1\gamma_2} \quad (19)$$

γ_1 *and* γ_2 are the surface energies for the contacting bodies.

f is the energy release rate for junction friction. It is a proportionality constant.

Their study agrees with Equation 19, which suggests that higher friction energy leads to increased adhesion, thereby enhancing friction. Their friction model verified the relevance of adhesion friction in traction.

2.4.1.2 Abrasion

Over time, as a tractor tire rotates on the ground, the soil causes the rubber particles of the tire tread to rub off. These particles then mix with the soil. In terms of the different types of wear, abrasive wear is considered the most common and accounts for more than 50% of wear events (Massola et al., 2016). The amount of abrasive wear of the tractor tire depends on the type of soil on the farm. For example, abrasive wear is relatively low when the tire runs on sandy, sandy-loam, and clay-loam soil. However, the tire will experience rapid wear on stony soil, as some of the stones may scratch or tear off the tread. Singh et al. (2017) note that the particle size and texture of the soil affect the abrasive wear on tillage implements.

2.4.1.3 Fatigue

The cords and rubber of a tractor tire are susceptible to fatigue failure. The alternating load on the tractor tires and the uneven soil surface of the field induce frequent stress and strain on the tires (Lin, 2023). Over time, the molecular chain of the rubber starts to break down. This leads to the continuous wearing of the rubber particles of the tire.

Incorrect tire pressure and overloading are key factors that cause fatigue in tires. These conditions lead to excessive flexing of the tire's sidewalls when they are operated beyond the designed limits. Over time, this stress and heat deform the molecular structure of the rubber and damage the tire’s internal components. The generated heat raises the temperature of the rubber and speeds up its oxidation. This process weakens the tire’s flexibility, resulting in cracks and poor adhesion.

2.4.2 Tire wear prediction

One of the major focuses of research on tire wear has been the prediction of tire wear. Many models have been developed to estimate tire wear as a function of sliding speed, friction, and surface terrain (Cho & Jung, 2007; Lepine & Cebon, 2018; Lupker et al., 2002; Moore, 1980). The conditions under which tires operate determine the factors that influence tire wear. Most researchers consider the factors that are most significant to their study in modeling tire wear. Le Maître et al. (1998) note that the ability of the model to provide a good analysis of tire-contact surface characteristics, which determine tread wear, demonstrates the quality of the model. Zhang et al. (2023) identify three main methods of predicting tire wear: theoretical method, empirical method, and finite element analysis.

2.4.2.1 Theoretical method

This method uses the principles of mathematics and physics to develop and simulate a model of how the tread of a tire wears. Li et al. (2012) established a formula to predict tire wear for different tires running under different conditions by analyzing the dependent variables (effect of temperature and vehicle dynamics) and independent variables (speed, tire pressure, and sprung mass). Their study revealed that by modifying the grounding characteristics, the cornering of the tire significantly affects the wear rate. Analyzing a two-dimensional contact patch of a tire, Nakajima and Hidano (2021) developed a theoretical model for the progress of tire that considers the pattern of the tire tread block. Their study used a calculated wear energy (by alternating slip angle and slip ratio) to predict tire wear progress. By making use of a modified theoretical model, Wang (2017) measured physical parameters to develop a predicted wear model. Their study analyzes the relationship between the contact features and the tire wear as a function of the structure of the tire and tire maneuvering parameters.

2.4.2.2 Empirical method

This method uses collected study data and observations to analyze various factors and the wear rate. Lupker et al. (2002) performed several tests, such as a material test of a tire compound, a well-controlled carousel test with truck tires, and a test with an articulated commercial truck on a public road. These tests obtain insight into the mechanism behind the phenomenon of truck tire wear. The study revealed that the long-distance transport vehicle traveling on the motorway recorded the lowest tread wear, while the vehicle used in extreme all-terrain off-road conditions recorded severe tread wear. This confirms the observation made by Lyasko (2010) that the tractive performance of a vehicle is influenced by the given surface condition on which the wheels are driven. Lepine and Cebon (2018) developed an empirical tire-wear model that is used to predict the wear for multi-axle vehicles based on route data and vehicle models:

$$\sigma\ (\alpha) = K\alpha^2 \tag{20}$$

Where

σ = is tire wear per unit area (mm/m^2)

K = wear coefficient = 132 g/m^2

α = angle of slip (^{0}), and

the total mass of rubber worn from the tire (ΔM) is given as

$$(\Delta \mathrm{M}) = w \int P\left(\propto (s)\right) ds \tag{21}$$

w = width of the tire (m)

s = tire traveling distance (km),

but the reduction of tread depth $\Delta h = \frac{\Delta M}{D\pi w\rho}$ (22)

Interestingly, the study showed that the rate of wear is independent of the tire's normal load, which simplifies their model. This agrees with the model for the rate of tire wear depth developed by Braghin et al. (2006) to predict the wear of a tire for a given maneuver as a function of road vehicle characteristics,

$$W_r = \frac{M/_{L_{CISA}}}{2\rho\pi r w} \tag{23}$$

where W_r is the amount of wear rate, W is the amount of wear, L_{CISA} is the total length of the Costruzioni Italiane Serrature e Affini (CISA) road course before each wear measurement, ρ is the density of the tread rubber compound, r is the tire normal radius, and w_t is the tire width (Braghin et al., 2006). Le Maître et al. (1998) evaluated the performance of tire wear in off-road vehicles in terms of severe use, medium use, and mild (highway and urban) use. They measured the rate of tire wear (g/100 km) for a full seasonal weather cycle to reduce the seasonal effect on the tire during their studies, as shown in Figure 2.14.

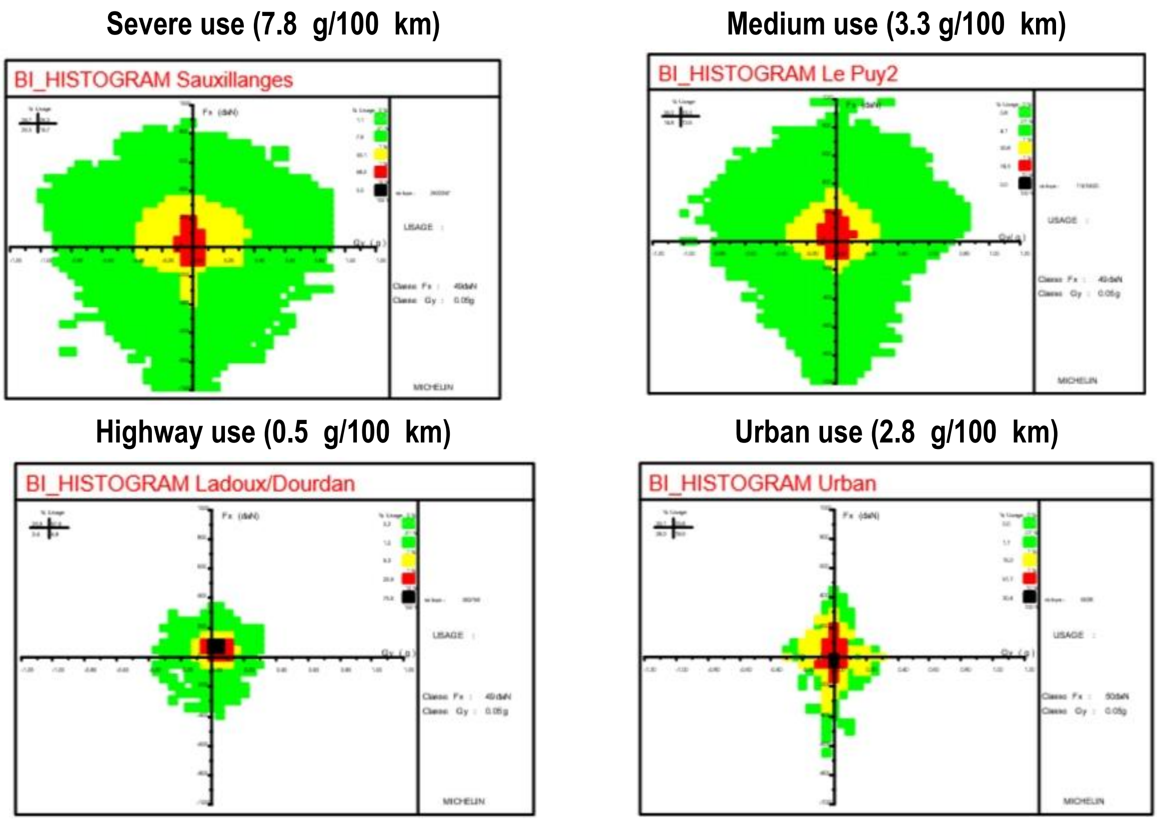

Figure 2.14. Wear rate by usage level (Le Maître et al., 1998).

To determine the tread life of the tires, Le Maître et al. (1998) measured the tread depth of the tires before and after each test, considering the following wear parameters: the routes and style of driving, different weather conditions under which the vehicle was operated, the vehicle, the tires, and the road surface. The tread life of the tires based on the three levels of usage is shown in Table 2.1 (Le Maître et al., 1998). Their study considered a wide range of parameters to reflect the actual conditions under which tires are used.

Table 2.1. Tire tread life based on distance traveled and level of usage (Le Maître et al., 1998).

Tire	Distance traveled (km)		
	Severe use (D10)	Medium use (D50)	Mild use (D90)
1	20,000	33,000	53,000
2	18,000	35,000	58,000

Note. Table shows the tread life of a car tire based on distance traveled.

Dorvlo et al. (2014) evaluated an on-farm rear tire using a 2WD tractor with an engine power rate of 56 kW that was aggregated with a three-bottom disc plow. The researchers measured the lug height before and after every operation to get the tire wear rate (mm/km), considering only one field operation (plowing) for 29 km of tractor travel. Their study reveals that the tractor rear tire wears at a rate of $493 \pm 12.4 \times 10^{-5}$ mm/km (Dorvlo et al., 2014). Due to different soil surfaces and properties under which the left rear tire ran (on an unplowed surface) and the right rear tire ran (in the plowed furrow) during the test, the left rear tire wore 6% more than the right rear tire. This supports the fact that soil parameters are key factors in determining the rate of tire wear (Le Maître et al., 1998; Wang, 2017).

2.4.2.3 Finite element analysis

Tamada and Shiraishi (2017) developed a wear progress simulation to evaluate the head- and toe-wear performance at the shoulder of the tire. They used a finite element tire model method by calculating the wear energy from the rolling simulation. Cho and Jung (2007) used an explicit finite element model to predict the pattern wear of a tire. The equation for wear rate is a function of slip velocity and tangential stress. They compared the tread wear to the test results of actual driving conditions for an indoor test. Their simulation wear results show a good correlation with the actual results of the indoor wear test. Most prediction models for tire wear on paved roads used the combination of theoretical and finite element analysis methods (Zhang et al., 2023).

2.5 Chapter Summary

This section includes a discussion of agricultural tires, tire-soil interaction, and tire wear. Agricultural tractor tires are designed for the conditions under which they will be used. The tire manufacturer's process and the composition of the materials determine the tire's type and characteristics, the quality of the tire, and the conditions under which the tire will be most effective.

The tire interacts with the soil to generate the tractive force needed for the tractor to pull the attached implement(s). Extensive studies have been conducted on tire-soil interaction. These have led to the development of both theoretical and empirical models to predict tractive effectiveness and fuel consumption by considering variables such as wheel slip, the static and dynamic loads of tractors, and friction. Most modern farmers prefer to use 4WD tractors for tillage work to achieve high tractive effectiveness, reduce fuel consumption, and reduce soil compaction.

As the tractor tire interacts with the soil, wear is inevitable. Various studies have been conducted and models developed to predict tire wear related to slip, friction, road vehicle characteristics, and soil surface terrain. Still, very little research has been conducted on tire wear relating to on-farm agricultural tractor tire use. Empirical research has been conducted to estimate the wear rate of agrarian tractor tires (Dorvlo et al., 2014). However, this research has some limitations. For example, a 2WD tractor, which most modern farmers do not use for tillage work, was used for the experiments. Also, the Dorvlo et al. (2014) study used only primary tillage (plowing) to estimate the depreciating life of the tire. Therefore, the focus of this research addresses these limitations.

CHAPTER 3: MATERIALS AND METHODS

3.1 Study Location and Site Selection

Akandem Farms Limited was selected as the location for the study due to farm management's willingness to collaborate with the research team (Figure A1). Akandem Farms has different farming fields in Builsa North in the Upper East Region of Ghana. Three Akandem Farm fields were selected for the study. The data collected during the 2023 farming season was used to develop the empirical wear prediction models, while the data collected during the 2024 farming season was used to validate the prediction models. This was to ensure that the study of the selected fields was conducted within the appropriate farming season.

Field 1 is off Wa-Sandema Road (latitude, 10°41'54.8"N; longitude, 1°16'52.8"W) and measures 9.7 ha (24 acres), as shown in Figure 3.1.

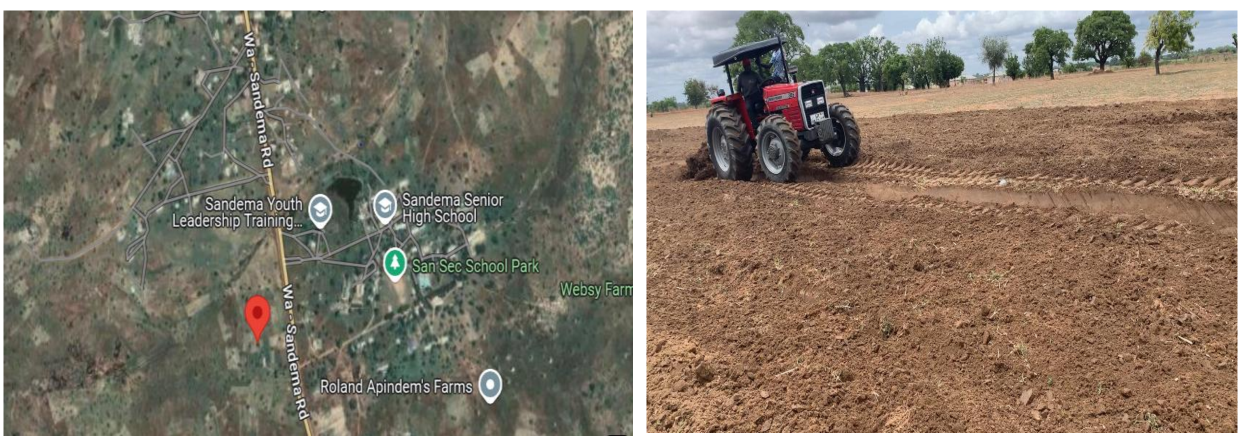

(a) (b)

Figure 3.1. Location and topography of Field 1.

Note. Image (a) shows the Google map location of Field 1 (red marker); image (b) shows the topography of Field 1 (author's work).

Fields 2 and 3, as shown in Figure 3.2, are located at Namonsa and are 15 ha (38 acres) and 16.2 ha (40 acres), respectively. All three fields have flat topography, as shown in Figures 3.1(b) and 3.2(b).

(a) (b)

Figure 3.2. Location and topography of fields 2 and 3.

Note. Image (a) is the Google map location of fields 2 and 3; image (b) is the topography of fields 2 and 3 (author's work).

3.2 Equipment and Instrument Selection

The following equipment and instruments were selected for the study.

3.2.1 Tractor

A Massey Ferguson 385 4WD tractor with a 56 kW engine, 49 kW PTO, and initial mileage of 832.2 km (Figure 3.3) was used for all field operations (plowing, harrowing, and planting). The tractor was outfitted with four tires manufactured by Panther Tire Limited. Two 12.4-24 tires with a W10 (single-well 10-inch) rim, an overall diameter of 1,160 mm, a section width of 315 mm, and a tire pressure of 2.3 bar were fitted on the front axle of the tractor. The two 18.4-30 tires fitted on the rear axles of the tractor had a W16 (single-well 16-inch) rim, an overall diameter of 1,524 mm, a section width of 467 mm, and a tire pressure of 2.9 bar.

The tractor was operated by a well-experienced operator who has been working with Akandem Farms for the past eight years. Prior to his employment at Akandem Farms, he plowed for individual small farm holders in the community. He completed all the field operations during the experiment for the 2023 and 2024 farming seasons.

Figure 3.3. Massey Ferguson 385 4WD tractor.

3.2.2 Implements

3.2.2.1 Plow

Figure 3.4 shows the Massey Ferguson four-disc pipe plow (width of 0.51 m) that was used to plow (primary tillage) the three fields under study

Figure 3.4. The disc plow.

During plowing and harrowing, the operator starts from the middle of the field and travels from one end to the other in a straight path. The return pass was done on the right and left sides of the first travel, with the right tires of the tractor typically running in the furrows as a guide to ensure parallel rows, as shown in Figure A7. The trajectory of the field plowing and harrowing continues like a “ripple effect”. Contrary to plowing and harrowing, planting was done starting along one side of the field and moving towards the other side in parallel adjacent passes, making use of planter markers to guide the tractor along those adjacent passes.

3.2.2.2 Harrow

Figure 3.5 shows the Massey Ferguson tandem disc harrow that was used to harrow (secondary tillage) the three fields under study. It has a width of 1.79 m, with 8 discs in front and 8 discs behind.

Figure 3.5. The disc harrow.

3.2.2.3 Planter

The Kuhn PPK 500 mechanical precision seed drill with a four-row planter that was used for planting is shown in Figure 3.6.

Figure 3.6. The Kuhn PPK 500 planter.

3.2.2.4 Digital depth micrometer gauge

A Fowler 54-225-456-0 IP54 digital depth micrometer with a measuring range of up to 150 mm (6 in) was used to measure the tread depth to determine the amount of lug wear. The digital depth micrometer has a resolution of 0.001 mm (0.00005 in) and an accuracy of ± 0.004 mm (0.00016 in), as shown in Figure 3.7.

Figure 3.7. A Fowler digital depth micrometer gauge (Copyright 2022 by Fowler High Precision).

3.3 Fabrication of Supporting Equipment

3.3.1 Micrometer base extension

The base of the micrometer was too small to sit on two adjacent tire lugs to take a correct reading. For this reason, a new wider base was fabricated and attached to the original base. Aluminum was used to prevent corrosion and to make the base lightweight. To further reduce the weight of the base, blind holes were created on the top surface. A rendering of the fabricated base is shown in Figure 3.8. A detailed drawing of the base is shown in Appendix A (Figure A2).

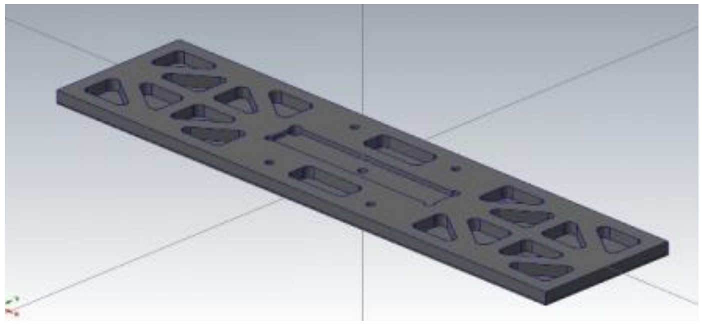

Figure 3.8. Rendering of fabricated base for micrometer.

3.3.2 Cylindrical core

A hollow cylindrical core (Figure 3.9) was fabricated to collect soil samples from the various fields. Galvanized steel was used to provide the necessary material strength, as the core would be driven into the soil. The core had a diameter of 76.2 mm and a height of 152.4 mm. These dimensions match the average depth at which both the plow and harrow discs cut into the soil.

3.4 EXPERIMENTS CONDUCTED

Experiments were carried out both in the field and in the laboratory. The field experiments took place at Akandem Farms (Section 3.1). The laboratory experiments were done at the University of Ghana Earth Science Laboratory and the University of Ottawa Geotechnical Laboratory.

3.4.1 Soil sample collection

Five data points were designated in each field, one in each of the four corners and one in the middle of the field, as shown in Figure A6. Using a mallet and a piece of wood, the 76.2 mm diameter cylindrical core is driven to a depth of 152.4 mm of the soil. Five soil samples, one from each of the five points, were collected as shown in Figure 3.9. Each sample was then dried in an oven for 24 hours at 105ºC. Ten grams of dried soil from each of the five samples were then collected and combined to create a single 50 g sample. This procedure was used to collect a 50 g soil sample from each field: Sample 1 (Field 1), Sample 2 (Field 2), Sample 3 (Field 3).

3.4.2 Soil texture

ASTM International (2017) standard *D7928: Standard test method for particle-size distribution (gradation) of fine-grained soils using the sedimentation (hydrometer) analysis* was used to determine the soil texture for each field of operation. The Uniform Soil Classification System (USCS) was used to classify the soils collected according to particle size.

Each soil sample was poured into a graduated cylindrical jar. To measure the percentage of sand and gravel (per USCS definition) in each field, two methods were used. A sieve grain size analysis was conducted to determine the distribution of soil particles larger than 0.075 mm, while a hydrometer analysis was used to analyze soil particles of less than 0.075 mm to determine the percentages of silt and clay (per USCS).

Figure 3.9. Collecting a soil sample using the cylindrical core.

3.4.3 Soil moisture

The initial mass of the soil sample collected from each data point was measured (M_{ws}). The sample was then dried at a temperature of 105ºC for 24 hours and weighed (M_{ds}). The percentage of moisture in the soil was determined using the formula

$$M_c = \left(\frac{M_{ws} - M_{ds}}{M_{ds}}\right) \quad (24)$$

where M_c is the soil moisture content, M_{ws} is the mass of wet soil, and M_{ds} is the mass of the dried soil. The method was repeated to obtain the soil moisture before every field operation.

3.4.4 Soil bulk density

The bulk density of the soil was assessed to measure soil compaction, i.e., the soil's capacity to support the tractor and the implements during field operations. As with the collection of soil samples to assess soil texture (Section 3.4.1), the cylindrical core method was used to determine bulk density (Figure 3.10) in accordance with ASTM D2937. The mass of the collected sample was then measured and the volume of soil in the cylindrical core was calculated. The bulk density of the sample was calculated using the formula

$$Bulk\ density\ (\rho_b) = \frac{Mass\ of\ sample\ soil}{Volume\ of\ sample\ soil} \tag{25}$$

This method was repeated to determine soil bulk density before any field operation.

Figure 3.10. Cylindrical core being pounded into the soil for sample collection.

3.4.5 Wheel slip

The right rear tire was marked to aid in counting the number of tire revolutions during field operation. For each field operation, the tractor was driven for five revolutions of the tire without engaging the implement, and the distance traveled was then measured (R_{d1}). Then, the implement was engaged for operation. The tractor was then driven for another five revolutions of the tire and the distance traveled by the tractor was again measured (R_{d2}). The wheel slip was calculated using the formula:

$$Wheel\ slip\ (i) = \frac{R_{d1} - R_{d2}}{R_{d1}} \times 100 \tag{26}$$

3.4.6 Draft force (field operation)

The draft force needed to pull each implement for each field operation was calculated using the formula suggested in American Society of Agricultural and Biological Engineers (ASABE) (2020) standard *ASAE D497.7 (R2020): Agricultural machinery management data,* i.e.,

$$D = F_e[\, A + B(s) + C(s^2)\,]w_i T \tag{27}$$

where *D* is the draft force of the implement (*N); F* is a dimensionless soil texture adjustment parameter; *e* is the soil coarse texture; *A*, *B,* and *C* are specific parameters of the tractor and/or implement; *s* is the field speed (km/h); w_i is the width of the attached implement (m); and *T* is the tillage depth (cm).

Each field operation (plowing, harrowing, planting) was classified according to the specific implement attached to the tractor and the draft force for each implement was calculated during its operation.

3.4.7 Tire wear measurement

Each tire was divided into four equal sections at an angle of 90º. Two lugs (the inner lug and the outer lug) were selected from each tire section. On each lug, the wear measurement was taken at three points, as shown in Figure 3.11(a). To ensure accuracy, the tires were thoroughly washed with water to remove dirt and mud before the readings were taken. The tire data points where the gauge plunger was positioned were marked with a white permanent marker to ensure consistency in data collection, as shown in Figure 3.11b. The points were remarked periodically because of tire wear and field operations to ensure the visibility of the data points.

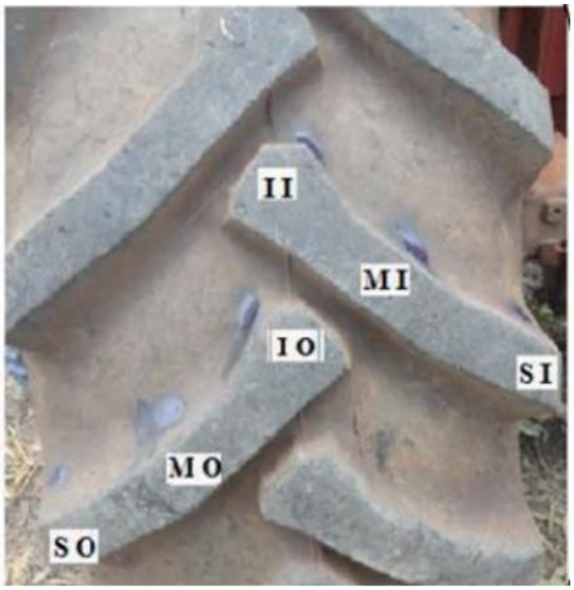

(a) Measurement locations (b) Measuring a lug

Figure 3.11. How tire wear was measured.

Note. II = inner lug; IO = inner of outer lug; MI = middle of inner lug; MO = middle of outer lug; SI = side of inner lug; SO = side of outer lug. Image (a) shows the points at which readings were taken on the lugs of each tire. From "Tractor Rear Tyre Wear Rate and Replacement Planning in Ghana," by S. Dorvlo, 2014, p. 6. Image (b) shows the measuring of a lug height.

Lug measurements were taken for each field operation in each field. To obtain the tire wear for each data point, the lug height was measured before and after each task on the field (Figure 3.11[b]). The wear was calculated using the formula

$$W_{L\,(mm)} = H_{Lb} - H_{La} \quad (28)$$

Where W_L is amount of lug wear, H_{Lb} is the lug height before a field operation, and H_{La} is the lug height after a field operation (Figure 3.12). Three readings were taken for each data point and the average of the three was recorded as the reading for the data point, and this average was recorded as the wear for that lug (data point).

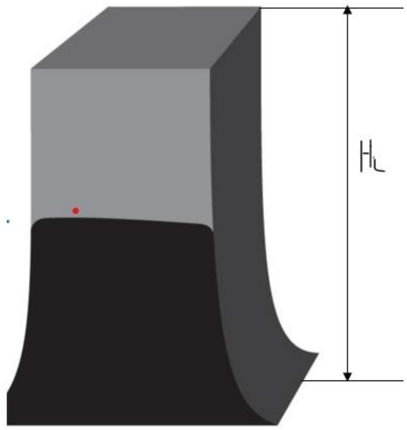

Figure 3.12. Cross-section of the measurement of H_L.

3.4.7.1 Tire lug wear rate

The wear rate of each lug was determined by the formula

$$W_r = \frac{W_L}{d} \tag{29}$$

Where

W_r = wear rate of the lug (mm/km)

W_L = amount of lug wear (mm)

d = distance traveled by the tractor during the field operation (km)

The experiment was repeated for all three field operations in the three fields.

3.5 Predictive Tire Wear Model

Study data was used to develop a tire wear rate model as a function of wheel slip, soil properties (bulk density, soil texture, and moisture content), and field operations (draft forces). The tire model was developed to anticipate the wear of a given soil condition and field operation.

The predictive model was developed using a multiple regression analysis using the enter method of version 27 of IBM SPSS Statistics (IBM Corp., 2020). The regression analysis examined how the independent variables (soil moisture, soil texture, draft force, speed, and slip) can predict the rate at which the tractor tire wears during field operation (dependent variable). The significance level of the regression model was 0.1.

3.5.1 Validation of the model

Vignola et al. (2007) recommend using a different dataset to validate a developed model, and this approach was followed for this study: the data collected during the 2023 farming season was used to develop the model, while the data collected during the 2024 season was used to validate the model. The same farm implements on the same fields were used to collect both sets of data.

Empirical models for the four tires were developed and validated. The accuracy of the models was tested by running a linear regression on SPSS between the predicted wear (W_p) and the measured wear (W_s). This was to determine the Pearson correlation (r) and the coefficient of determination (r^2) between the predicted and measured wear for the four empirical models developed for the four tires.

CHAPTER 4: RESULTS AND DISCUSSION

4.1 Study Data

Study data was collected during the 2023 and 2024 farming seasons. The data collected during the 2023 season was used to develop the predicted tire-wear models, and the 2024 data was used to validate the models. This section analyzes the soil test results and tire wear measurements from fields 1, 2, and 3.

4.1.1 Soil properties

4.1.1.1 Soil texture

Table 4.1. Proportion of soil types for the 2023 and 2024 farming seasons.

Field	Sand (%)	Silt (%)	Clay (%)	Texture classification
1	62	26	12	Sandy loam
2	52	36	12	Sandy loam
3	44	38	18	Loam

Table 4.1 shows the percentages of soil types in fields 1, 2, and 3 for the 2023 and 2024 farming seasons. Field 1 exhibits a high rate of tire wear in sandy soil compared with the other fields. The soil type percentage indicates the texture of the soil. The soil texture classifications are based on these percentages, as shown in Table 4.1 using the US Department of Agriculture (USDA) soil texture classification triangle. The soil types for fields 1, 2, and 3 (with sand percentages of 62%, 52%, and 44%, respectively) are appropriate for growing corn and soybeans in the Upper East Region of Ghana. These results agree with Tetteh et al. (2016), who report that the texture of the subsoil in that region of Ghana is sandy loam and is suitable for growing cereals.

4.1.1.2 Soil bulk density (ρ_b)

Table 4.2 shows the bulk density of the soil for fields 1, 2, and 3 during each farm operation in the 2023 and 2024 farming seasons.

Table 4.2. Soil bulk density by field, field operation, and year.

Field	Plowing (g/cm^3)		Harrowing (g/cm^3)		Planting (g/cm^3)	
	2023	2024	2023	2024	2023	2024
1	1.53	1.55	1.63	1.65	1.62	1.64
2	1.62	1.63	1.63	1.72	1.64	1.64
3	1.63	1.65	1.67	1.72	1.73	1.64

The lowest soil bulk density (1.53 g/cm^3) was recorded during plowing on Field 1 (2023 farming season), and the highest was recorded during planting on Field 3 (2023 farming season). The soil density increases in each field as the field operations progress from plowing to planting. Research has shown that the bulk density of untilled soil is higher than that of tilled soil (Amer et al., 2021; Lyasko, 2010; Sharma & Warren, 2024). Therefore, one may expect that the measurement of bulk density taken during plowing should be higher than the other field operations since the soil sample for plowing (primary tillage) would be taken before the soil had been tilled. However, it was observed that because the topsoil had already been tilled (before harrowing and planting), driving the cylindrical core into the topsoil faced less resistance and moved deeper, beyond the tilled surface to the untilled subsoil. This increased the soil bulk density observed during harrowing and planting. This observation agrees with Mari et al. (2011) and Sharma & Warren (2024), whose experiments concluded that bulk density is a dynamic property of soil, varies within small distances, and increases with depth. During harrowing (secondary tillage), the clumps of soil are broken down into fine and even layers of soil. This allows the cylindrical core to penetrate deeper into the soil when collecting samples prior to planting. Hence, the bulk density for planting becomes higher than for harrowing, as shown in Table 4.3.

4.1.1.3 Soil moisture

Table 4.3 shows the soil moisture of the three fields during each farming operation. The soil moisture content of Field 1 during the 2023 growing season for plowing (10%) was higher than for the other field operations, and the lowest was recorded on Field 3 during planting of the same farming year (4.33%).

Table 4.3. Percentage of soil moisture in each field during each field operation.

Field	Plowing (%)		Harrowing (%)		Planting (%)	
	2023	2024	2023	2024	2023	2024
1	10.02	10.65	7.29	7.01	5.48	5.60
2	4.83	5.31	4.36	4.03	8.13	7.92
3	4.80	4.71	4.33	4.42	7.90	7.75

None of the soil moisture content results for the 2023 and 2024 farming seasons fell within the optimum moisture content range for tillage work (18% to 20%) suggested by P. Cardei et al. (2020).

Northern Ghana is considered a dry farming area (rain-distress location) due to the severity of the drought (Kpenekuu et al., 2024). Farmonaut (n.d.) reports that in 2024, Northern Ghana experienced one of its worst droughts in history, which led to the U.S. government providing a $1.7 million lifeline for the 9,800 Ghanaian farmers affected by the severe drought in that region. In conventional farming, most farmers in northern Ghana depend on a rain-fed farming system. The farmers wait for the “first rain” (as the locals call it) before they commence any soil-working operation. This first rain provides the soil moisture necessary for effective plowing.

Plowing is the first field operation that turns the firm soil. Effective plowing can take place within a range of soil moisture levels; however, the drawing resistance of the plow can increase significantly when the soil moisture content falls outside the most appropriate range.

The optimum moisture ranges for plowing as suggested by P. Cardei et al. (2020), Amer et al. (2021), and Mari et al. (2011)are 18% to 20%, 9% to 12%, and 13% to 20%, respectively.

However, Table 4.3 shows that the soil moisture percentages measured for this study are outside these ranges. In other words, the moisture content results are too low for effective tillage. Lower moisture increases soil cohesion, resulting in very high plowing resistance. According P. Cardei et al. (2020), a plow will experience specific resistance of between 61,000 Pa and 75,000 Pa in sandy loam and loam soil (Table 4.1) that has an optimum moisture range of 18% to 20%. However, because none of the moisture content results for the three fields fall within this range, the specific resistance of the plow will increase to between 30% and 50% of the minimum plowing resistance (P. Cardei, 2019). Again, since the soil is untilled, the plowing resistance increases by 30%, and the resistance for tilled soil increases by 10%. This agrees with the results in Table 4.3, indicating that the draft force for plowing is greater than that for harrowing.

4.1.2 Data from the 2023 farming season

4.1.2.1 Draft force, slip, and speed of the tractor

The data from Table B1 is plotted in Figure 4.1, making it easy to compare the relationship between draft force (D), slip (i), and tractor speed (S) during the use of the different farm implements (plow, harrow, planter) on each field.

Taking all of the parameters for the soils for each field and for the tractor and implements, the ASABE (2020) standard model for draft force (Equation 27) was used to calculate the draft force of the implements. Figure 4.1 indicates that plowing exhibits a higher draft force in each field (Field 1 = 12.82 kN, Field 2 = 13.47 kN, and Field 3 = 13.24 kN) than other field operations. Because plowing is the first tillage work on the soil, the power unit (tractor) requires a high force at the hitch to pull the plow through the soil. The results in Table 4.4 overestimate the specific draft force for fields 1, 2, and 3 for the 2023 growing season by 19.9%, 26.0%, and 24.0%, respectively, compared with the specific draft force for plowing (3.79 N/cm^2) modeled by Ahmadi (2016). However, to develop his model, Ahmadi (2016) used a three-blade disc plow to work on silty clay loam soil with a bulk density of 1.5 g/cm^2, while in this study, a four-disc plow was used to plow fields 1, 2, and 3, which had a level of soil moisture below the recommended range. This may have increased the draft force, as Walters (2024) suggested. It should be noted that the ASABE (2020) standard model for a moldboard plow was used to determine the draft force, even though a four-disc plow was used in this study. As discussed above, it was appropriate to use the draft force results from Table 4.4. The Hendrick (1988) model for the specific draft force for a disc plow working on Davidson loam soil at the forward speed of the plow is given by:

$$D_s = 2.4 + 0.045\, S^2 \tag{30}$$

where D_s is the specific draft force (N/cm^2) and S is the forward speed of the plow (km/h). Therefore, the formula for the draft force for the disc plow is given by:

$$D = D_s \times w_p \times T \times N \tag{31}$$

Where D is the draft force (kN) for the disc plow, w_p is the width (m) of the plow, T is the depth of tillage (cm), and N is the number of discs. Table 4.4 presents the results obtained by inputting the plow's parameters for 2023 into equations (30) and (31).

Table 4.4. Specific draft force and draft force for disc plow using Hendrick's formula.

Field	Plowing operation (2023 farming season)	
	Specific draft force (N/cm^2)	Draft force (kN)
1	4.73	14.71
2	5.14	15.97
3	4.99	15.54

Comparing the draft force for the four-disc plow presented in Figure 4.1 versus Table 4.4, it is observed that the draft force for plowing (2023 farming season) shown in Table 4.4 for fields 1, 2, and 3 is 14.74%, 18.55%, and 17.38% higher, respectively, than the draft force shown in Figure 4.1, respectively (based on the Table B1 data of 12.82, 13.47, and 13.24 kN, respectively). Also, for the 2024 farming season, the draft force for fields 1, 2, and 3 in Table 4.4 is only 11.88%, 15.29%, and 14.46% higher, respectively, than the draft force shown in Figure 4.14 (based on the Table B1 data of 12.61, 13.35, and 13.13 kN, respectively). This justifies the appropriateness of using the ASABE (2020) draft force model for the moldboard plow to determine the study's draft force, even though a disc plow was used.

It is well established (theoretically and experimentally) that the variation of the implement's draft force is a function of the working speed (Naderloo et al., 2009; Okoko, 2018; Walters, 2024). For instance, the equations of the models developed by Ahmadi (2016) and the ASABE (2020) are order 2 polynomials with respect to the speed of the plow. However, from Figure 4.1, the draft force is inversely proportional to the speed of the tractor. This is because, in addition to speed as a function of the draft force, the parameters for the conditions of the soil and the implements are key variables in determining the draft force. Walters (2024) indicates that when a moldboard plow is run at a speed of 8.04 km/h, the draft force in medium-textured soil is higher than in coarse-textured soil. The results of the relationship between the draft force and the speed of the tractor as depicted in Figure 4.1 agree with the data provided on soil resistance by Siemens & Bowers (1999) and recorded in Walters (2024).

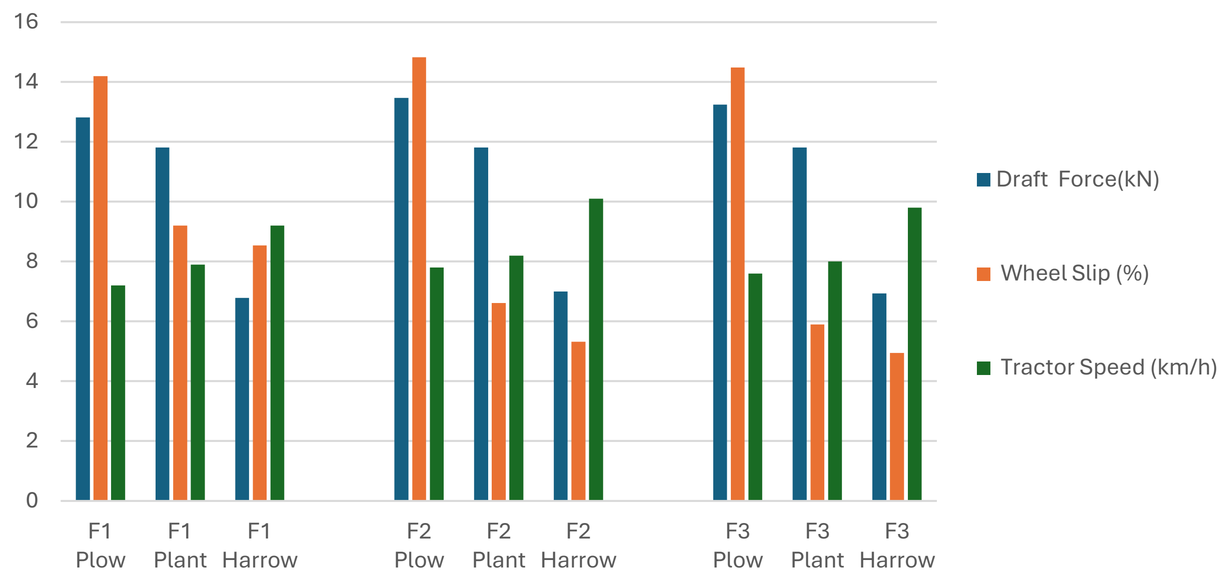

Figure 4.1. Draft force, wheel slip, and tractor speed by field and field operation (2023 data values).

Note. F1 = Field 1; F2 = Field 2; F3 = Field 3. Implement widths were as follows: plow = 0.51 m, harrow = 1.79 m, and planter = 4 rows.

4.1.2.2 Wear rate (W_r)

4.1.2.2.1 Wear rate on Field 1

Figure 4.2 shows the wear rate of each tire lug during plowing, harrowing, and planting on Field 1. The total distance, including headland turns, that the tractor traveled during the plowing, harrowing, and planting operations on Field 1 is 75.1, 59.1, and 46 km, respectively. On average, the wear rate of the inner lugs of the tires is slightly higher than the outer lugs. The inner lug of the rear right tire shows the highest wear rate. It is expected that the tire lugs will experience an even wear rate. However, during the tractor's operation, the tractor's wheels could misalign, causing a toe-out. A toe-out occurs when the front ends of the tractor's wheels point outward, away from the tractor's central axis, causing wear on the inner edges of the tires. Markel (2016) notes that the wear of the inner edge of a tire is considered the most common problem that most tire technicians see. Therefore, the results in Figure 4.2 reveal a tire wear problem that most tire users are familiar with.

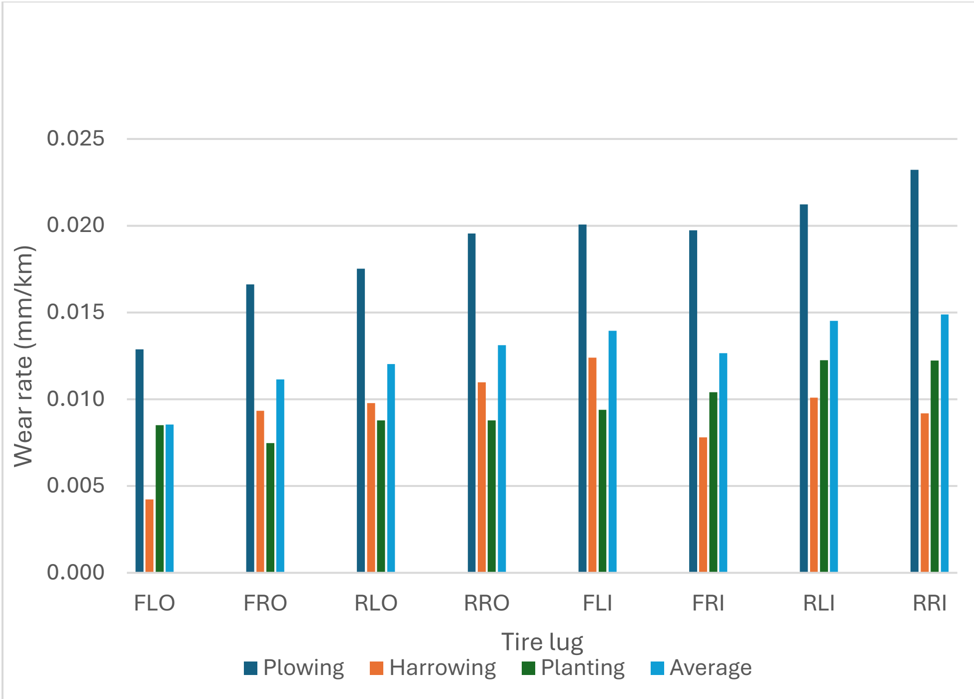

Figure 4.2. Wear rate of tire lugs on Field 1 by lug location and field operation.
Note. FLI = front left inner; FLO = front left outer; FRI = front right inner; FRO = front rear outer; RLI = rear left inner; RLO = rear left outer; RRI = rear right inner; RRO = rear right outer.

The wear rate of each tire is calculated as the average of the inner and outer lugs of the respective tire. Figure 4.3 shows the wear rate of each tire during each operation on Field 1. On average, the rear right tire shows the highest tire wear rate, and the front left tire shows the lowest. The rear left tire experiences a wear rate that is between 14.9% and 16.3% higher than the wear rate for the front left tire, and the rear right tire shows a wear rate that is between 14.91% and 15.01% higher than the wear rate for the front right tire. Because the diameter of the front tires is smaller than the rear tires, the lugs on the front tires come into contact with the soil more often than the lugs on the rear tires. One might expect this would cause the front tires to wear faster than the rear tires. However, because the tractor pulls the implements (additional load) at the rear, the rear tires have to work harder to maintain grip (traction) during field operations, thus increasing wear.

In the case of 4WD-assisted tractor configurations, it is important to note that the distribution of weight (static and dynamic) between the two axles and the need to accommodate wider steering angles are the key reasons why the front tires are smaller than the rear tires (smaller tires can pivot more than larger ones without hitting the side of the tractor frame). However, according to Bouma (n.d.), the need for sufficient traction to pull the required loads is one of the reasons why a tractor's rear tires are made larger than their front tires. A close look at the wear rate data shows that, for the rear tires, the rear right tire experienced a 5.14% higher wear rate than the rear left tire while, for the front tires, the front right tire recorded a 5.46% higher wear rate than the front left tire. This variation could be a result of the right tires being run in the plowed furrows more than the left tires due to the method that the tractor operator used during field operations. During a field operation, especially plowing, it was observed that because the soil in the furrow was loosened, the right tires experienced more slippage than the left tires, which run on firmer ground. It is commonly observed that the slippage of the right tires causes the front wheels to turn left, requiring the operator to force the wheels back onto the right track.

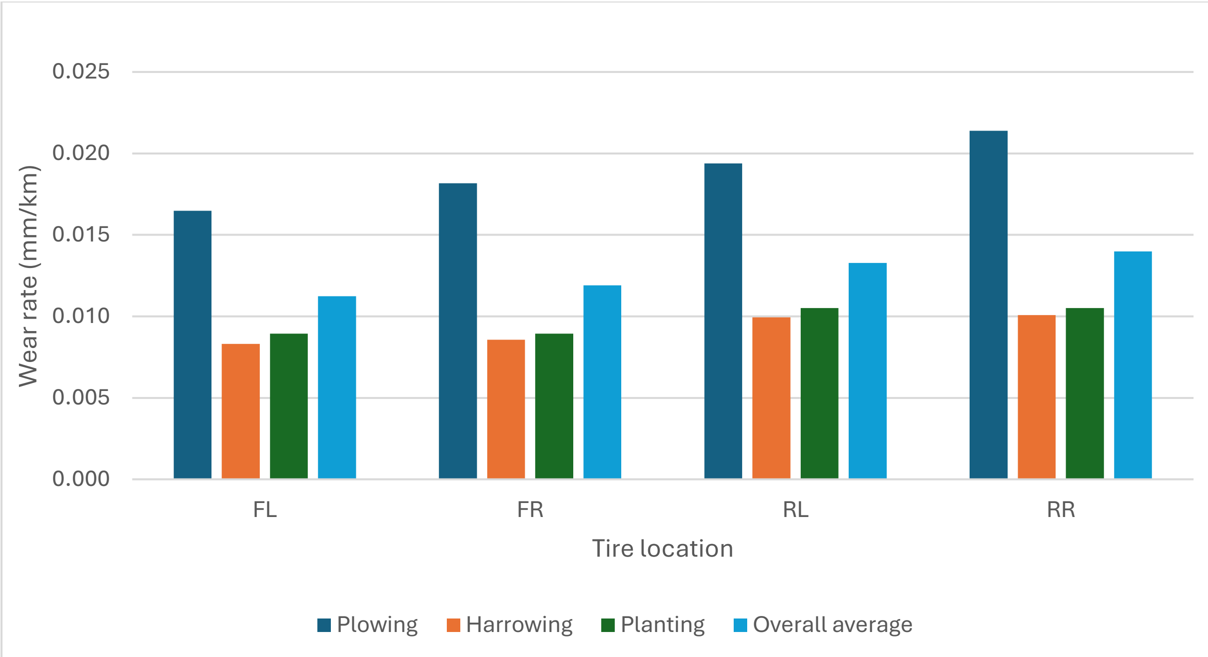

Figure 4.3. Average rate of tire wear on Field 1 by tire location and field operation.
Note. FL = front left; FR =front right; RL = rear left; RR = rear right.

To determine the variation in the tire wear rate on Field 1 for each field operation, the two-way analysis of variance (ANOVA) factor was tested using the wear rate data in Figure 4.3.

The ANOVA test results for Field 1 (Table 4.5) show a significant difference in the average tire wear rate due to the tire's position. In other words, the tire's location on the tractor affects the rate at which the tire wears, which means that all tires experience different wear rates. Also, at a 95% CI, there is a significant difference in the average wear rate of the tires depending on the specific field operation the tractor performs.

Table 4.5. ANOVA results for the variation of means of tire wear rates and field operations on Field 1.

Variation	SS	df	MS	F	P-value	η^2
Tires	1.42×10^{-7}	3	4.74×10^{-8}	7.96	0.02	4.76
Field operations	2.35×10^{-6}	2	1.17×10^{-6}	197.15	3.41×10^{-6}	5.14
Within	3.57×10^{-8}	6	5.95×10^{-9}	—	—	—

Note. ANOVA = analysis of variance; df = degree of freedom; η^2 = effect size; F = F statistic; MS = mean square; SS = sum of squares.

In the study, the draft force of the various implements was used to categorize the field operations. Therefore, the effect of field operations on the tire wear rate means that draft force plays a significant role in tire wear. This finding is supported by the relationship between the draft force of the implements pulled by the tractor and tire wear rate, as shown in Figure 4.8.

4.1.2.2.2 Wear rate on Field 2

Figure 4.4 shows the rate of wear of the tractor lugs on Field 2. The total distances, including the headland turns the tractor covered during plowing, harrowing, and planting on Field 2, were 91.1 km, 71.5 km, and 54.7 km, respectively.

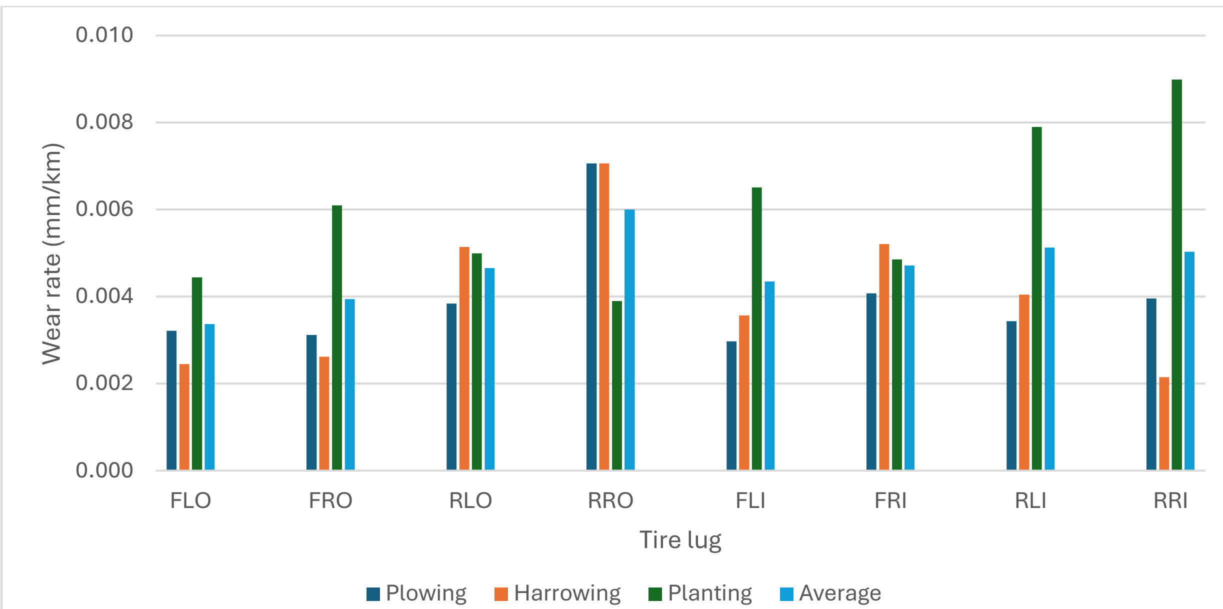

Figure 4.4. Wear rate of tire lugs on Field 2 by lug location and field operation.
Note. FLI = front left inner; FLO = front left outer; FRI = front right inner; FRO = front rear outer; RLI = rear left inner; RLO = rear left outer; RRI = rear right inner; RRO = rear right outer.

The outer lug of the rear right tire shows the highest wear rate, while the outer lug of the front left tire shows the lowest wear rate. On average, the outer lugs of the tires experience a higher wear rate than the inner lugs of the tire. A careful observation of the toe-in alignment of the front and rear wheels of the tractor during field operation in Field 2 gives insight into the possible reason for the tires' inner lugs wearing more than the outer lugs. The vigorous work of the tractor during operations may cause wheel misalignment. Toe-in is a wheel misalignment where the edges of the wheels point inward toward the central axis of the tractor. The wear of the inner lugs more than the outer lugs may also be caused by a negative camber angle of the wheels. In his study of truck tire assessment, Lupker et al. (2002) notes that the tire's outer shoulder wears significantly more than the inner shoulder due to a positive camber angle of 0.6 to 0.7 degrees of front tires.

Figure 4.5 shows the wear rate of each tire as the tractor carried out all three operational practices of Field 2. The rear right tire shows the highest wear rate among all field operations, while the front left tire experiences the lowest wear rate.

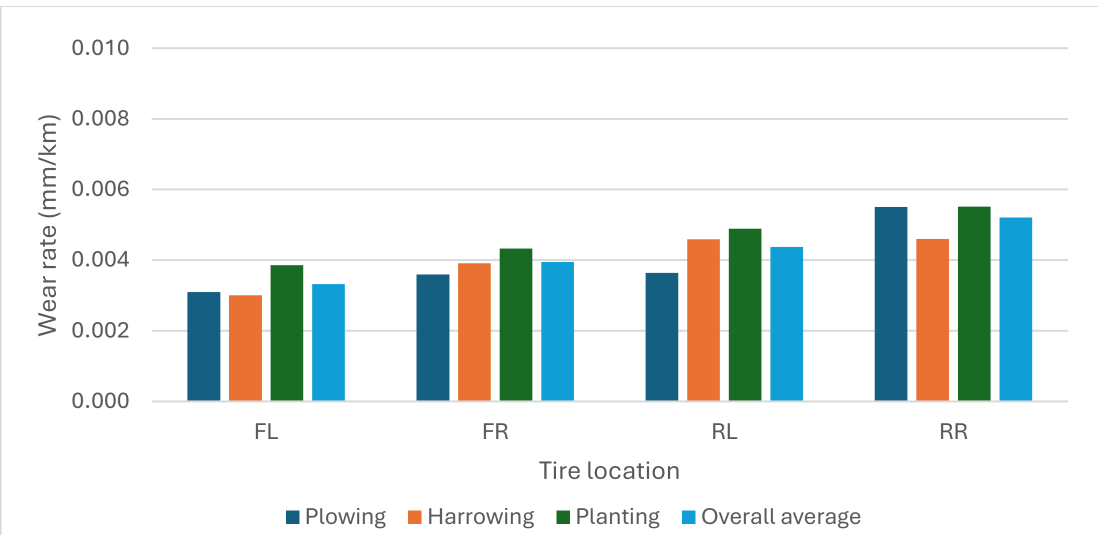

Figure 4.5. Average rate of tire wear on Field 2 by tire location and field operation.
Note. FL = front left; FR = front right; RL = rear left; RR = rear right.

Figure 4.3 shows that plowing generated the highest values of tire wear rate on Field 1, while planting generated the highest wear rate on Field 2 (Figure 4.5).

This may be explained by the presence of small pockets of gravel that were observed on Field 2 during field operations (Figure A3), even though the soil is sandy loam. Since the paths of travel between field operations will naturally differ, it is possible that the path taken during planting caused the tires to have more contact with these small pockets of gravel, thus increasing wear rate, compared with the path taken during plowing. This concurs with the findings of this study, which show the wear rate increases as the percentage of coarse particles in the soil increases (Figure 4.13).

A two-way ANOVA test was run using the data from Figure 4.5 to analyze the variation of the mean wear rate between the positions of the tires and the field operations, as shown in Table 4.6.

Table 4.6. ANOVA results of the variation of means of tire wear rates and field operations on Field 2.

Variation	SS	df	MS	F	P-value	η^2
Tires	5.66×10^{8}	3	1.89×10^{-8}	11.77	0.01	4.76
Field operations	1.16×10^{8}	2	5.78×10^{-9}	3.60	0.09	5.14
Within	9.63×10^{9}	6	1.60×10^{-9}	—	—	—

Note. ANOVA = analysis of variance; df = degree of freedom; η^2 = effect size; F = F statistic; MS = mean square; SS = sum of squares.

The effect of the specific field operation on the wear rate of the tires on Field 2 is significant ($p < 0.1$); the wear rate for harrowing is 1.7% higher than for plowing, and the wear rate for planting is 13.3% higher than for harrowing. During harrowing, the tractor runs on furrowed soil that is looser than the firm soil experienced during plowing. Therefore, the wheels of the tractor will not have much grip on the soil, causing an increase in wheel slippage. Tire wear increases as wheel slip increases, a fact supported by the results shown in Figure 4.9. Again, harrowing further loosens the soil; therefore, during planting, the tractor runs on soil that is more loose, which may increase slippage. In addition, the weight of the seeds and the fertilizer adds more load, increasing the ground pressure of the contact area of the soil and the tractor wheel. Macmillan (2002) argues that the rolling resistance of wheels on soft soil depends directly on (but is not necessarily proportional to) the weight on the wheels and is also proportional to the ground pressure. Thus, the wear rate increases as the wheels' rolling resistance (force) increases, as shown in Figure 4.8.

From Table 4.6, the positions of the tires of the tractor influence the wear rate of the tires significantly on Field 2. The table also shows a significant difference between the mean wear of the tires' positions, since the p-value is less than 0.1 ($p < 0.006$). The wear rate of the right tires (rear right and front right) is higher than that of their corresponding left tires (rear left and front left). The mean wear rate for the rear right tire is 16.12% higher than that of the rear left tire, and the mean wear rate for the front right tire is 18.67% higher than that of the front left tire. This observation is similar to the wear rate of the tires observed on Field 1 (Figure 4.3), except that the wear rates in Field 2 are higher than in Field 1. During field operations on Field 2, it was observed that even though the soil is sandy loam, there is some gravel in some pockets of the field (Figure A3), and the tractor had to work through this gravel. This could influence the wear of the tires in Field 2.

4.1.2.2.3 Wear rate on Field 3

The wear rate for each lug of the tire on Field 3 is shown in Figure 4.6. The tractor traveled 196.6, 78.0, and 58.5 km for plowing, harrowing, and planting, respectively. During planting, the outer lugs of the rear right tires show the highest wear rate, and the outer lugs of the front left tire show the lowest wear rate. Similar to the rate of lug wear on Field 2, the outer shoulder wears more than the inner shoulder of the tires on Field 3. It was observed that the tractor had the same toe-in misalignment on Field 3 as on Field 2.

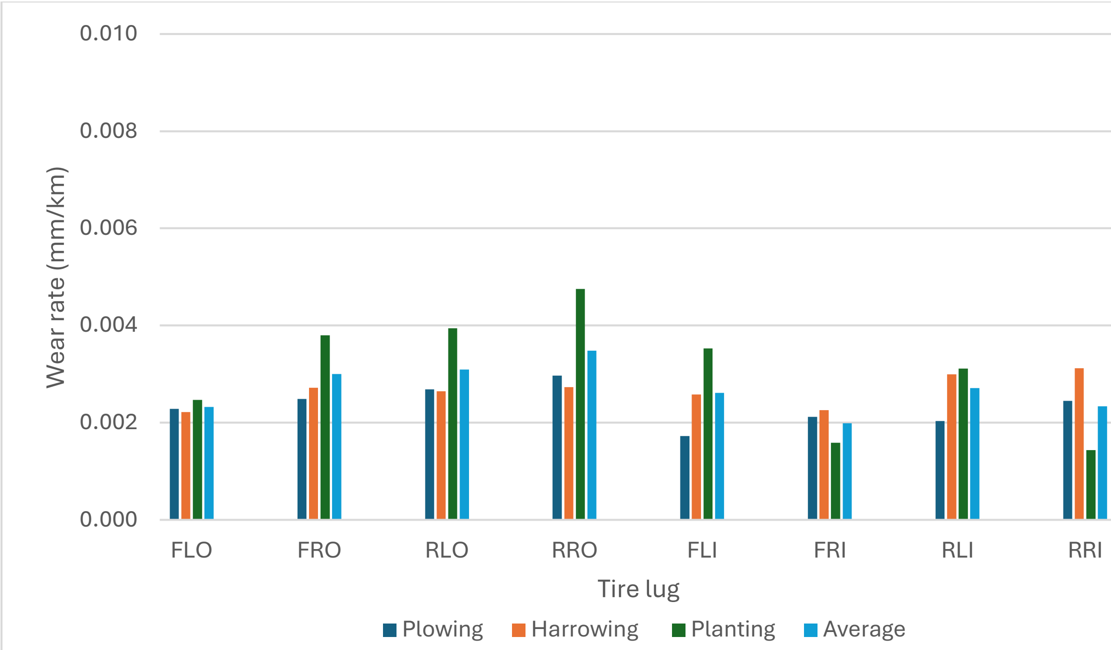

Figure 4.6. Wear rate of tire lugs on Field 3 by lug location and field operation.
Note. FLI = front left inner; FLO = front left outer; FRI = front right inner; FRO = front rear outer; RLI = rear left inner; RLO = rear left outer; RRI = rear right inner; RRO = rear right outer.

Figure 4.7 shows the wear rate of each tire on Field 3, with the highest wear rates occurring during planting. It was observed that all the tires showed almost the same wear rate on Field 3. The average wear rate of the front right tire was only 0.8% higher than that of the front left tire, and the wear of the rear right tire was only 0.34% higher than the rear left tire. The tractor experiences the lowest slippage on Field 3 compared with the other fields (Table B1), and high slippage usually occurs on the tires on the right side of the tractor on all three fields. Therefore, less slippage of the tractor will cause less wear on the tires on the right side of the tractor; hence, there will not be much difference in wear between the tires on either side of the tractor.

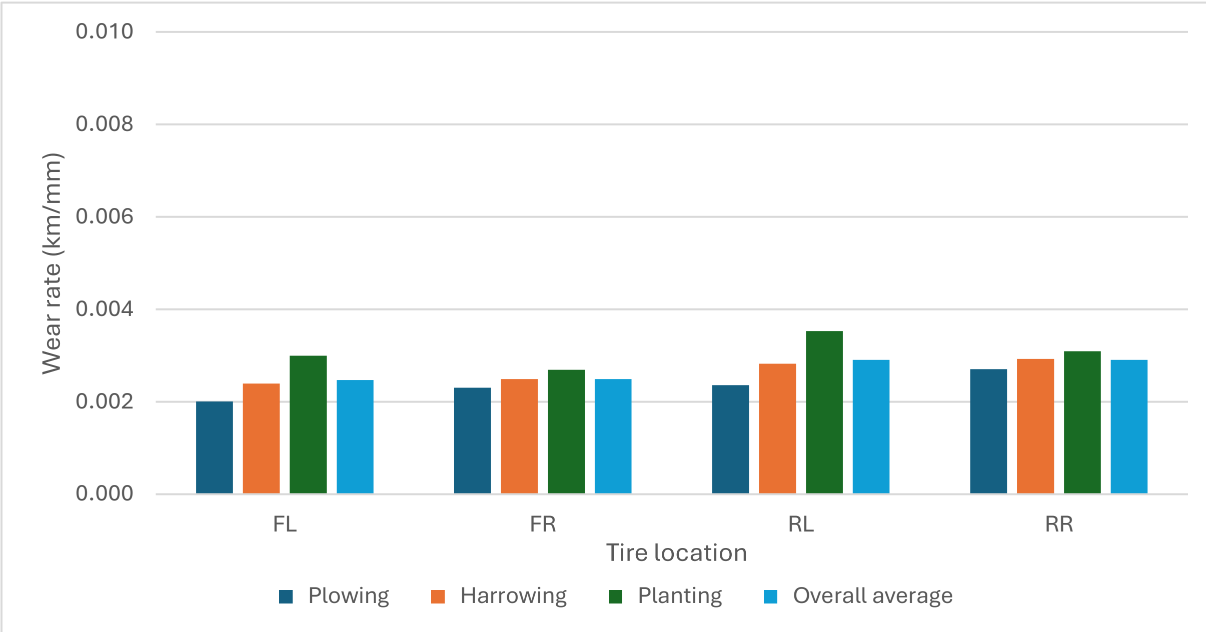

Figure 4.7. Average rate of tire wear on Field 3 by tire location and field operation.
Note. FL = front left; FR =front right; RL = rear left; RR = rear right.

Table 4.7 shows the ANOVA test for the wear rates of the tires and the field operations on Field 3. The table shows that at a 95% CI, there is a significant difference between the wear rates of the tires (i.e., the tire's position affects the amount of wear it experiences). Therefore, the tires do not wear uniformly under the tractor but experience different levels of wear. Also, at a 95% CI, there is a significant difference in wear rates for the different field operations.

Table 4.7. ANOVA result for the variation of means of tire wear rates and field operations on Field 3.

Variation	SS	df	MS	F	P-value	$η^2$
Tires	5.45×10^{-9}	3	1.82×10^{-9}	4.21	0.06	4.75
Field operations	1.09×10^{-8}	2	5.43×10^{-9}	12.59	0.01	5.14
Within	2.59×10^{-9}	6	4.31×10^{-10}	—	—	—

Note. ANOVA = analysis of variance; df = degree of freedom; $η^2$ = effect size; F = F statistic; MS = mean square; SS = sum of squares.

The results from the field tests clearly show that the wear rates of the tires on the right side of the tractor are higher than those of their corresponding tires on the left side of the tractor. This could be attributed to the operational method used by the operator during the operation. The operator adopted the one-way method of plowing because a one-way disc plow was used. With this method (unidirectional plowing), the tires on the right side of the tractor always run in the furrows (soft soil), and the tires on the left side of the tractor run on unplowed (firm) soil for every field pass. Moreover, to ensure uniform harrowing, the operator usually ran the right tires of the tractor on the already harrowed furrow as a guide. This again makes the right tires run on a softer soil than the left ones. It was observed that because the right tires always run on soft soil, they experienced excessive slip, forcing the tractor's front wheel to move to the left and causing the operator to forcibly turn the steering wheel to the right. The results confirm why the right tires wear faster than the left tires of the tractor, which might also be the cause of the asymmetrical wear of the lugs. Therefore, it can be claimed that the method of plowing significantly influences the rate of tire wear.

The results in figures 4.5, 4.6, and 4.7 show that the tire wear rate on Field 1 is higher than on Field 2, and higher on Field 2 than on Field 3. This may be attributed to the fact that the percentage of sand in Field 1 (62%) is more than that of Field 2 (52%), and the percentage of sand in Field 2 is higher than in Field 3 (44%). The higher the percentage of sand, the higher the wear rate of the tire.

4.1.2.2.4 Effects of individual variables on wear rate

Figure 4.8 shows the tire's lug wear rate in comparison to the tractor's draft force for all three fields of operation. The results generally reveal that the draft force does not appear to affect the tire wear rate when the draft force is 7.5 to 12 kN; this is followed by an increase in wear rate when the draft force is between 12 and 13 kN, and then by a rapid decrease in wear rate when the draft force is more than 13 kN. Draft force is the resistance that the tractor experiences when pulling the implements through the soil. In addition to the soil type, speed and depth of operation, implement type, and soil conditions are key factors that influence the draft force. Assuming all of these factors are held constant, except for the implement type and conditions as variables then, as the draft of the implement increases, the tractor will require more power to pull the implement. Again, as the weight on the wheels increases, the wheels sink deeper into the soft soil, thereby increasing the ground pressure, which in turn leads to a higher rolling resistance of the wheels. Macmillan (2002) argues that as the coefficient of rolling resistance of the tractor wheels on soft soil increases, the ground pressure also increases; however, this is contrary to the length of the contact area. Therefore, significant traction is required to pull the implement, resulting in a high rate of wear, especially on soft soil, as shown in Figure 4.8.

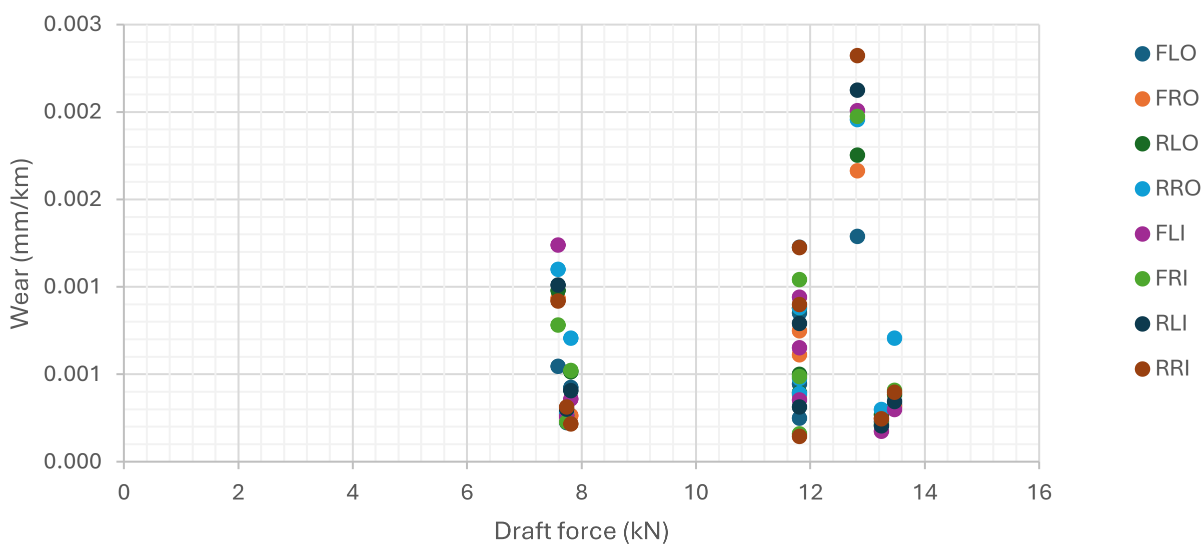

FLI = front left inner; FLO = front left outer; FRI = front right inner; FRO = front rear outer; RLI = rear left inner; RLO = rear left outer; RRI = rear right inner; RRO = rear right outer.

Figure 4.8. Wear rate of tire lug versus draft force.

The wear rate of the tire lug in comparison to the tractor's wheel slip for all three fields is demonstrated in Figure 4.9. Close observation of the results reveals that, on average, the wear rate of the tire lugs increases with increasing slip in the range of 5% to 14% and then decreases rapidly as the wheel slip continues to increase. The wheel slip is the amount of soil the tractor wheel deforms horizontally. At 0% wheel slip, there is no soil deformation and power consumption, whereas, at 100% slip, zero forward thrust occurs, and all of the tractor power is consumed in soil deformation and displacement. Walters (2024) suggests that to maximize traction, wheel slip must range between 8% to 15%, depending on the type of tractor and soil condition.

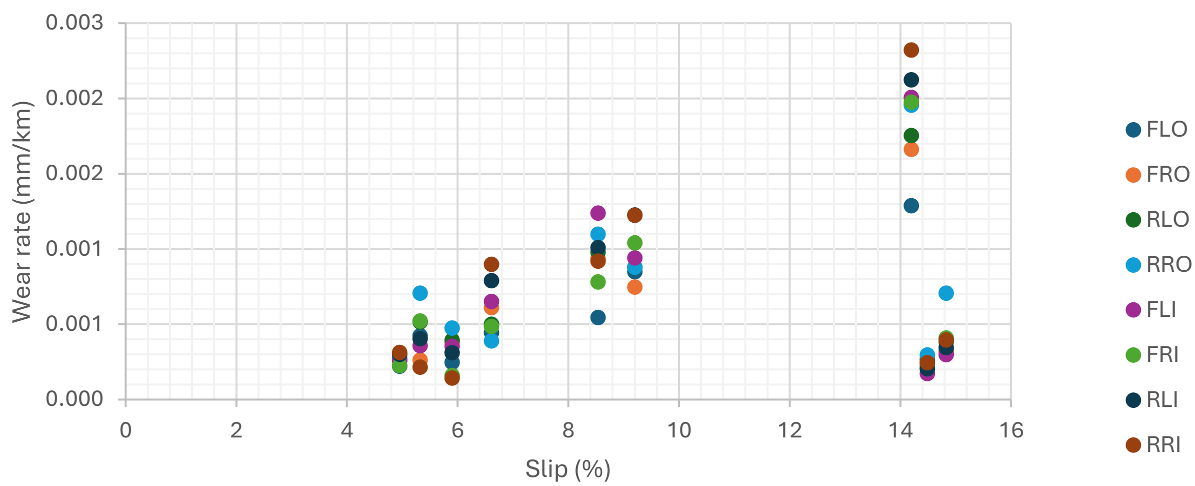

FLI = front left inner; FLO = front left outer; FRI = front right inner; FRO = front rear outer; RLI = rear left inner; RLO = rear left outer; RRI = rear right inner; RRO = rear right outer.

Figure 4.9. Wear rate of tire lug versus tractor wheel slip.

From Figure 4.9, most of the implements experienced slippage within the suggested slip range percentage. However, the slippage for harrowing and planting on fields 2 and 3 falls below the slip range. This may be attributed to the bulk density of the soil during operation (Table 4.2).

Figure 4.10 compares the tire lug's wear rate and the tractor's operating speed on fields 1, 2, and 3. The wear rate of the lugs is inversely proportional to the speed. The tire wear rate decreases with increasing speed. The results in Figure 4.10 contradict the study of the impact factor of tire wear conducted by Liet al. (2012). Their study reveals that tire wear increases with speed, although it was conducted on a tarred road. Generally, higher speed generates more friction between the tire and the (paved) surface, leading to increased temperatures. This makes the tire rubber softer, causing excessive tire tread wear at higher speeds. However, in agricultural soil-tire interactions, the slow movement of the tire increases contact time with the deformable soil and the tire's ground contact area, which increases soil resistance and friction, thereby accelerating tire wear. Thus, due to the deformable nature of the soil, slippage may occur, leading to a reduction in the tractor's forward movement. As part of this process, wheel slip increases, generating higher temperatures between the tire and the deformable soil, which accelerates tire wear. Consequently, tire wear on agricultural soil increases as tire speed decreases (Figure 4.10), and the slow traffic on the soil increases soil compaction in the vertical and longitudinal direction while expanding the soil in the lateral direction (Shahgholi & Abuali, 2015).

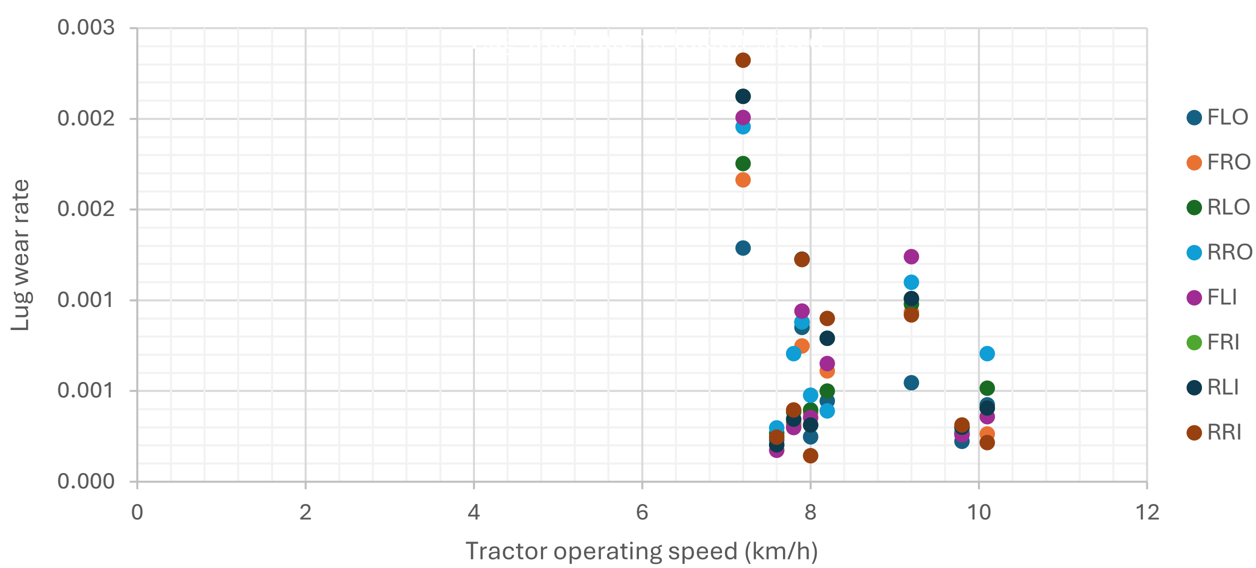

FLI = front left inner; FLO = front left outer; FRI = front right inner; FRO = front rear outer; RLI = rear left inner; RLO = rear left outer; RRI = rear right inner; RRO = rear right outer.

Figure 4.10. Wear rate of tire lug versus tractor operating speed.

Figure 4.11 demonstrates inverse proportionality between lug wear rate and soil bulk density across the three fields (i.e., the wear rate of the lugs decreases as soil bulk density increases). The tractor tire-soil interaction is a soft wheel on a soft surface interaction, where both surfaces deform during interaction. Accordingly, the high bulk density of the soil reduces the amount by which the soil deforms under the wheels. As the soil is compacted at a higher bulk density, it may reduce the amount of soil displaced under the wheels of the tractor. This results in a reduced area of the two contacting surfaces and the contacting time (Shahgholi & Abuali, 2015), thus decreasing both rolling resistance and wheel slippage. As the bulk density of the soil decreases, the normal load of the tractor and the implement causes the wheel to sink into the soil, resulting in motion resistance. The torque on the wheel generates shearing as the tire-soil interacts to develop draft force and slippage; therefore, an increase in soil bulk density reduces tractor tire wear. Studying the effect of tire wear particles (TWPs) on soil-water retention of different soil textures, Verdi and Naseri (2024) conclude that TWPs increase as the bulk density of the soil decreases. Their conclusion agrees with the results of this study on the relationship between the wear rate of the tractor tires and soil bulk density (Figure 4.11).

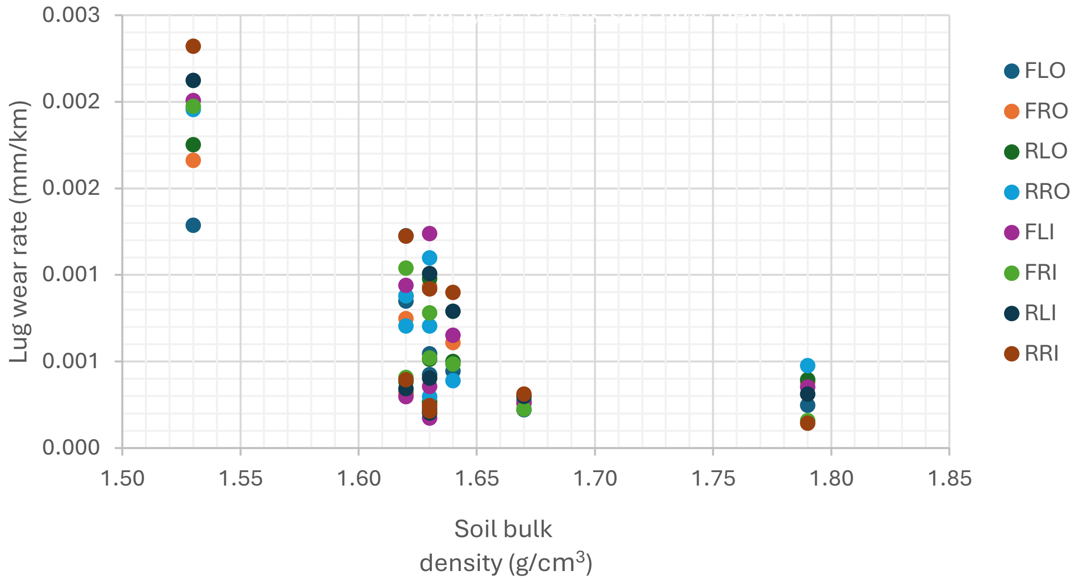

FLI = front left inner; FLO = front left outer; FRI = front right inner; FRO = front rear outer; RLI = rear left inner; RLO = rear left outer; RRI = rear right inner; RRO = rear right outer.

Figure 4.11. Wear rate of tire lug versus bulk density of the soil.

Figure 4.12 illustrates the lug wear rate versus soil moisture for the fields under study. The result reveals that the tire lug wear rate is proportional to the soil moisture. Agricultural soil (a combination of sand, silt, and clay) derives its strength from internal friction and cohesion. Therefore, the soil moisture content may influence the strength of the soil. For the tractor to experience effective traction, the soil moisture must fall within a recommended range as suggested by Amer et al. (2021), P. Cardei et al. (2020), and Mari et al. (2011). Al Nuaimi and Al Rijabo (2020) note that as soil moisture increases, the draft force needed to pull the implement increases. They argue that increasing moisture content increases the adhesion of the soil, which increases clods and soil resistance to the movement of the implement in the soil. Therefore, a high draft force is needed to pull the tillage tool through the soil as the moisture of the soil increases. The results of the relationship between the draft force and the wear rate of the tractor tire in this study (Figure 4.34) reveal that as the draft force increases, the wear rate of the tractor tires increases. Also, increasing soil moisture may increase tire slippage, as indicated by

Al Nuaimi and Al Rijabo (2020). Hence, the soil moisture may influence the wear rate of the tire, as shown in the results of this study.

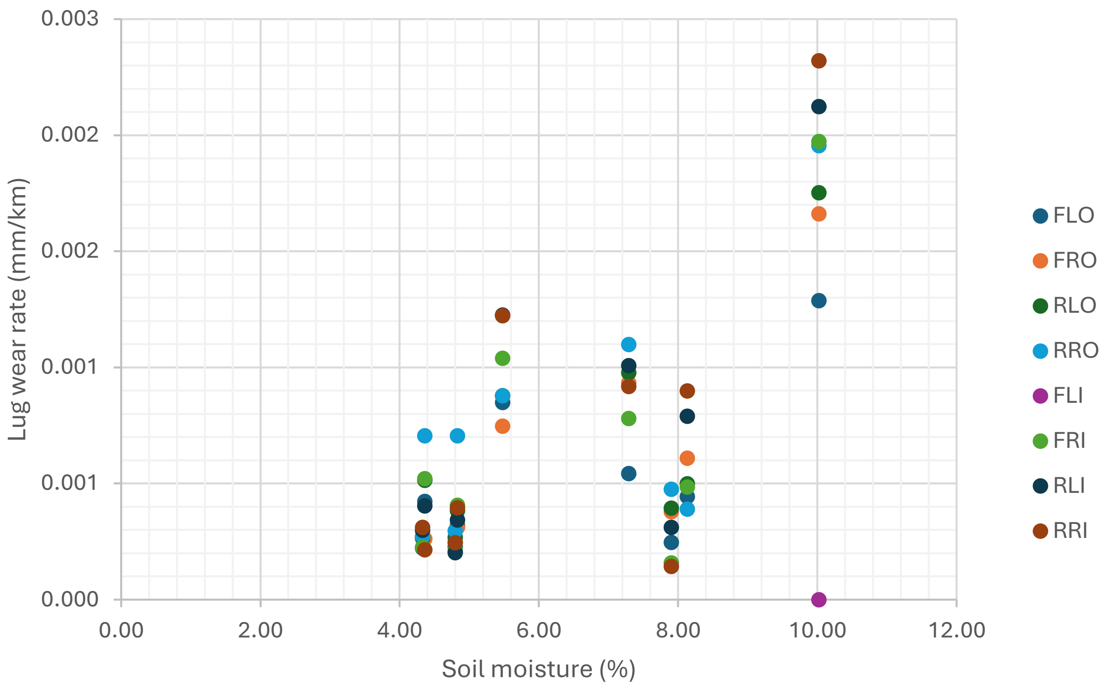

FLI = front left inner; FLO = front left outer; FRI = front right inner; FRO = front rear outer; RLI = rear left inner; RLO = rear left outer; RRI = rear right inner; RRO = rear right outer.

Figure 4.12. Wear rate of tire lug versus moisture of the soil.

Figure 4.13 shows the rate of tire lug wear versus soil texture. A tractor lug operating on sandy loamy soil exhibits a higher wear rate compared to loamy soil. The results reveal that the wear rate of the lugs of the tires reduces as the percentage of sand in the field reduces and the percentage of silt increases. Field 1 has a higher ratio of sand and contains a high percentage of coarse particles. This causes high wear on the tire lug. The high percentage of sand in Field 1 makes the soil looser than in Field 3. This increases wheel slippage and reduces traction. Excessive wheel spinning on coarse particles generates friction, accelerating the wear of the tire trea

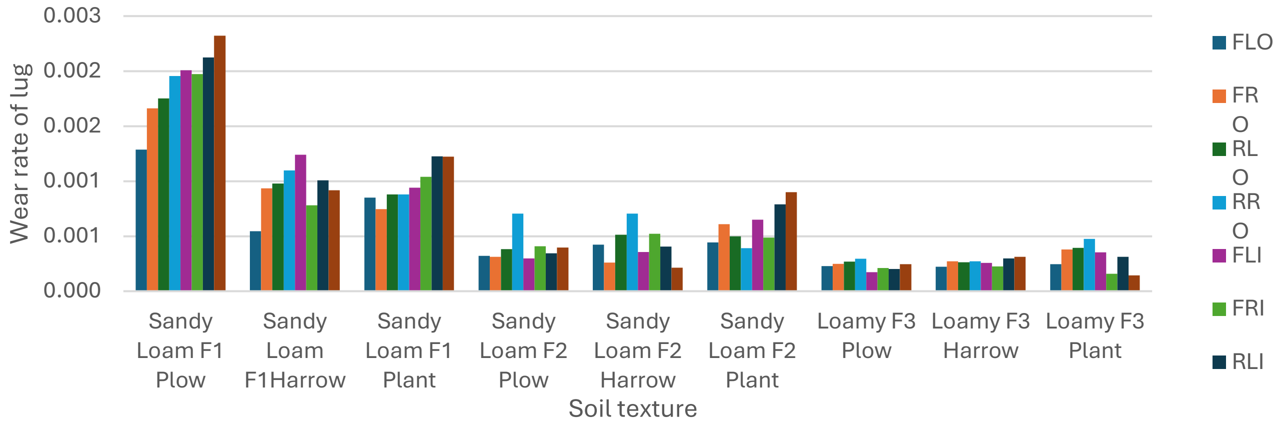

Figure 4.13. Wear rate of tire lug versus type of soil and soil texture.

4.1.3 Data from the 2024 farming season

4.1.3.1 Draft force, slip, and speed

Figure 4.14 shows the draft force, slip, and operational speed of the tractor during the 2024 farming season.

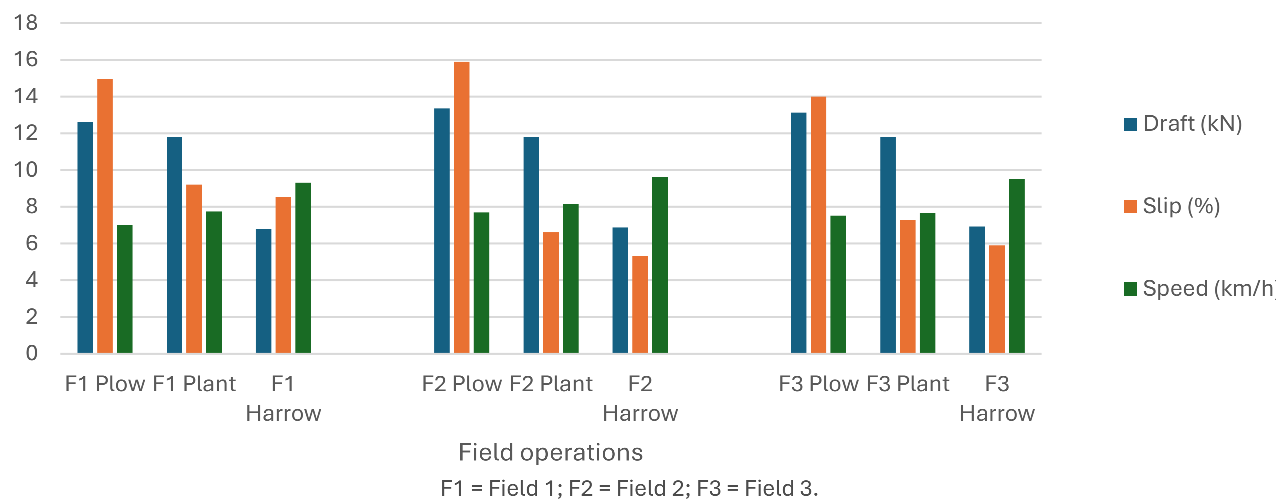

Figure 4.14. Draft force, slip, and tractor speed by field operation on each field.

Note. Data on draft, slip, and speed for the 2024 farming season.

The tractor experienced a reduction in draft force for plowing of 10.3%, 0.89%, and 0.83% on fields 1, 2, and 3, respectively, compared to the 2023 farming season. Additionally, the draft force for harrowing during the 2024 growing season on fields 1, 2, and 3 is reduced by

10.03%, 11.9%, and 12.8%, respectively, compared to the 2023 season. It was observed that during the 2024 farming season, the tractor operated at a reduced speed for all field operations (Table B1) compared to the 2023 season. Speed is a key variable in determining the draft force of the tractor, as noted in the ASABE (2020) standard and the Hendrick (1988) model for draft force. Therefore, the variation in the tractor's speed strongly influences the draft of the tractor, as shown in Figure 4.14. The results also reveal that on most occasions during the 2024 operations, the tractor experienced a higher percentage of slips compared with 2023. This might cause the reduction of the speed of the tractor, as shown by the results in Figure 4.14.

4.1.3.2 Wear rate

This section presents the results of the wear rate of the tire lugs for all three fields.

4.1.3.2.1 Wear rate for Field 1

Figure 4.15 exhibits the results of the wear rate for each tire lug during the field operations on Field 1. Including the headland turns, the tractor travels 75.0, 59.0, and 46 km for plowing, harrowing, and planting, respectively. All of the tire lugs experienced a higher wear rate during plowing than during the other field operations, with the inner lug of the rear right tire showing the highest wear rate. The tractor experienced a higher draft for the primary tillage to turn the soil effectively. The higher draft force needed for the primary tillage accounts for the higher wear rate that the tire lugs experienced during plowing.

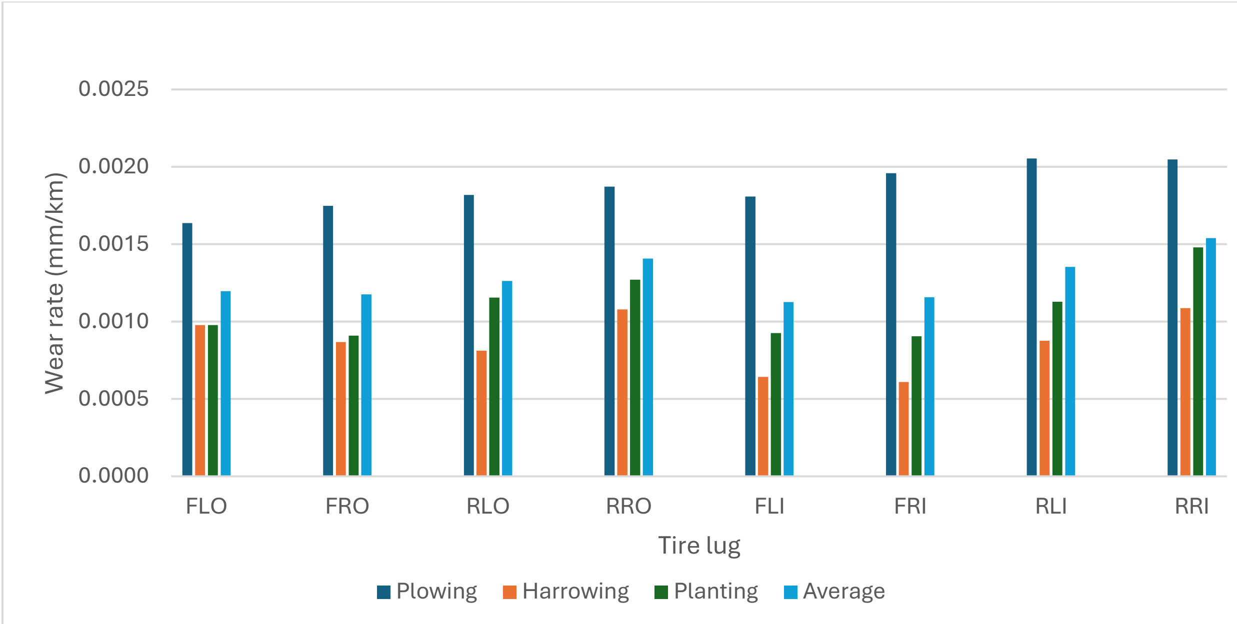

Figure 4.15. Rate of tire lug wear on Field 1.

Note. FLI = front left inner; FLO = front left outer; FRI = front right inner; FRO = front rear outer; RLI = rear left inner; RLO = rear left outer; RRI = rear right inner; RRO = rear right outer.

Figure 4.16 shows the wear rate of the tractor tires on Field 1. The wear rate of the right tires of the tractor is higher than that of the left tires. This pattern is similar to the one observed during 2023 field operations. The wear rates of the front right and rear left tires during the 2023 farming season (Figure 4.3) are 2.0% and 1.6%, respectively, higher than the corresponding tire wear rates during the 2024 season (Figure 4.16), and the wear rates of the front left and rear right for the 2024 season are 3.3% and 5.2%, respectively, higher than the corresponding tire wear rates during the 2023 season. On average (Figure 4.16), the wear rate of the front right tire is 0.4% higher than the front left tire of the tractor, and the rear right tire is 12.7% higher than the rear left tire. The reason for this variation is discussed in section 4.1.3.2. However, one may conclude there is no significant difference in the wear rate between the front left and front right tires, or between the rear left and rear right tires.

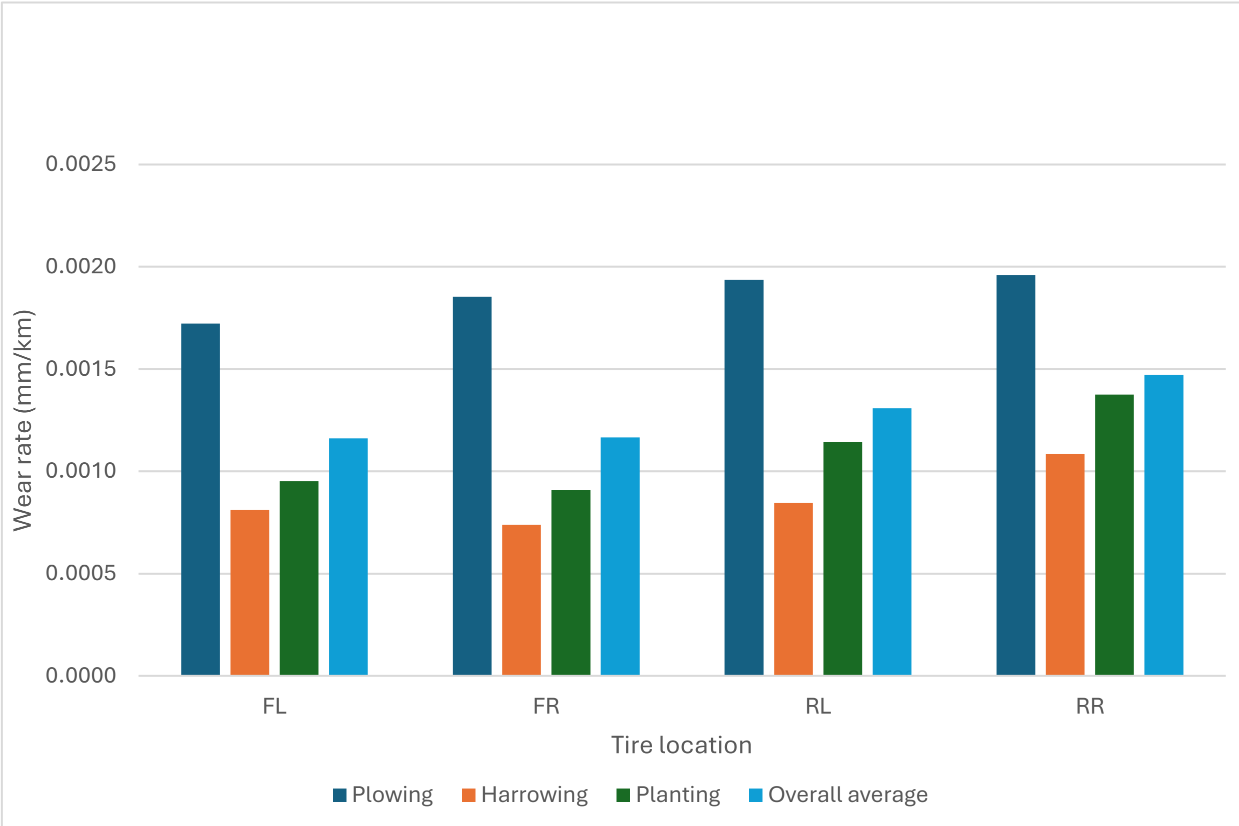

Figure 4.16. Average rate of tire wear by field operation on Field 1.
Note. FL = front left; FR = front right; RL = rear left; RR = rear right.

4.1.3.2.2 Wear rate for Field 2

Figure 4.17 shows the wear rate of the lugs of the tractor on Field 2. The tractor traveled a total distance of 91.0 km for plowing, 71.5 km for harrowing, and 54.6 km for planting. The outer lug of the rear left tire experienced the highest wear rate. The highest wear rate was experienced during plowing; however, all of the lugs exhibit almost the same average wear rate.

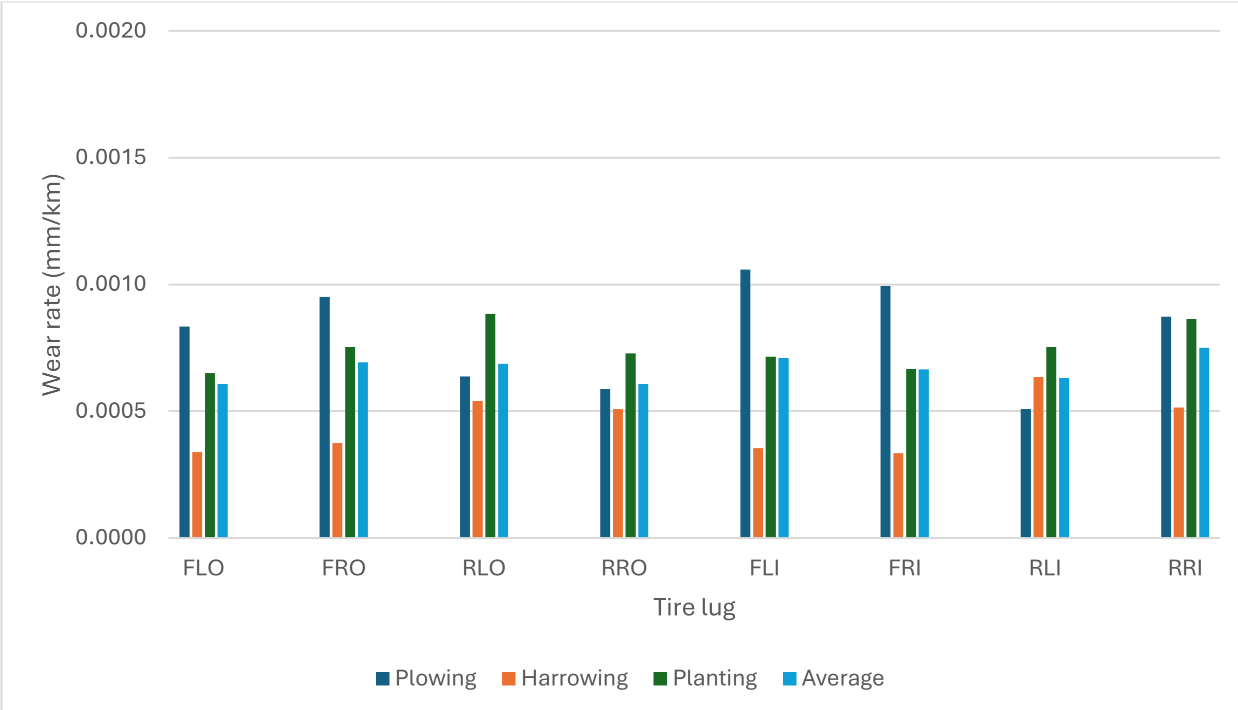

Figure 4.17. Wear rate of tire lugs by location and field operation on Field 2.
Note. FLI = front left inner; FLO = front left outer; FRI = front right inner; FRO = front rear outer; RLI = rear left inner; RLO = rear left outer; RRI = rear right inner; RRO = rear right outer.

The rate at which the tires wear on Field 2 is shown in Figure 4.18. On average, the tires on the right side of the tractor wear faster than those on the left side of the tractor. The wear rate of the front right tire is 3.1% higher than the front left tire, and the wear rate of the rear right tire is 3.0% higher than the rear left tire.

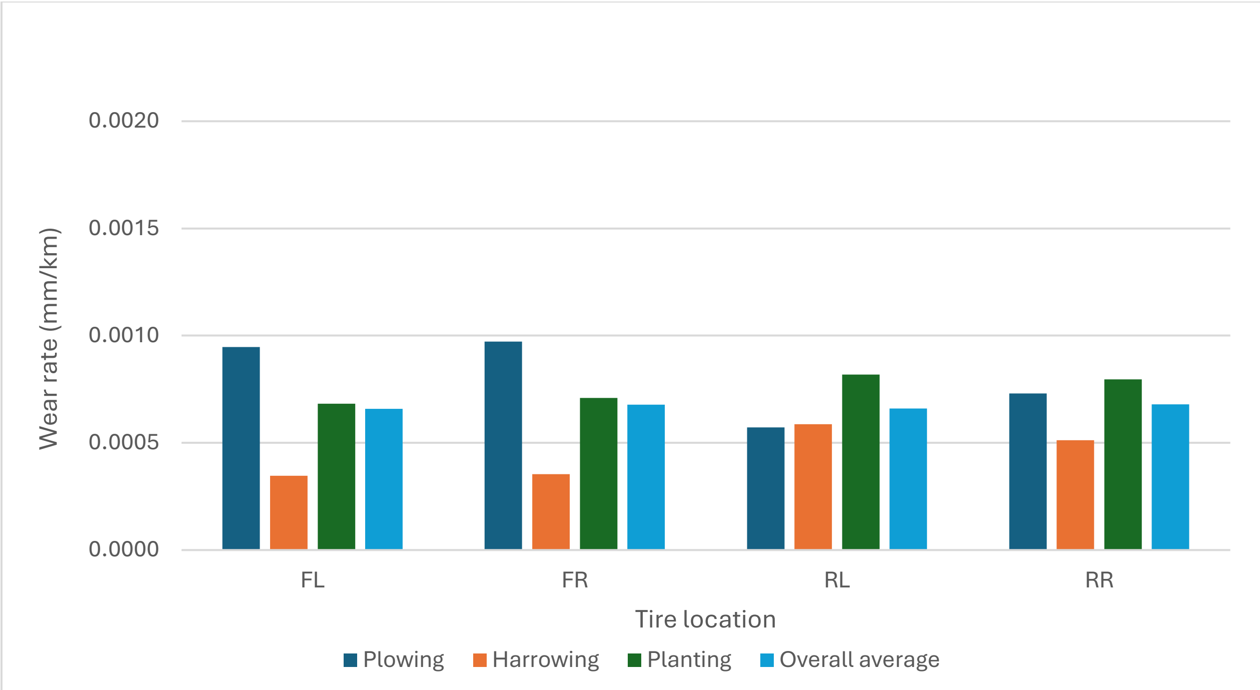

Figure 4.18. Average tire wear rate on Field 2 by tire location and type of field operation. *Note*. FL = front left; FR = front right; RL = rear left; RR = rear right.

4.1.3.2.3 Wear rate for Field 3

Figure 4.19 shows the wear rate of the tire lugs on Field 3. The outer and inner lugs of the rear right tire show a high wear rate during plowing compared with the other lugs. Compared with fields 1 and 2, the outer and the inner lugs of the rear right tire experienced a high wear rate on Field 3 during plowing.

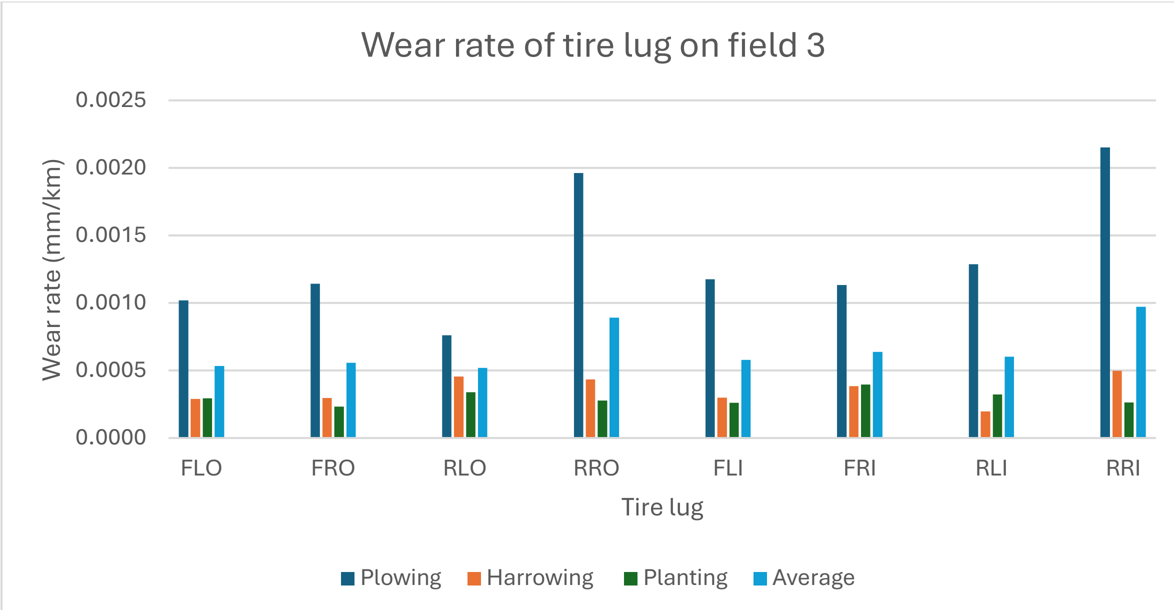

Figure 4.19. Wear rate of tire lugs on Field 3 by lug location and field operation.
Note. FLI = front left inner; FLO = front left outer; FRI = front right inner; FRO = front rear outer; RLI = rear left inner; RLO = rear left outer; RRI = rear right inner; RRO = rear right outer

Figure 4.20 shows the wear rate of the tires on Field 3. The rear right tire shows a very high wear rate during plowing. On average, the rear left tire experiences the lowest wear rate.

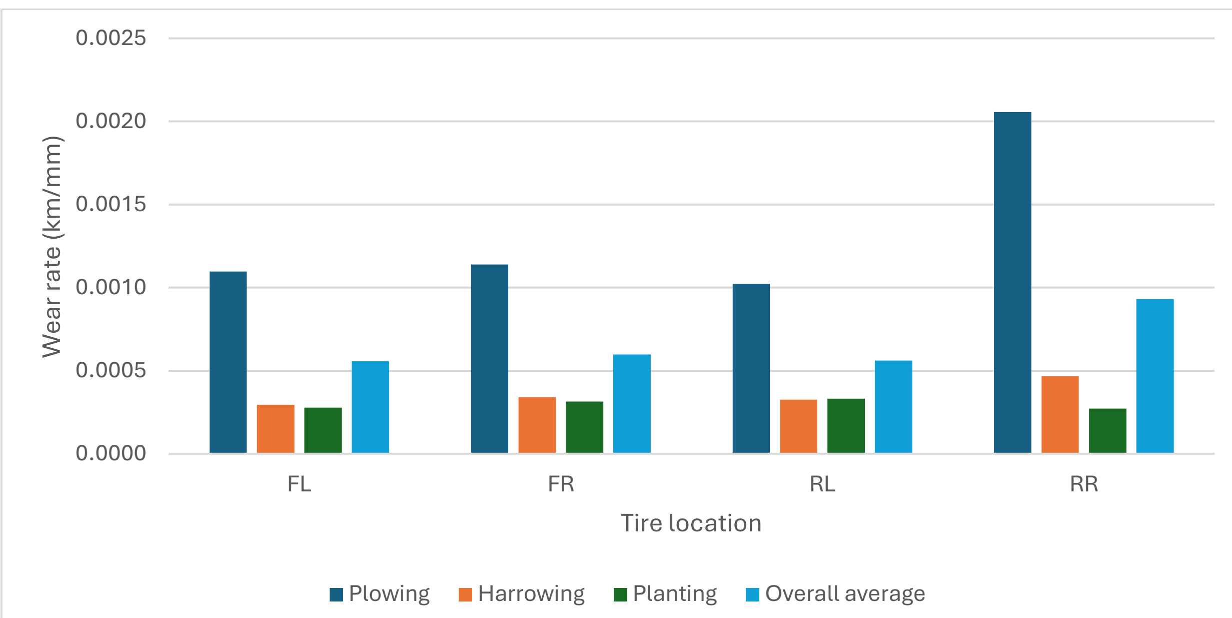

Figure 4.20. Average wear rate of tires on Field 3 by tire location and field operation.
Note. FL = front left; FR = front right; RL = rear left; RR = rear right.

4.1.3.2.4 Effect of independent variables on wear rate

The relationship between the wear rate of the tire lugs and the draft force of the tractor for all the fields of operation is shown in Figure 4.21. The tire lug wear rate increases marginally with increasing draft in the range 7 to 12 kN; this is followed by an increase between 12 to 13 kN and then a rapid decrease beyond 13 kN. This observation is similar to the 2023 farming season.

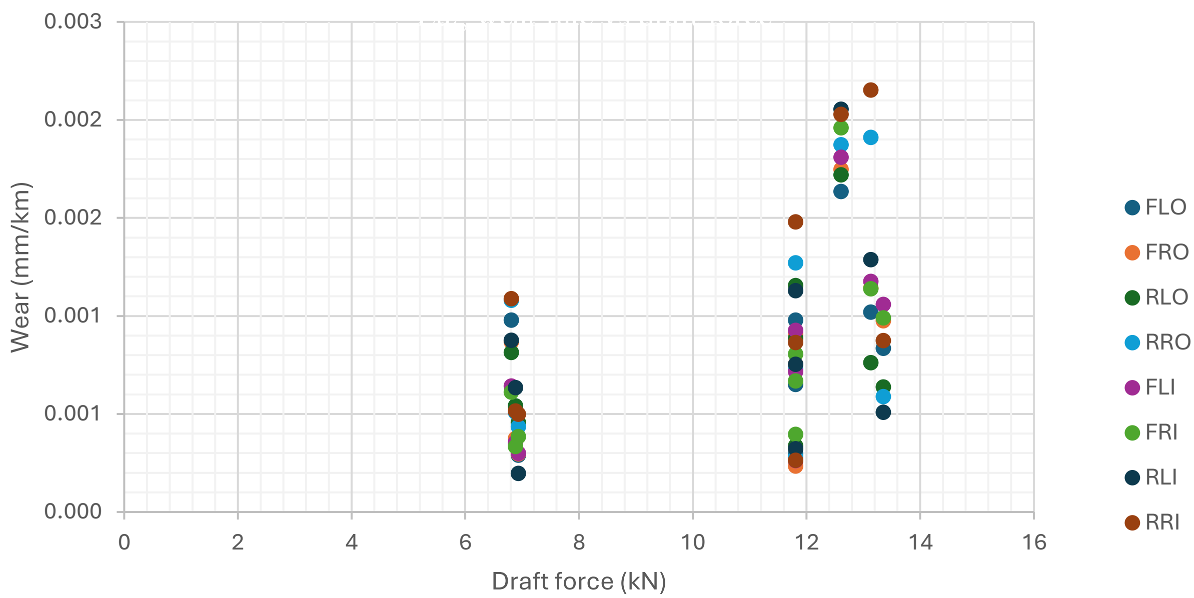

FLI = front left inner; FLO = front left outer; FRI = front right inner; FRO = front rear outer; RLI = rear left inner; RLO = rear left outer; RRI = rear right inner; RRO = rear right outer.

Figure 4.21. Rate of lug wear versus draft force.

Figure 4.22 shows the rate of wear of the tire lugs in comparison to the tractor's wheel slip. The wear rate of the tire lugs increases with increasing slip in the range of 5% to 15% and then decreases. These results confirm the observation of the relationship between the tractor wheel slip and the wear rate of the tire lugs for the 2023 farming season.

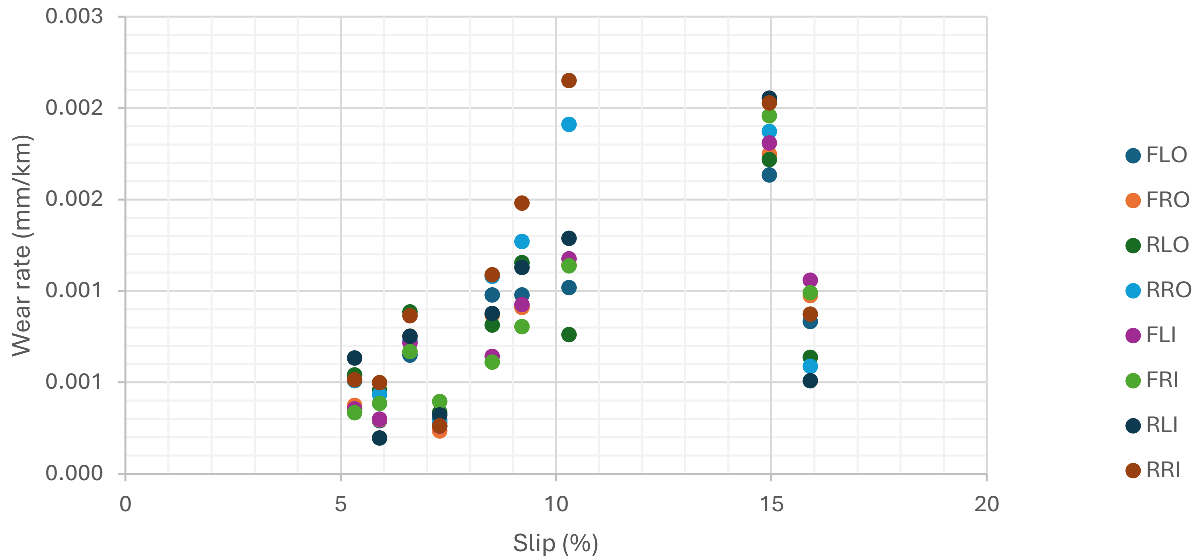

FLI = front left inner; FLO = front left outer; FRI = front right inner; FRO = front rear outer; RLI = rear left inner; RLO = rear left outer; RRI = rear right inner; RRO = rear right outer.

Figure 4.22. Rate of lug wear versus tractor wheel slip

Figure 4.23 demonstrates the comparison between the wear rate of the tire lug and the speed of the tractor. The results reveal that the wear rate of the tire lugs decrease with increasing speed. This observation is similar to the 2023 farming season. However, there was a reduction in tractor speed for all field operations except for harrowing on Field 2.

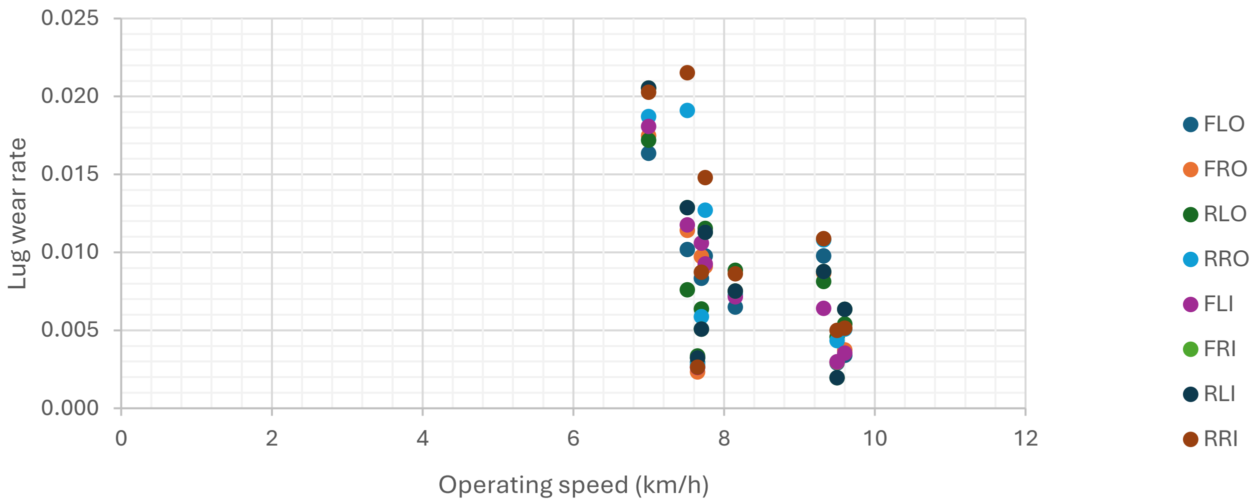

Figure 4.23. Rate of lug wear versus tractor operating speed.

Figure 4.24 compares the wear rate of each tire lug and the soil bulk density. The tire lugs wear rate decreases with increasing bulk density in the 1.55 to 1.65 g/cm^2; this is followed by 1.70 g/cm^2 and then by a rapid decrease. Generally, soil bulk density is inversely proportional to the wear rate of the tire lug. The soil bulk density for plowing and planting in the 2024 farming season is 1.2% and 2.3%, respectively, higher than in the 2023 farming season. The relationship between the soil bulk density and the wear rate of the tire lug is the same for both farming seasons.

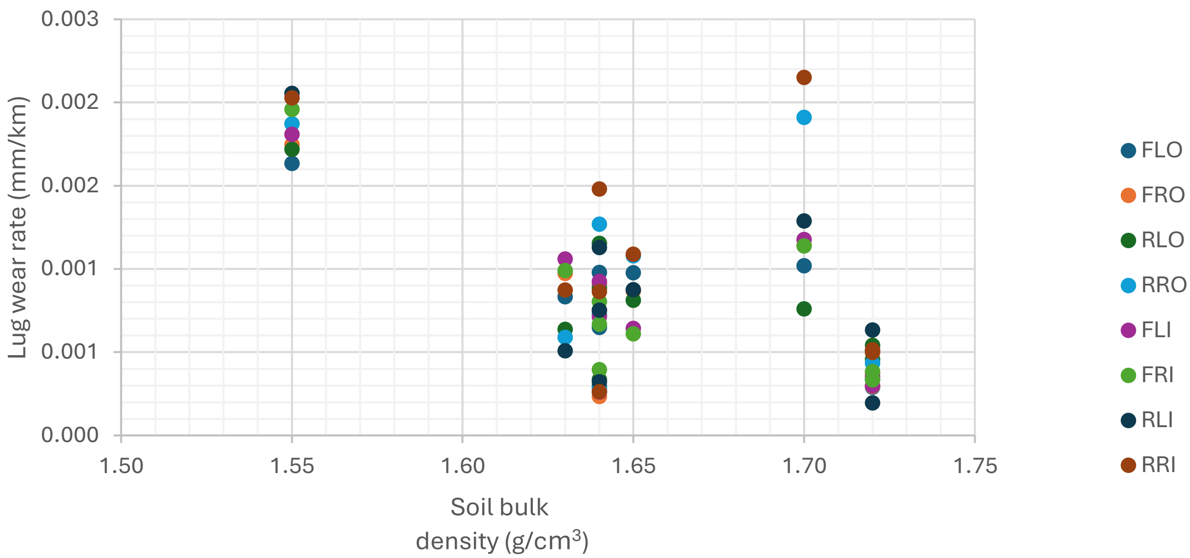

FLI = front left inner; FLO = front left outer; FRI = front right inner; FRO = front rear outer; RLI = rear left inner; RLO = rear left outer; RRI = rear right inner; RRO = rear right outer.

Figure 4.24. Rate of lug wear versus the soil bulk density.

Figure 4.25 shows the relationship between the wear rate of the tire lugs and the soil moisture content for all three fields. It is generally observed that the wear rate of the lugs increases with increasing soil moisture. This is similar to the 2023 farming season.

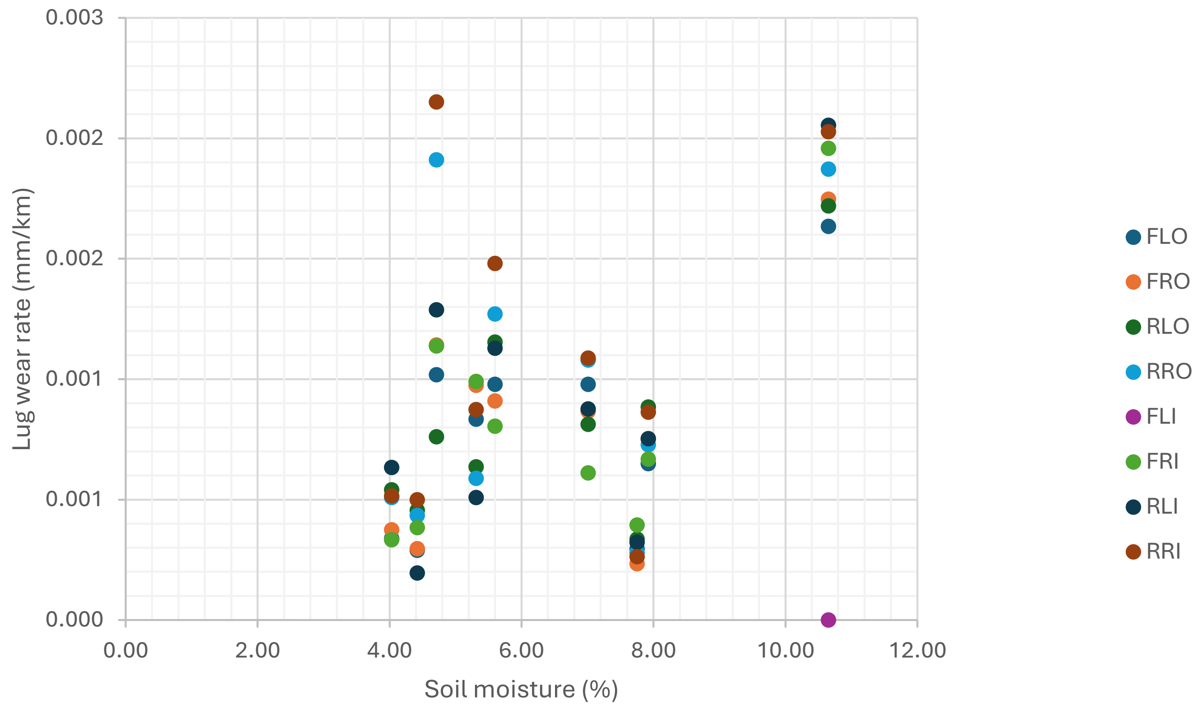

FLI = front left inner; FLO = front left outer; FRI = front right inner; FRO = front rear outer; RLI = rear left inner; RLO = rear left outer; RRI = rear right inner; RRO = rear right outer.

Figure 4.25. Tire lug wear rate versus soil moisture.

Figure 4.26 compares the wear rate of the tire lug with the texture of the soil. It is observed that the wear rate of the tire lugs decreases as the percentage of sand in the soil increases. However, the wear rate of the lug during the plowing in Field 3 shows an unusual increase, which did not occur during the 2023 farming season. This may be attributed to the tire lugs coming into contact with a foreign material in the soil, which caused excessive wear to the lugs.

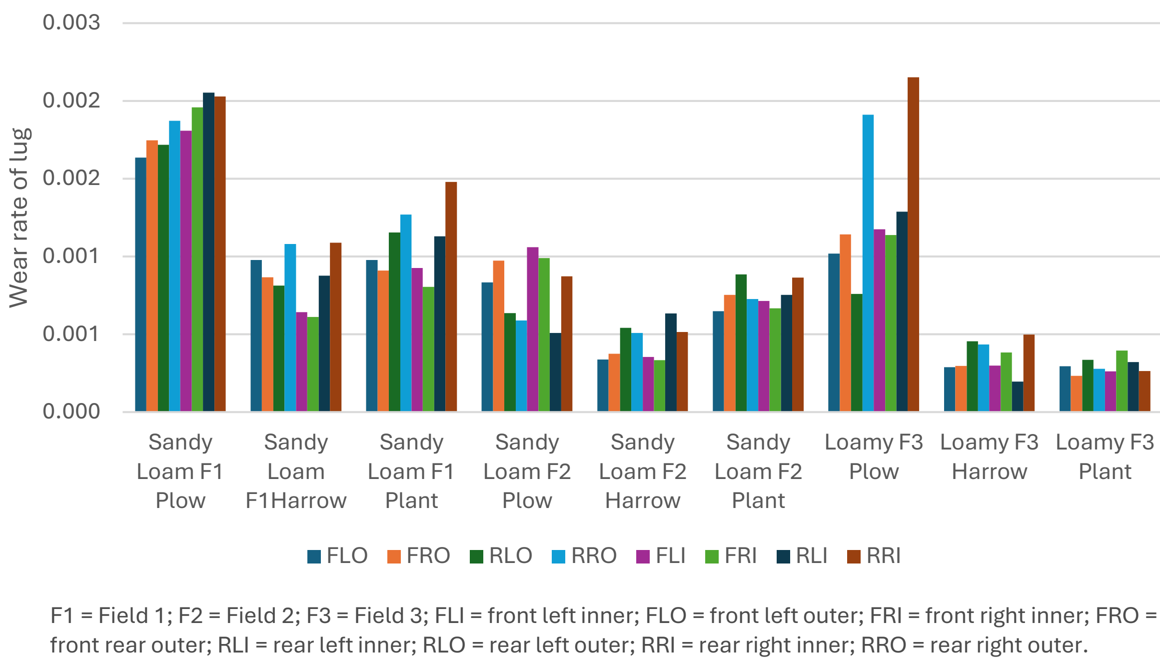

Figure 4.26. Rate of tire lug wear by soil type, field, and field operation.

4.2 Development of Prediction Models

The prediction models for all four tractor tires were developed using data collected during the 2023 farming season. The models were developed for all the tires because each tire operates under different conditions. For all three field operations, the rear tires travel over rolling surfaces that have been affected by the front tires, while the front tires operate on untraveled surfaces. There is an additional lateral difference for the plowing operation as the right tires travel at the bottom of the last furrow from the previous field pass while it is not the case for the left tires.

4.2.1 Model for front left tire

Table 4.8 presents the results of the overall multiple regression, which identifies the independent variables that are significant and insignificant in determining the tire wear rate for the front left tire under study. The regression is statistically significant (R^2 = 0.76, F (5,65) =

17.50). The p-value for draft force ($p = 0.01$), wheel slip ($p = 0.11$), tractor speed ($p = 0.01$), and the bulk density of the soil ($p < 0.01$) are less than or approximately equal to the alpha value of 0.10. However, the moisture of the soil is not significant to the wear rate of the tire, since the p-value ($p = 0.53$) is greater than 0.1.

Table 4.8. Coefficients and significant levels of the individual variables for the front left tire

Model	Estimate	Standard error	95% confidence interval		P-value	t stat
			Lower limit	Lower limit		
Constant	2.00×10^{-2}	4.45×10^{-3}	0.11	2.90×10^{-2}	< 0.01	4.39
Draft force	-2.19×10^{-4}	8.12×10^{-5}	-3.82×10^{-4}	-5.70×10^{-5}	0.01	-2.70
Wheel slip	-4.63×10^{-5}	2.87×10^{-5}	-1.04×10^{-4}	1.10×10^{-5}	0.11	-1.61
Speed	-6.60×10^{-4}	2.50×10^{-4}	-1.16×10^{-3}	-1.66×10^{-4}	0.01	-2.66
Bulk density	-6.8×10^{-3}	1.45×10^{3}	-9.7×10^{-3}	-3.90×10^{-3}	< 0.01	-4.69
Soil moisture	2.96×10^{-5}	4.66×10^{-5}	-6.35×10^{-5}	1.23×10^{-4}	0.53	0.64

To improve the developed model, a regression test was conducted on each independent variable significant to the tire's wear rate. The results of the test used to determine the model for the predicted wear rate of the front left tire are shown in Table B2. The regression model is given as

$$\mathrm{W}_{r(FL)} = (2.90 \times 10^{-5})\mathrm{D} + (3.50 \times 10^{-5})i + (-1.80 \times 10^{-4})\mathrm{s} + (-6.70 \times 10^{-3})\rho_b + 1.26 \times 10^{-2} \quad (32)$$

Where:

$\mathrm{W}_{r(FL)}$ = the predicted tire wear rate for the front left tire

D = the draft force (kN)

i = the wheel slip of the tractor (%)

s = the tractor's speed (km/h) and

ρ_b = the soil bulk density (g/cm^3).

4.2.2 Model for front right tire

Table 4.9 shows the significance level of the independent variables that are significant in determining the wear rate of the front right tire. The results indicate that the draft force ($p = 0.03$), the speed of the tractor ($p = 0.05$), and soil bulk density ($p < 0.01$) significantly influence the wear rate of the tire. However, the wheel slip of the tractor and the soil moisture are not significant because their p-values are greater than 0.1

Table 4.9. Coefficients and significant levels of the individual variables for the front right tire.

Model	Estimate	Standard error	95% confidence interval		P-value	t stat
			Lower limit	Upper limit		
Constant	1.91×10^{-2}	6.04×10^{-4}	7.07×10^{-3}	3.12×10^{-2}	< 0.01	3.30
Draft force	-2.10×10^{-4}	1.03×10^{-4}	-4.10×10^{-4}	1.09×10^{-6}	0.03	-2.17
Slip	-3.22×10^{-5}	3.64×10^{-5}	-1.05×10^{-4}	4.33×10^{-5}	0.38	-0.88
Speed	-5.90×10^{-4}	3.21×10^{-4}	-1.23×10^{-3}	5.54×10^{-5}	0.05	-1.99
Bulk density	-7.00×10^{-3}	$2.06\ x^{-3}$	$-1.11\ x^{-2}$	-2.88×10^{-3}	< 0.01	-3.20
Soil moisture	5.76×10^{-5}	6.04×10^{-5}	-6.30×10^{-5}	1.78×10^{-4}	0.52	0.64

A regression test was conducted on each of the three independent variables that are significant to the tire's wear rate. The results in Table B3 were used to determine the predicted model of the tire's wear rate. The equation of the regression model for the front right tire is given as

$$\mathrm{W}_{r(FR)} = (2.40\ \mathrm{x}10^{-5})\mathrm{D} + (-2.10\ \mathrm{x}10^{-4})\mathrm{s} + (-8.3 \times 10^{-3})\rho_b + 1.60\ \mathrm{x}10^{-2} \quad (33)$$

Where

$\mathrm{W}_{r(FR)}$= the predicted tire wear rate for the front right tire (mm/km)

D = the draft force (kN)

s = the tractor's speed (km/h)

ρ_b = the soil bulk density (g/cm^3)

4.2.3 Model for rear left tire

The p-values of the independent variables that are significant and insignificant in determining the wear rate of the rear left tire are shown in Table 4.10. This reveals that the effects of draft force ($p = 0.01$), wheel slip ($p = 0.11$), tractor speed ($p = 0.01$), and soil bulk density ($p < 0.01$) significantly influence the wear rate of the rear left tire.

Table 4.10. Coefficients and significant levels of the individual variables for the rear left tire.

Model	Estimate	Standard error	95% confidence interval		P-value	t stat
			Lower limit	Upper limit		
Constant	2.3×10^{-2}	5.33×10^{-3}	1.27×10^{-2}	3.41×10^{-2}	< 0.01	4.39
Draft force	2.58×10^{-4}	9.56×10^{-5}	-4.49×10^{-4}	-6.71×10^{-5}	0.01	-2.70
Wheel slip	-5.43×10^{-5}	3.37×10^{-5}	1.22×10^{-4}	1.31×10^{-5}	0.11	-1.61
Speed	7.80×10^{-4}	2.94×10^{-4}	$-1.37 \times ^{-3}$	-1.94×10^{-4}	0.01	-2.69
Bulk density	-8.00 × 10-3	1.70×10^{-3}	-1.14×10^{-2}	-4.59×10^{-3}	< 0.01	-4.68
Soil moisture	3.51×10^{-5}	5.49×10^{-5}	-7.45×10^{-5}	1.44×10^{-4}	0.53	0.64

The model was developed using the regression analysis on each of the independent variables that significantly influence the tire wear, as shown in Table B4. The equation of the model is given as

$$W_{r(RL)} = (3.40\ \text{x}10^{-5})D + (4.10\ \text{x}10^{-5})i + (-2.10\ \text{x}10^{-4})s + (-7.9\ 0\ \text{x}10^{-3})\rho_b\ 1.50\ \text{x}10^{-2} \quad (34)$$

Where

$W_{r(RL)}$= the predicted tire wear rate for the rear left tire (mm/km)

D = the draft force (kN)

i = the wheel slip of the tractor (%)

s = the tractor's speed (km/h) and

ρ_b = the soil bulk density (g/cm^3

4.2.4 Model for rear right tire

Table 4.11 shows the p-values of the independent variables that significantly affect the wear rate of the right tires. The results indicate that three of the independent variables, draft force (p = 0.04), tractor's speed (p = 0.05), and soil bulk density (p < 0.01), significantly influence the wear rate of the rear right tire.

Table 4.11. Coefficients and significant levels of individual variables for the rear right tire.

Model	Estimate	Standard error	95% confidence interval		P-value	t stat
			Lower limit	Upper limit		
Constant	2.45×10^{-2}	7.01×10^{-3}	1.05×10^{-2}	3.85×10^{-2}	< 0.01	3.50
Draft force	-2.49×10^{-4}	1.19×10^{-4}	-4.90×10^{-4}	-1.05×10^{-5}	0.04	-2.09
Slip	-4.65×10^{-5}	4.24×10^{-5}	-1.31×10^{-4}	1.30×10^{-5}	0.277	-1.10
Speed	-7.4×10^{-4}	3.72×10^{-4}	-1.48×10^{-3}	3.69×10^{-5}	0.05	-2.00
Bulk density	-8.99×10^{-3}	2.36×10^{-3}	-1.37×10^{-2}	-4.28×10^{-3}	< 0.01	-3.81
Soil moisture	4.66×10^{-5}	7.09×10^{-5}	-9.52×10^{-5}	1.88×10^{-4}	0.51	0.66

The results of the regression analysis used to determine the predicted model for the tire wear rate are shown in Table B5. The regression model equation to predict the wear rate of the rear right tire is given as

$$W_{r(RR)} = (4.00 \text{ x}10^{-5})D + (-2.50 \text{ x}10^{-4})s + (-9.9 \text{ x}10^{-3})\rho_b + 1.9 \text{ x}10^{-2} \quad (35)$$

Where

$W_{r(RR)}$= the predicted tire wear rate for the rear right tire (mm/km)

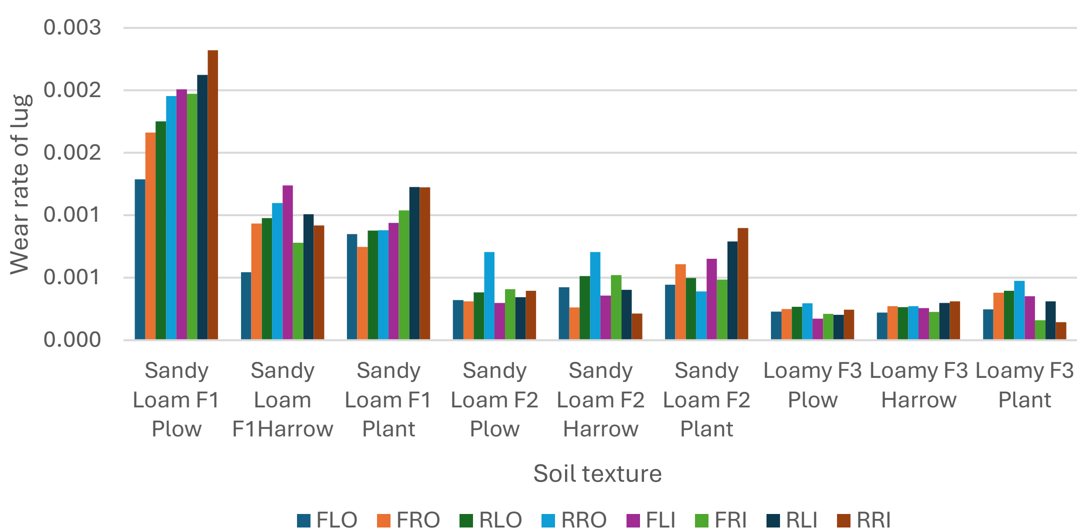

F1 = Field 1; F2 = Field 2; F3 = Field 3; FLI = front left inner; FLO = front left outer; FRI = front right inner; FRO = front rear outer; RLI = rear left inner; RLO = rear left outer; RRI = rear right inner; RRO = rear right outer.

D = the draft force (kN)

i = the wheel slip of the tractor (%) and s = the tractor's speed (km/h).

Table 4.12 provides a summary of the developed models for the four tires. The coefficients of the draft force, speed, and soil bulk density of the front left tire are higher than those of the front right tire by 20.8%, 14.3%, and 19.3%, respectively. However, the constant value of the right tire is 26.9% higher than that of the front left tire; hence, the front right tire has a higher wear rate than the front left tire. Additional discussion on this can be found in section 4.1.2.2.1.

Table 4.12. Summary of the developed models.

Tire	Developed model
Front left	$W_{r(FL)} = (2.90 \text{ x}10^{-5})D + (3.50 \times 10^{-5})i + (-1.80 \text{ x}10^{-4})s + (-6.70 \times 10^{-3})\rho_b + 1.26 \text{ x}10^{-2}$
Front right	$W_{r(FR)} = (2.40 \text{ x}10^{-5})D + (-2.10 \text{ x}10^{-4})s + (-8.3 \times 10^{-3})\rho_b + 1.60 \text{ x}10^{-2}$
Rear left	$W_{r(RL)} = (3.40 \text{ x}10^{-5})D + (4.10 \text{ x}10^{-5})i + (-2.10 \text{ x}10^{-4})s + (-7.9\,0 \text{ x}10^{-3})\rho_b + 1.50 \times 10^{-2}$
Rear right	$W_{r(RR)} = (4.00 \text{ x}10^{-5})D + (-2.50 \text{ x}10^{-4})s + (-9.9 \text{ x}10^{-3})\rho_b + 1.9 \text{ x}10^{-2}$

The coefficients for tractor speed and soil bulk density for the rear left tire are 16.0% and 20.2% higher than the speed and soil bulk density for the rear right tire, respectively. However, the coefficient for the draft force and the constant for the rear right tire are 17.7% and 26.7% higher than for the rear left tire, respectively. Hence, the rear right tire wears faster than the left tire. Additional discussion on can be found in section 4.1.2.2.1.

4.3 Validation of the Models

The data collected during the 2024 farming season (Table 4.13) for the five independent variables was used to validate the developed models. The predicted wear for the rear right, rear left, front right, and front left tires was calculated using equations 32, 33, 34, and 35 respectively.

Table 4.13. Values for independent variables for model validation.

Field	Operation	Draft (kN)	Slip (%)	Speed (km/h)	Bulk density (g/cm^3)	Moisture (%)
1	Plow	12.61	14.95	7.00	1.55	10.65
	Harrow	6.81	8.52	9.32	1.65	7.01
	Plant	11.81	9.21	7.75	1.64	5.60
2	Plow	13.35	15.90	7.70	1.63	5.31
	Harrow	6.88	5.32	9.60	1.72	4.03
	Plant	11.81	6.61	8.15	1.64	7.92
3	Plow	13.13	14.00	7.51	1.65	4.71
	Harrow	6.93	5.90	9.50	1.72	4.42
	Plant	11.81	7.30	7.65	1.64	7.75

4.3.1 Comparison of the predicted versus measured wear values

To validate the developed model, the correlations between the predicted wear rate and the measured wear rate for all four tires were tested. The scatter plot in Figure 4.27 shows a comparison between the predicted and measured wear values for the tractor's front left tire.

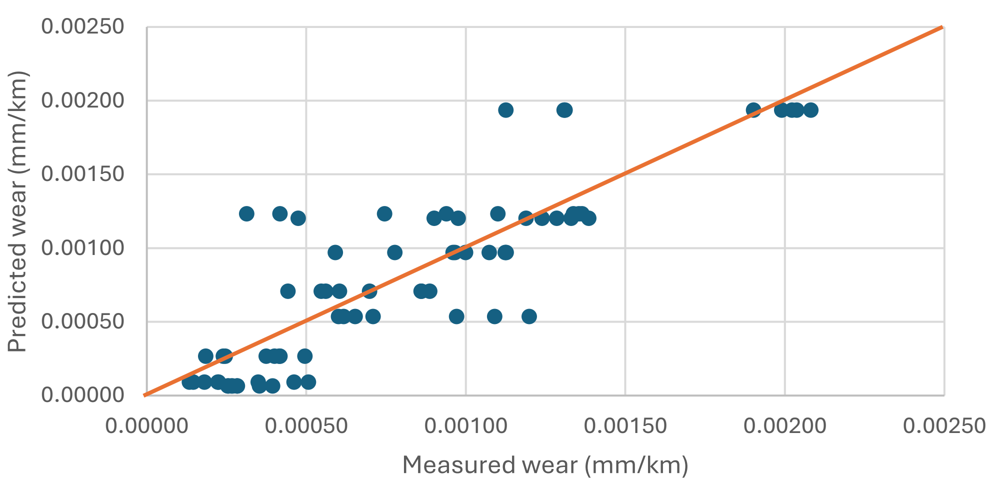

Figure 4.27. Predicted wear versus measured wear of the tractor's front left tire.

The Pearson correlation (r) of the predicted and the measured wear was 0.84 and statistically significant ($p < 0.001$). The model has a determination coefficient (r^2) of 0.73, as shown in Figure A8. Figure 4.27 reveals a good agreement between the measured wear and the predicted wear of the tractor's front left tire.

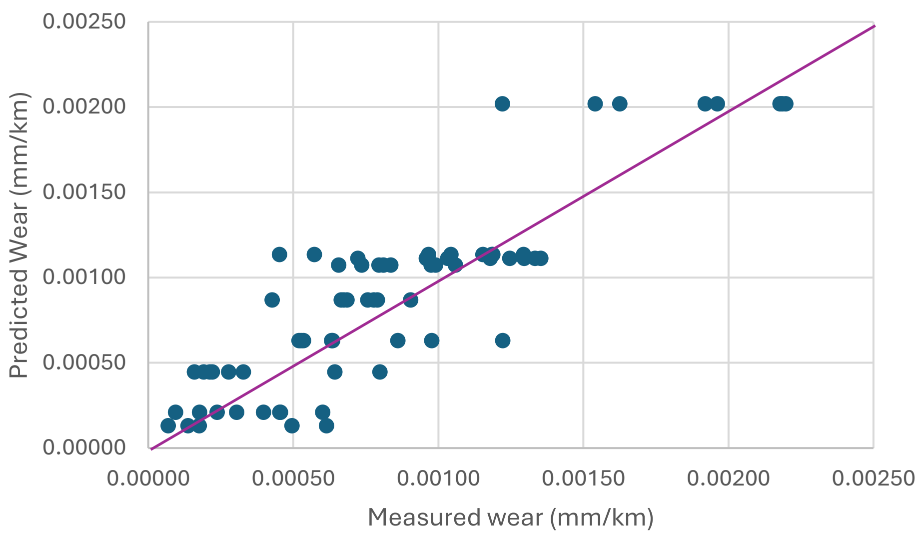

Figure 4.28. Predicted wear versus measured wear of the tractor's front right tire.

The Pearson's correlation analysis reveals a good agreement between the measured wear value and the predicted wear value, with an r value of 0.83 for the front right tire of the tractor. The correlation is statistically significant ($p < 0.001$). Figure 4.28 shows that the coefficient of determination between the predicted wear rate and the measured wear for the front right tire is 0.77.

Figure 4.29 shows the positive linear relationship between the measured wear and the predicted wear of the rear left tire of the tractor under study.

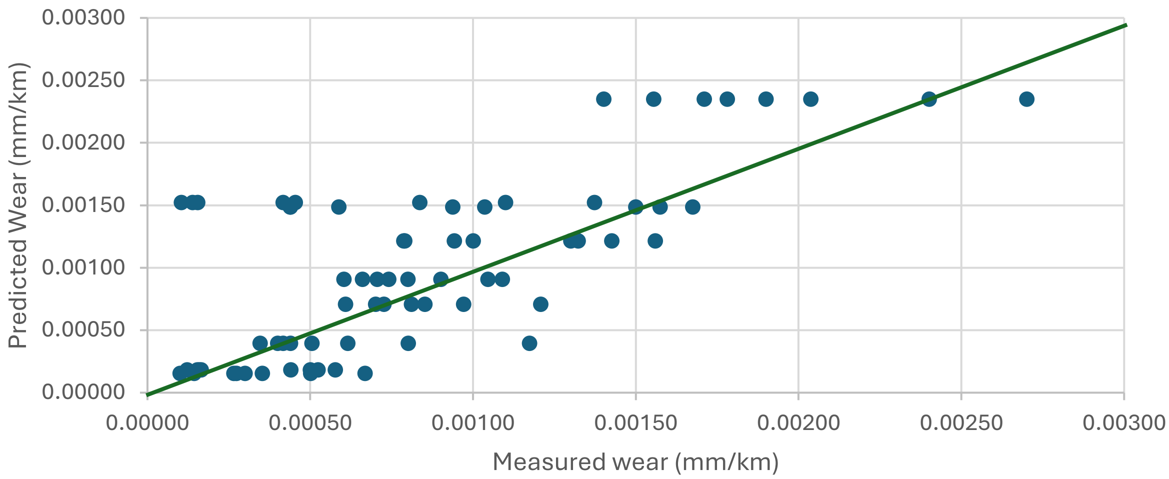

Figure 4.29. Predicted wear versus measured wear of the tractor's rear left tire.

Note. Pearson correlation (r) of 0.71 and determination coefficient (r^2) of 0.51.

Figure 4.29 shows a good relationship between the measured and predicted wear values of the rear left tire with a correlation of 0.71 and a significant level of $p < 0.001$. It has an r^2 value of 0.51.

Figure 4.30 shows a good correlation between the measured wear and predicted wear values of the rear right tire.

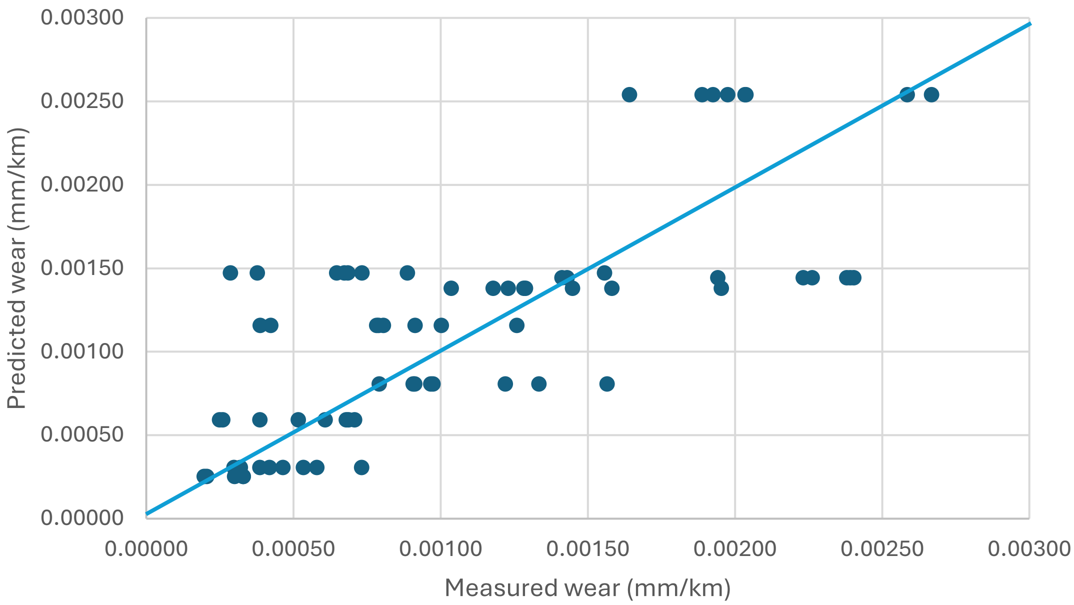

Figure 4.30. Predicted wear versus measured wear of the tractor's rear right tire.

The Pearson correlation of the measured and predicted wear of the rear right tire shows a good correlation of 0.75 and a significant level of $p < 0.001$. The relationship between the predicted and measured wear has an r^2 value of 0.56. The accuracy of correlations was tested by using an error histogram.

4.3.2 The error histogram

Using the developed models, the estimated wear rate was calculated for each data point (P_w) and was compared to the corresponding measured wear rate (M_w). The error (Ɛ) was then calculated as

$$Error\ (\varepsilon) = P_w - M_w \qquad (36)$$

The error histogram was conducted for the four tire models. The models are deemed accurate when the estimated wear rate shows a minimal error and the symmetric distribution of the errors centers around zero.

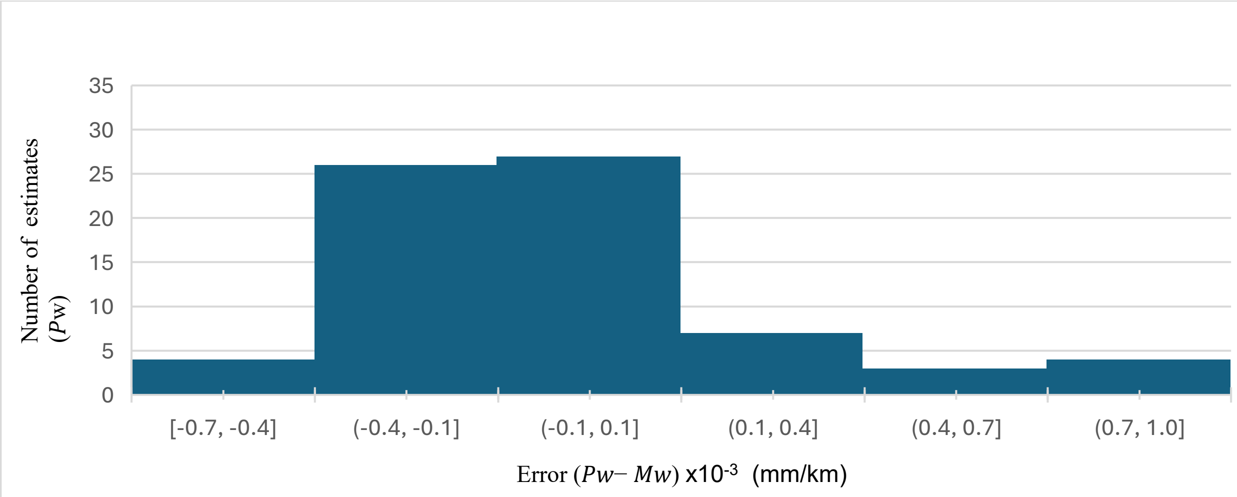

Figure 4.31. Error histogram for front left tire correlation.

Figure 4.31 illustrates a symmetrical distribution of the error for the front left tire model, indicating that the model neither overpredicts nor underpredicts the wear rate. The highest number of estimates is recorded between -0.1 × 10^{-3} and 0.1 × 10^{-3} mm/km error. 66.2% of the estimates fall within the interval of -0.20 × 10^{-3} to 0.20 × 10^{-3} mm/km error bar for the front left tire.

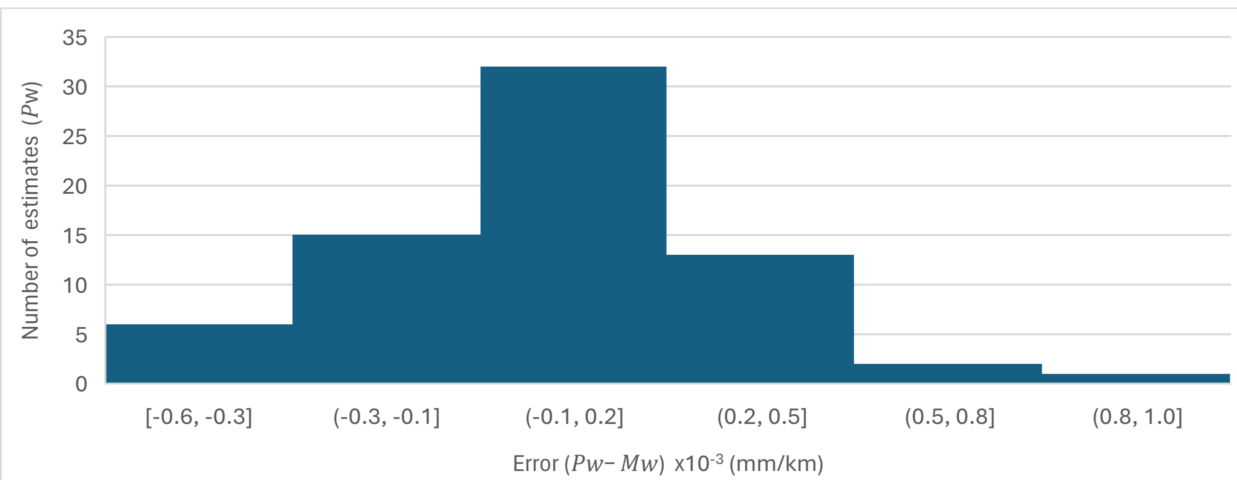

Figure 4.32. Error histogram for front right tire correlation.

The error histogram for the front right tire (Figure 4.32) shows a symmetrical distribution of the error, with the highest number of estimates recorded between -0.1 × 10^{-3} and 2.0 × 10-

^{3} mm/km. The model shows no overprediction or underprediction of the wear rate. The analysis shows that 58.6% of the number estimates of the front right tire are within the range of -0.20 $\times 10^{-3}$ to 0.20×10^{-3} mm/km of the error.

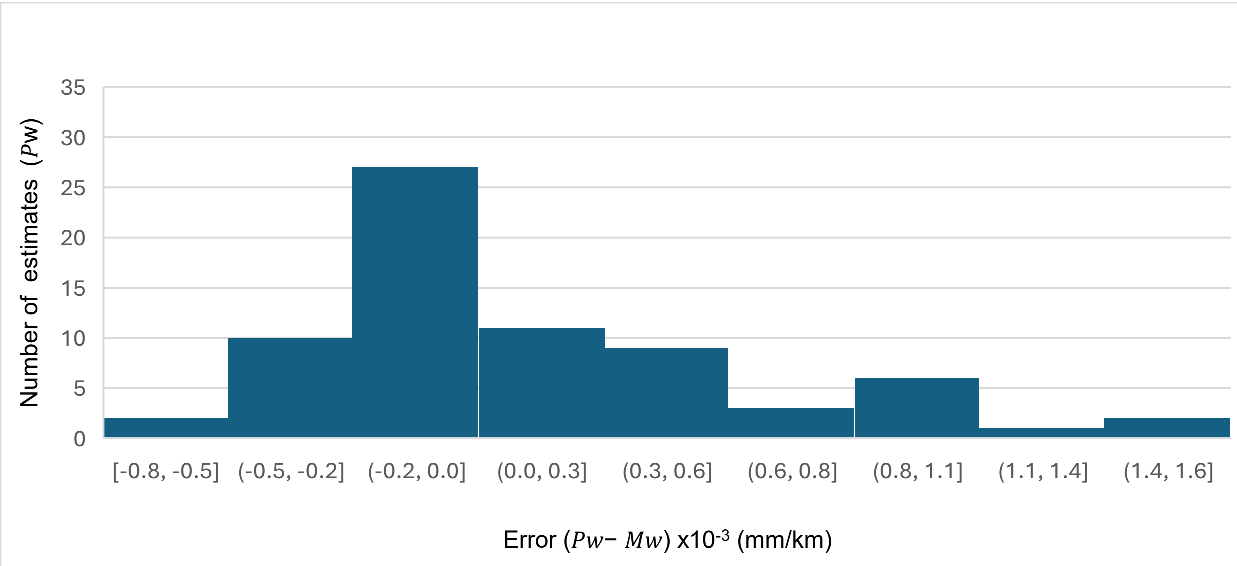

Figure 4.33. Error histogram for rear left tire correlation.

Figure 4.33 shows that the error for the rear left tire is symmetrically distributed at the center zero, with the highest number of estimates within the range of -0.2×10^{-3} and 0.0×10^{-3} mm/km of the error. 46.5% of what the rear left tire model predicts is between the error interval of -0.20×10^{-3} to 0.20×10^{-3} mm/km.

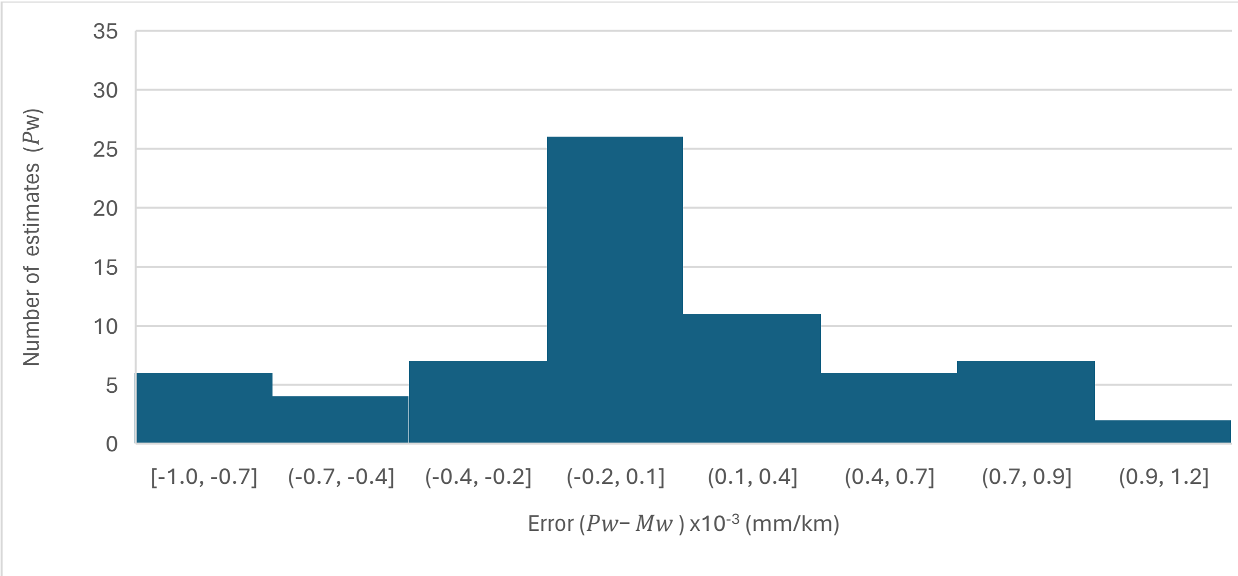

Figure 4.34. Error histogram for rear right tire correlation.

The error histogram for the rear right tire clearly shows a symmetrical distribution. The highest number of estimates falls between -0.2 × 10^{-3} and 0.1× 10^{-3} mm/km of the error. The model indicates no overprediction or underprediction of the wear rate. The results show that 43.7% of the predictions have an error ranging from -0.200 × 10^{-3} to 0.200 × 10^{-3} mm/km.

4.4 Sensitivity Analysis

Using Microsoft Excel, a sensitivity analysis was performed on four independent variables to assess the relative contributions of each to the predicted tire wear rate. These independent input variables, which are significant to the model, were varied systematically to assess their impact on the tire wear rate. Each independent variable was adjusted by plus or minus 10%, 20%, and 30% from its base value while keeping other parameters constant.

4.4.1 Effect of draft force

Changes in draft force (D) have a sensitive effect on each of the four tire models. The regression parameter for D (in mm/km per incremental kN of draft force) for the front left, front right, rear left, and rear right tire is 2.90×10^{-5}, 2.40×10^{-5}, 3.40×10^{-5}, and 4.00×10^{-5} mm/km per incremental kN, respectively. The relative difference between the predicted values of unit wear rate due to draft force is 66.7% (ranging from 2.40×10^{-5} to 4.00×10^{-5} mm/km per incremental kN). The predicted unit wear rate of the tires mounted on the front axle ranges from 2.40×10^{-5} to 2.90×10^{-5} mm/km per incremental kN, and the rate for those mounted on the rear axle ranges from 3.40×10^{-5} to 4.00×10^{-5} mm/km per incremental kN.

The right tires wear more and faster than the left tires. For example, when the base value of the draft force is increased by 10%, the wear rate of the front right and front left tire increases by 2.1% and 1.9%, respectively, while the wear rate for the rear right tire and the rear left tire increases by 2.9% and 2.8%, respectively. Using the preceding percentage increases in tire wear rates, the analysis indicates that the rear tires wear out faster than the front tires. This is further discussed in section 4.1.2.2.1.

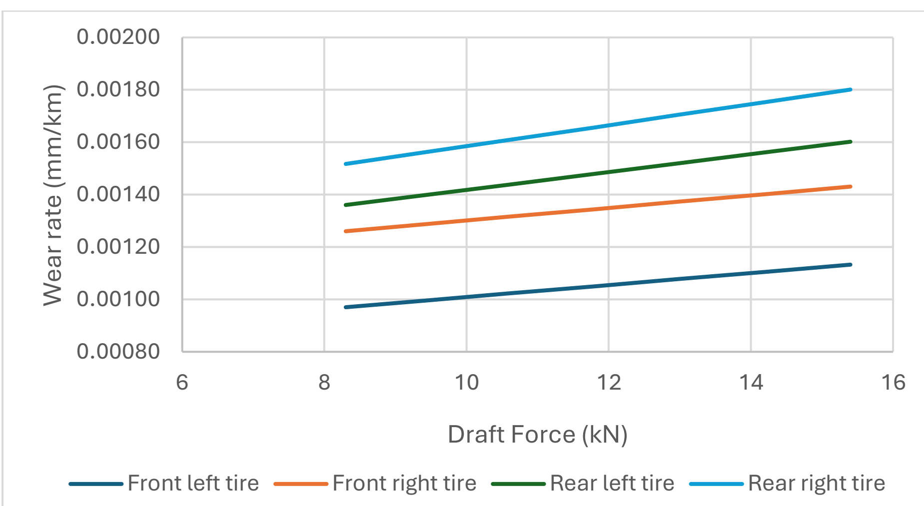

Figure 4.35. Sensitivity analysis of wear rate versus draft force by tire location.

4.4.2 Effect of wheel slip

The regression parameter for *i* (in mm/km per incremental percentage of wheel slip) for the front left and rear left tire is 3.50×10^{-5} and 4.10×10^{-5} mm/km per incremental percentage of slip, respectively. The relative difference between the predicted values of unit wear rate due to wheel slip in mm/km per incremental percentage is 17.1% (ranging from 3.50×10^{-5} to 4.10×10^{-5} mm/km per incremental percentage).

The sensitive analysis of wheel slip reveals that the rear tires wear out faster than the front tires. The wear rate of the rear and front tires is increased by 2.5% and 2.2%, respectively, when the base value of the wheel slip is increased by 10%. However, because wheel slip is not significant in determining the wear rate for either the front right or rear right tires, its sensitivity is constant. Further discussion on this can be found in sections 4.1.2.2.1 and 4.1.2.2.4.

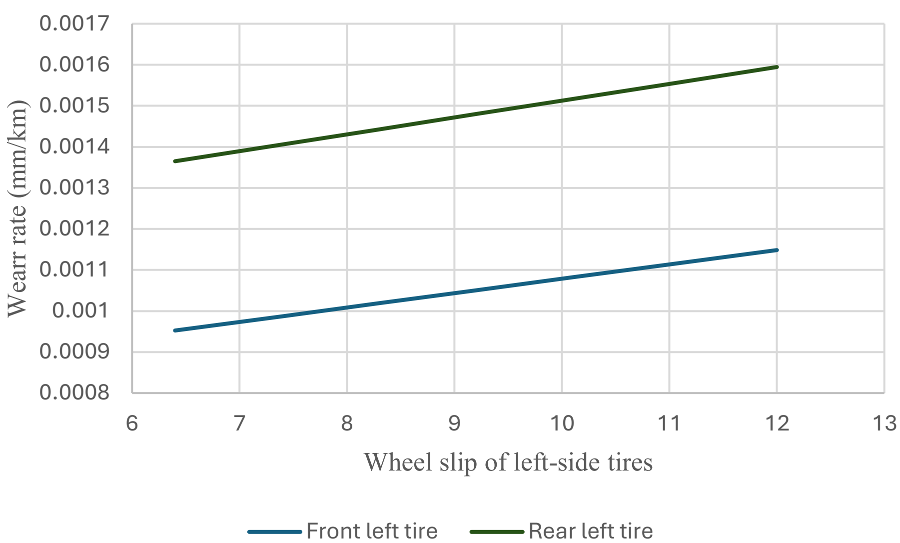

Figure 4.36. Sensitivity analysis of wear rate versus wheel slip.

4.4.3 Effect of tractor speed

Figure 4.37 illustrates the impact of tractor speed on all tire models. The regression parameters for S (in mm/km per incremental km/h of speed) for the front left, front right, rear left, and rear right tires are -1.80 × 10^{-4}, -2.10 x10^{-4}, -2.10 × 10^{-4}, and -2.50 × 10^{-4} mm/km per incremental km/h, respectively. The relative difference between the predicted unit wear rate due to speed (mm/km per incremental km/h of speed), which ranges from -2.50 × 10^{-4} to -1.80 × 10^{-4}, is 28.0%. The predicted unit wear rate of the tires mounted on the front and rear axles ranges from -2.10 × 10^{-4} to -1.80 × 10^{-4} and -2.50 × 10^{-4} to 2.10 × 10^{-4} mm/km per incremental km/h of speed, respectively.

At a reduced speed, the right tires wear more and faster than the left tires. For example, the wear rate of the front right tire and the front left tire increased by 12.5% and 9.9%, and the wear rate on the rear right and the rear left tires increased by 12.1% and 11.4%, respectively, when the base speed of the tractor is reduced by 10%. From the analysis, the rear tires wear faster than the front tires. Further discussion on this can be found in sections 4.1.2.2.1 and 4.1.2.2.4.

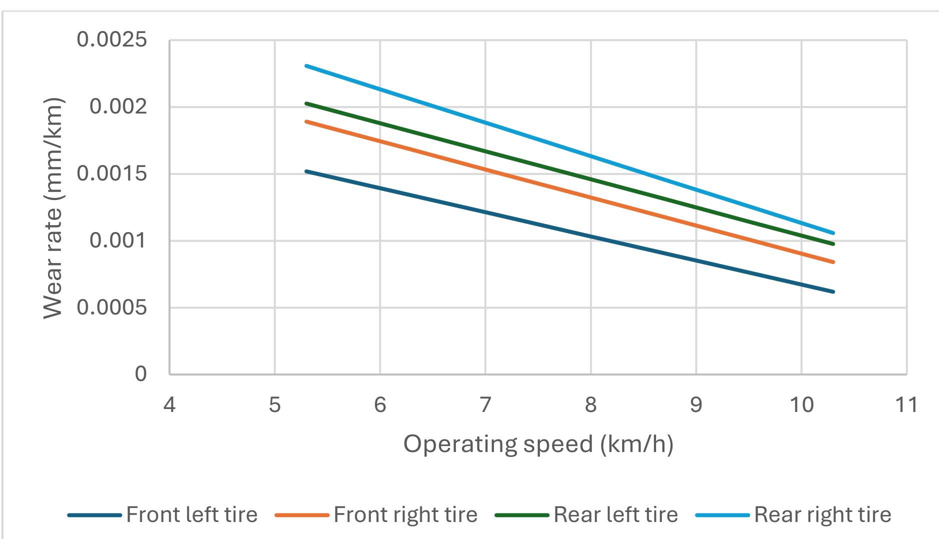

Figure 4.37. Sensitivity analysis of wear rate versus tractor operating speed.

4.4.4 Effect of soil bulk density

The regression parameter for ρ_b (in mm/km per incremental g/cm^3 of soil bulk density) for the front left, front right, rear left, and rear right tires is -6.70 × 10^{-3}, -8.30 × 10^{-3}, -7.90 × 10^{-3}, and -9.90 × 10^{-3} mm/km per incremental g/cm^3 of soil bulk density, respectively. The relative difference between the predicted unit wear rate due to soil bulk density (mm/km per incremental g/cm^3), ranges from -9.90 × 10^{-3} to -6.70 × 10^{-3} mm/km per incremental g/cm^3 is 32.32%. The predicted unit wear rate of the tires mounted on the front and rear axles ranges from -8.30 × 10^{-3} to -6.70 × 10^{-3} mm/km per incremental g/cm^3 and -9.90 × 10^{-3} and 7.90 × 10^{-3} mm/km per incremental g/cm^3, respectively.

The sensitivity effect of the soil bulk density on the predicted models is very high compared to the other independent variables. The right tires wear faster than the left tires at a lower soil bulk density; when the soil bulk density was reduced by 10%, the wear rates for the front right and left tires increased by 98.8% and 73.9%, respectively, while the wear rates for the rear right and left tires increased by 95.6% and 85.4%, respectively. This is further discussed in sections 4.1.2.2.4 and 4.4.5. The negative values for the tire wear rates when the bulk density is greater than 1.76 g/cm^3 (Figure 4.38) mean that the tire wear prediction models are not valid when the soil bulk density is higher than 1.76 g/cm^3.

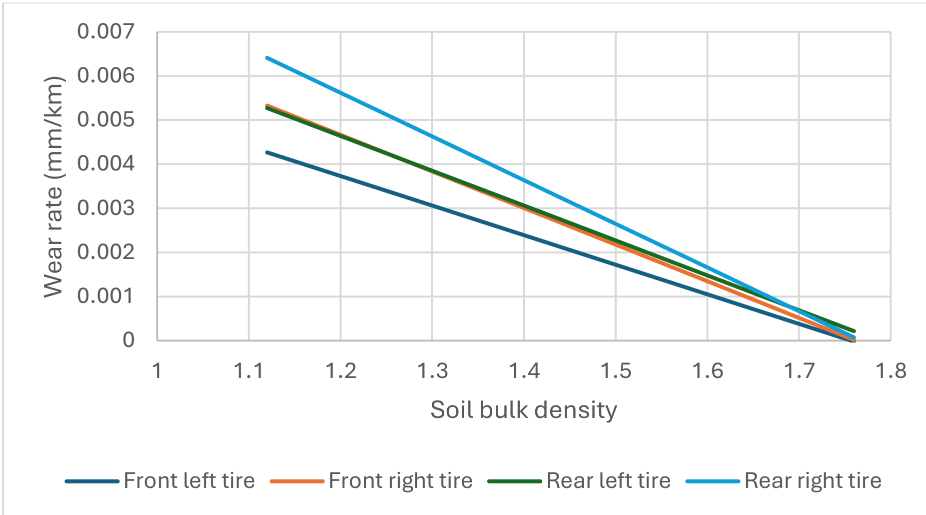

Figure 4.38. Sensitivity analysis of wear rate versus the bulk density of the soil.

4.4.5 Relative contribution of the four independent variables to predicted tire wear

From the example in section 4.5.1, the front left tire wears at a rate of 0.00015 mm/km using a draft force of 11.81 kN, a wheel slip of 7.90%, a speed of 8.20 km/h, and a soil bulk density of 1.73 g/cm^3 during planting. In that example, three values—draft force (0.00034), wheel slip (0.00028), and the constant value (0.0126)—contributed positively to the wear rate of the tire, while the speed (-0.00148) and soil bulk density (-0.01159) contributed negatively. The main contributor to the predicted wear rate for the front left tire is the constant value. The two positive contributors (draft and wheel slip) are two orders of magnitude smaller than the constant value. The predicted wear rate is reduced when the tractor is operated at a higher speed or on firmer soils (i.e., soils with higher bulk density values). The tractor tires are in constant interaction with the soil during every field operation, providing the necessary support for effective tillage. The soil bulk density is key in influencing the soil condition (the stiffness or abrasiveness of the soil) to provide efficient traction when the tractor operates under varying loads (plowing, harrowing, and planting). USDA (2008) notes that soil bulk density for plant growth in sandy soil should be between 1.6 and 1.8 g/cm^3. A very low soil bulk density will increase the pressure of the tire on the soil contact area. The average pressure exerted by tires on deformable surfaces is approximately equal to the tire inflation pressure (Wulfsohn, 2009). The tire-soil contact area is inversely proportional to the density of the soil, i.e., the contact area is larger when the tire is on low-density soils and smaller when it is on high-density soils. A very low soil bulk density will retard the speed of the tractor and increase slippage and wear. Conversely, a higher soil bulk density will result in increased draft requirements, in addition to increasing wheel slip. Given that these two independent variables (draft force and wheel slip) contribute positively to tire wear rate in the prediction models, the predicted tire wear rate values will be higher for field operations that are completed on firmer soils. Therefore, the soil bulk density is fundamental to determining the wear of the tire.

The model shows a high baseline value (constant) when all the independent variables are simultaneously zero. However, during a field operation, the independent variables (speed and soil bulk density) cannot simultaneously be zero. If the tractor is not pulling any implement, then the draft force will be zero (the tires will only need to provide a tractive force equal to the value of the rolling resistance), and wheel slip will be close to zero. Nau (2020)notes that the presence of a constant is key in multiple regression models, regardless of its statistical significance. A high constant provides the best fit to data because it absorbs the in-sample errors to reduce bias (the model will not over-predict or under-predict the wear rate). A constant value may indicate the correction of a significant variable or variables that might be omitted in developing the model. This may include the pressure of the tire or gravel or other debris on the soil (as discussed in section 4.1.2.2.2). Li et al. (2012) note that the air pressure of a tire influences its wear. Even though the tires were inflated to the required pressure before each operation, there could have been variations in air pressure during the field operations.

4.5 USE OF THE MODELS

The lifespan of a tractor tire is the total distance the tire can travel until its amount of wear reaches the maximum recommended by the manufacturer. To use the model to predict the maximum surface area that a tractor tire can cover before needing replacement, the following parameters must be determined:

1. Total lug height (H_T): This is the initial lug height of a new tire. The lug heights of the front and rear tires (the tires for the 2023 farming season were almost new) used in this study were approximately 48 mm and 60 mm, respectively.
2. Replacement lug height (H_r): This is the lug height at which the tire should be replaced. Generally, manufacturers recommend that a tire be replaced when the lug height is 60% of that of a new tire (Tractor Tyre Expert, 2021b). Therefore, the wearable lug heights (the amount of wear available) for the front and rear tires used in this study is

$$\varepsilon = 0.40 \times 48 \; and \; 0.40 \times 60$$

$$= 19.2 \text{ mm and } 24 \text{ mm}$$

and the replacement lug heights for the front and rear tires used in this study are 28.8 mm and 36 mm, respectively (i.e., 48.0 – 19.2 = 28.8; 60 – 24.0 = 36).

3. The final parameter is the predicted wear rate (W_r), which is calculated for each tire using the developed models. The cross-section of the tire lug is not the same from top to bottom (it increases as the tire lug wears down). Because the predicted wear rate models do not account for this, they should be considered conservative (i.e., they may over-predict tire wear as the lugs wear down).

4.5.1 Allowable tire wear

The independent variables in Table 4.14 are used together with equations 32, 33, 34, and

35 to determine the average wear rate for the corresponding field operation of the four tires on the tractor. For example, Equation 32 is used to calculate the predicted average wear rate for the front left tire during planting (W_{rp}) as follows:

$$W_{rh} = (2.9 \times 10^{-5})\mathrm{D} + (3.50 \times 10^{-5})i + (-1.80 \times 10^{-4})\mathrm{s} + (-6.7 \times 10^{-3})\rho_b + 0.0126$$

using data from Table 4.15, where D = 11.81 kN, i = 7.90%, s = 8.20 km/h, and ρ_b = 1.73 g/cm^3.

Therefore

$$W_{rp} = 0.00015 \text{ mm/km.}$$

Since the tractor covers a surface area during operation, it is appropriate to determine the distance traveled by the tractor in terms of the area it covers during each operation. Therefore, the wear rate value in ha is given as

$$W_r\left(\frac{mm}{Ha}\right) = W_r\left(\frac{mm}{km}\right) \times \left(\frac{10}{w_i\,(m)}\right) \tag{37}$$

The time required for the tire to travel before needing replacement is given by

$$Time\ (h) = (Total\ distance\ travelled\ (km))/(Speed\ (km/h)) \tag{38}$$

Table 4.14 shows the data for the independent variables used to determine the lifespan of the tires.

Table 4.14. Data for determining the lifespan of a tractor tire.

Field operation	Draft force (kN)	Slip (%)	Speed (km/h)	Soil bulk density (g/cm^3)	Soil moisture (%)
Plowing	12.61	9.30	7.50	1.68	4.71
Harrowing	7.81	8.50	8.60	1.70	4.42
Planting	11.81	7.90	8.20	1.73	5.64

4.5.2. Area covered by the tires

Table 4.15 presents the key predicted results before the replacement of each tire. The detailed calculations are presented in Appendix D. The maximum surface area that can be covered by the front left, front right, rear left, and rear right tires before needing replacement is 3,221, 2,719, 3,101, and 1,717 ha, respectively. The lower limits of the replacement intervals (in hours) for the front and rear tires (Table 4.16) fall within the average lifespan of 1,700 to 3,000 hours for front tires and 2,000 to 3,000 hours for rear tires, as recommended by Firestone (Tractor Tyre Expert, 2021b). However, the upper limits for the front left, front right, rear left, and rear right are higher by 29%, 14%, 13%, and 0.3%, respectively, than the upper limits of the recommended average lifespan.

Table 4.15. Key predicted wear rate (W_p) results for each tire by field operation.

Parameter	Field operation	Front tires		Rear tires	
		Left	Right	Left	Right
W_r, mm/km	Plowing	0.69×10^{-3}	0.78×10^{-3}	0.86×10^{-3}	0.1×10^{-2}
	Harrowing	0.12×10^{-3}	0.19×10^{-3}	0.19×10^{-3}	0.23×10^{-3}
	Planting	0.15×10^{-3}	0.20×10^{-3}	0.23×10^{-3}	0.20×10^{-3}
W_r, mm/ha	Plowing	7.67×10^{-3}	8.67×10^{-3}	9.56×10^{-3}	11.11×10^{-3}
	Harrowing	6.28×10^{-4}	1.06×10^{-3}	1.06×10^{-3}	1.28×10^{-3}
	Planting	6.44×10^{-4}	8.58×10^{-4}	9.87×10^{-4}	8.58×10^{-3}
Total W_r, mm/ha		8.94×10^{-3}	10.59×10^{-3}	11.61×10^{-3}	20.97×10^{-3}
Maximum surface area (ha)		3,221	2,719	3,100	1,716
Replacement interval (h)		2,970 to 4,285	2,437 to 3,516	2,784 to 4,017	2,492 to 3,596

4.5.6 Determining when to swap tires

To ensure the two front and rear tires wear uniformly, it is vital to determine when to swap the tires. The front tires are to be used to cover X ha before they are swapped. If both tires are used for an area (X ha) before they are swapped and then used for another area (X ha), then

left tire total wear = $\chi \times (10.59 \times 10^{-3}) + \chi \times (8.94 \times 10^{-3}) = 19.53 \times 10^{-3}\chi$

right tire total wear = $\chi \times (8.94 \times 10^{-3}) + \chi \times (10.59 \times 10^{-3}) = 19.53 \times 10^{-3}\chi$

since the total replacement lug height of 28.8 mm, then

$$19.53 \times 10^{-3}\chi = 28.8$$

$$\Rightarrow \chi = {}^{28.8}/_{19.53\ \times 10^{-3}} \approx 1{,}474.65 \text{ ha}$$

To ensure that the front tires wear uniformly, the tires are to be interchanged after they have covered approximately 1,474.65 ha. For the rear tires:

Left rear tire total wear

$= \chi \times (20.97\ \times 10^{-3}) +\ \chi\ \times (11.61\ \times 10^{-3}) = (32.58 \times 10^{-3})\chi$

Right rear tire total wear

$=\ \chi \times (11.61\ \times 10^{-3}) +\ \chi\ \times (20.97\ \times 10^{-3}) = (32.58\ \times 10^{-3})\chi$

Since the height at which the tires should be replaced is 36 mm, then

$$(32.58\ \times 10^{-3})\chi = 31$$

$$\Rightarrow \chi = {}^{36}/_{(32.58\ \times 10^{-3})}\ =\ 1{,}104.97 \text{ ha}$$

therefore, the left tire and the right tire at the rear of the tractor should be swapped after every 1,104.97 ha of travel to enable the tires to wear uniformly.

It is essential to note that these estimates were calculated within the context of this study, where the tractor (and the tires mounted on it) are exclusively used to complete plowing, harrowing, and planting on the three fields each year. Any other use of the tractor (either off-field or on-field operation) will result in a different predicted tire lifespan value for each year.

CHAPTER 5: CONCLUSION AND RECOMMENDATIONS

5.1 CONCLUSION

Effective management of a tractor's tires enhances the tractor's performance, improves traction, and supports crop growth by reducing the potential (unintentional) harm a tractor can do to the soil (e.g., due to excessive compaction). To manage tires efficiently, it is important to predict the rate at which a tire wears. Several tire-wear models have been developed and applied by researchers and industry professionals in the tire sector. Most of these models are for on-road tires, ranging from small vehicles to trucks; very few studies have been conducted on wear rates for off-road tires. However, no model has been developed to predict the wear rate of a tire on agricultural soil. The purpose of this study was to create a model to predict the wear rate of agricultural tractor tires and identify which field operations contribute to a high wear rate. This study was also conducted to provide tire users with a good understanding of the wear rates of their tires, enabling them to develop an effective tire management plan, maximize efficient field operation, and reduce preventable delays during the farming season. The following observations were made during the study.

- Although the moisture content of the soil did not significantly affect the wear rates of the tires in developing the models, the drought in the Northern Region of Ghana during the two farming seasons (2023 and 2024) required the tractor to engage a high draft force to pull the implements through the soil.
- The differences in soil texture reveal variations in the rate at which the tires wear. Tires working in sandy loam soil wear more than those working in loam soil. The higher the tire wear rate, the higher the percentage of sand in the soil. The tire wear rate increases with a decrease in soil bulk density.

- The type of field operation significantly influenced the rate at which a tractor tire wore. The tires experienced a high rate of wear during plowing and planting. For all three fields, the four tires experienced different wear rates for plowing and planting, respectively:
    - the front left tire had wear rates of 35.7% and 35.3%
    - the front right tire had 37.4% and 32.5%
    - the rear left tire had 34.5% and 34.7% and
    - the rear right tire had 39.1% and 31.9%.
- The tires on the right side of the tractor wore faster than those on the left.
- The model for the front left tire is significantly affected by the draft force, wheel slip, speed of the tractor, and bulk density. The model has a good correlation (*r*) of 0.84, and 66.2% of the estimated errors fall within a margin of error of -0.20×10^{-3} to 0.22×10^{-3} mm/km.
- The model for the front right tire is significantly influenced by the draft force, the wheel slip of the tractor, and soil bulk density. The model shows a good correlation of 0.83, and 58.6% of the estimated errors fall within a margin of error of -0.200×10^{-3} to 0.22×10^{-3} mm/km.
- The model for the rear left tire is significantly affected by the draft force, wheel slip, speed of the tractor, and bulk density. It has a good correlation of 0.71, with 46.5% of the estimated errors falling within a margin of error of -0.200×10^{-3} to 0.22×10^{-3} mm/km.
- The model for the rear right tire is significantly affected by the draft force, wheel slip, and soil bulk density. It exhibits a correlation of 0.61, and 43.7% of the estimated number of errors fall within a margin of error of -0.200×10^{-3} to 0.22×10^{-3} mm/km.

- The maximum surface areas that the front left tire, the front right tire, the rear left tire, and the rear right tire can cover before needing replacement are between 2,719 and 3,221, and 1,716 and 3,100 ha, respectively.
- The tires experienced physical damage due to the nature of the field during operation. Because the tractor operated on large fields for extended period, the tires were exposed to stones, wood debris, stumps, and crop residue such as stover on the fields. All of these objects can tear and prick the tires.

5.2 Recommendations

1. Since the method used to conduct a field operation affects the pattern of tire wear, it is important to engage an experienced operator.
2. To ensure a uniform wear rate, the front tires should be interchanged after covering an area of 1,475 ha, while the rear tires should be swapped after covering an area of 1,105 ha.
3. Within the context of this study, the front tires should be replaced after covering 2,720 to 3,211 ha and the rear tires should be replaced after covering 1,717 to 3,101 ha to maximize safety and minimize operational cost.

5.3 Areas for Future Study

This study analyzed data and developed a model to predict the rate at which tractor tires will wear during field operations. Separate models were developed for the four tires of the tractor. However, after observing the wear pattern of the tires and making deductions from the analysis of the results, there are potential areas for future research work:

1. Need for a model for soil with a sufficient level of moisture: The data for this thesis was collected in real time over two seasons during which a drought occurred and the soil moisture level fell below the recommended range. Such low percentages of soil moisture may be the reason why soil moisture content was not significant in developing the prediction models for this study. Therefore, there is a need to develop a wear-rate model for a tractor operating on soil with a level of moisture that falls within the recommended range, given that most farmers aim to carry out tillage and planting work on soil that has an appropriate level of soil moisture to improve the efficiency of field operations and increase crop yield.
2. Need for condition-specific prediction models: It will likely be impossible to develop a universal, "one-size-fits-all" tire-wear prediction model. The farming landscape is being redefined because most farmers are adopting the use of modern tractors and implements to increase yield, reduce costs, and manage the soil more effectively. Therefore, the development of condition-specific prediction models that use modern farm machinery would serve an important purpose.
3. Need to understand economic implications related to tire wear: In addition to new models developed using modern farm machinery, future studies could be conducted on the economic impacts of tire wear on farmers. The studies could focus on how wear rate influences fuel consumption and how to plan and budget effectively for the management and replacement of tractor tires.
4. The methodological and analytical frameworks of this study could be applied to other situations. With more situation-specific tire wear data available, it will eventually be possible to develop and validate general tire wear prediction models, similar to other

standardized prediction models (e.g. ASABE standard ASAE D497.7 MAR2011 (R2020)).

5. Future studies may also consider the use of machine learning techniques in data collection and the prediction of the model for tire wear.

REFERENCES

Ahmadi, I. (2016). Development and assessment of a draft force calculator for disk plow using the laws of classical mechanics. *Soil and Tillage Research*, *163*, 32–40. https://doi.org/10.1016/j.still.2016.04.013

Al Nuaimi, B., & Al Rijabo, S. (2020). Design and manufacture of chisel plow shares and their effect on some field performance indicators. *Tikrit Journal for Agricultural Sciences*, *20*(1), 10–19. https://doi.org/10.25130/tjas.20.1.2

Amer, K. Z., Swain, K. H., & Abbas Jebur, H. (2021). The impact of plowing depth and soil moisture on some technical indicators using disk plow. *International Journal of Agricultural and Statistical Sciences*, *17*(1), 177–180. https://connectjournals.com/file_full_text/3355201H_177-180.pdf

American Society of Agricultural and Biological Engineers. (2020). *ASAE D497.7 MAR2011 (R2020): Agricultural machinery management data*, https://elibrary.asabe.org/abstract.asp?aid=36431

Association of Equipment Manufacturers. (2022). *AEM United States AG tractor and combine report March 2022*. https://www.aem.org/AEM/media/docs/Statistics/US-Month-Ag-Report-3-2022.pdf

ASTM International. (2017). *ASTM D7928: Standard test method for particle-size distribution (gradation) of fine-grained soils using the sedimentation (hydrometer) analysis*, 1–25. https://doi.org/10.1520/D7928-17

Bauer Built Tire and Service. (2025, January 14). *Types of tractor tires*. https://www.bauerbuilt.com/bauer-built-blog/understanding-the-3-types-of-tractor-tires/

Bohnert, L., & Kenady, T. (1975) A comparative analysis of radial and bias R-1 drive wheel tractor tires. *SAE Technical Paper 751185*. https://doi.org/10.4271/751185

Botta, G. F., Tolon-Becerra, A., Tourn, M., Lastra-Bravo, X., & Rivero, D. (2012). Agricultural traffic: Motion resistance and soil compaction in relation to tractor design and different soil conditions. *Soil and Tillage Research*, *120*, 92–98. https://doi.org/10.1016/j.still.2011.11.008

Bouma, C. (n.d.). *6 reasons why rear wheels on a farm tractor are bigger*. Farm Tractor Addict. https://tractoraddict.com/why-rear-wheels-on-tractor-are-bigger/

Braghin, F., Cheli, F., Melzi, S., & Resta, F. (2006). Tyre wear model: Validation and sensitivity analysis. *Meccanica*, *41*(2), 143–156. https://doi.org/10.1007/s11012-005-1058-9

Brassart, F. P. (1994). *Traction and agricultural tractor tire selection studies* [Doctoral dissertation, Louisiana State University]. https://repository.lsu.edu/gradschool_disstheses/5855/

Bridgestone Americas Tire Operations. (n.d.-a). *Radial tires vs bias ply tires*. https://commercial.firestone.com/en-us/agriculture/tire-expert-center/bias vs-radial

Bridgestone Americas Tire Operations. (n.d.-b). *Understanding the anatomy of a tire*. https://commercial.firestone.com/en-us/agriculture/tire-expert-center/tire-construction

Briscoe, B. J., & Sebastian, K. S. (1993). An analysis of the "durometer" indentation. *Rubber Chemistry and Technology*, *66*(5), 827–836. https://doi.org/10.5254/1.3538347

Callister, W. D., Jr. (2006). *Materials science and engineering: An introduction* (7th ed.). John Wiley & Sons, Inc.

Cardei, P. (2019). *Soil moisture influence in the soil tillage operations*. https://doi.org/10.13140/RG.2.2.28028.69768

Cardei, P., Sfiru, R., Muraru, S., & Condruz, P. (2020). Soil moisture influence in the soil tillage operations. *E3S Web of Conferences, 180*. https://doi.org/10.1051/e3sconf/202018003002

Carroll, E., Stone, M. L., & Smith, D. W. (2006). Traction and transport devices. Chapter 13. In *Off-Road Vehicle Engineering Principles* (Vol. 2003, pp. 351–382). American Society of Agricultural and Biological Engineers

Chang, W.-H., Juang, R.-T., Huang, M.-H., & Sung, M.-F. (2021). Estimation of tire mileage and wear using measurement data. *Electronics*, *10*(20), 2531. https://doi.org/10.3390/electronics10202531

Chen, Y., Cavers, C., Tessier, S., Monero, F., & Lobb, D. (2005). Short-term tillage effects on soil cone index and plant development in a poorly drained, heavy clay soil. *Soil and Tillage Research*, *82*(2), 161–171. https://doi.org/10.1016/j.still.2004.06.006

Cho, J. C., & Jung, B. C. (2007). Prediction of tread pattern wear by an explicit finite element model. *Tire Science and Technology, 35*(1), 276–299. https://doi.org/10.2346/1.2804913

Clark, S. K. (1971). *NBS monograph 122: Mechanics of pneumatic tires,* 445–500. [U.S.] National Bureau of Standards. https://nvlpubs.nist.gov/nistpubs/Legacy/MONO/nbsmonograph122.pdf

Dadi, W., Mulugeta, M., & Semie, N. (2023). Impact of urbanization on the welfare of farm households: Evidence from Adama Rural District in Oromia regional state, Ethiopia. *Heliyon,10* (1). https://doi.org/10.1016/j.heliyon.2023.e23802

Dorvlo, S. Y. (2015, January). *Tractor rear tyre wear rate and replacement planning in Ghana*. University of Ghana. https://www.researchgate.net/publication/341463162_Tractor_rear_tyre_replacement_strategy_for_Ghana

Dorvlo, S. Y., Mahama, A. A., & Baryeh, E. A. (2014). Evaluation of on-farm rear tyre wear rate in Ghana. *Journal of the Ghana Science Association*, *15*(2), 119–128. https://www.researchgate.net/publication/341462896_Evaluation_of_on-farm_rear_tyre_wear_rate_in_Ghana

Enyart, J. (2008, October 22). Radial tire technology: The importance of radial over bias for farming. *Tire Review.* Babcox Media Inc. https://www.tirereview.com/radial-tire-technology-the-importance-of-radial-over-bias for-farming/

Farmonaut. (n.d.). *Urgent: US Unleashes $1.7M Lifeline for Ghana's Drought Crisis – Farmers' Salvation Amid Devastating Crop Losses*. Farmonaut Technologies Private Limited. https://farmonaut.com/news/urgent-us-unleashes-1-7m-lifeline-for-ghanas-drought-crisis-farmers-salvation-amid-devastating-crop-losses

Garciano, L. O., Upadhyaya, S. K., & Jones, R. A. (2010). Measurement of soil parameters useful in predicting tractive ability of off-road vehicles using an instrumented portable device. *Journal of Terramechanics*, *47*(5), 295–305. https://doi.org/10.1016/j.jterra.2010.07.002

Gent, A. N. (2012). *Engineering with rubber: How to design rubber components*. Carl Hanser Verlag GmbH Co KG.

Gent, A. N., & Walter, J. D. (2006). *Pneumatic tire*. University of Akron Mechanical Engineering Faculty Research. 854. http://ideaexchange.uakron.edu/mechanical_ideas/854

Gharibkhani, M. (2014). A mathematical model for determining rolling resistance of agricultural tire to control energy losses. *Tarım Makinaları Bilimi Dergisi, 10*(3), 183–187. ISSN: 1306-0007.

Gharibkhani, M., Mardani, A., & Vesali, F. (2012). Determination of wheel-soil rolling resistance of agricultural tire. *Australian Journal of Agricultural Engineering*, *3*(1), 6–11. ISSN:1836-9448

Goodyear Tire and Rubber Co. (2004, June 1). *Pros and cons of radial vs. bias ply tires in construction*. ForConstructionPros.Com. https://www.forconstructionpros.com/equipment/fleet-maintenance/tires/article/10307455/goodyear-tire-rubber-co-pros-and-cons-of-radial-vs-biasply-tires-in-construction

Heinrich, G., & Klüppel, M. (2008). Rubber friction, tread deformation, and tire traction. *Wear*, *265*(7–8), 1052–1060. https://doi.org/10.1016/j.wear.2008.02.016

Hendrick, A. (1988). *CRC handbook in agriculture* (Vol. 1). Boca Raton, CRC Press.

IBM Corp. (2020). IBM SPSS Statistics for Windows (Version 27.0) [Computer software].

Ivanov, R. (2016). Tire wear modeling. *Transport Problems*, *11*(3), 111–120. https://www.researchgate.net/publication/308823341_Tire_wear_modeling

Jarrett, V. H. (1995). Radial tractor tires–how good they are? *All Current Publications.* Paper 564. 739–745. https://digitalcommons.usu.edu/extension_curall/564

Jenane, C., & Bashford, L. L. (2000). Tractive performance of a mechanical front-wheel assist tractor as related to forward speeds. *Journal of Agricultural Engineering Research*, *77*(2), 221–226. https://doi.org/10.1006/jaer.2000.0569

Jerry. (2002, May 4). *Could someone tell me the difference between FWA and FWD?* [discussion forum]. Yesterday’s Tractor Co. https://www.yesterdaystractors.com/cgi-bin/viewit.cgi?bd=ttalk&th=307848

Kichler, C. M., Fulton, J. P., Raper, R. L., McDonald, T. P., & Zech, W. C. (2011). Effects of transmission gear selection on tractor performance and fuel costs during deep tillage operations. *Soil and Tillage Research*, *113*(2), 105–111. https://doi.org/10.1016/j.still.2011.03.002

Kpenekuu, F., Antwi-Agyei, P., Nimoh, F., Osei, M. A., & Guodaar, L. (2024). Understanding drought risk management in vulnerable communities in dryland farming systems: Evidence from northwest Ghana. *International Journal of Disaster Risk Reduction*, *100*. https://doi.org/10.1016/j.ijdrr.2023.104186

Le Gal, A., Yang, X., & Klüppel, M. (2005). Evaluation of sliding friction and contact mechanics of elastomers based on dynamic-mechanical analysis. *Journal of Chemical Physics*, *123*(1). https://doi.org/10.1063/1.1943410

Le Maître, O., Süssner, M., & Zarak, C. (1998). Evaluation of tire wear performance. *SAE Technical Papers*, *724*. https://doi.org/10.4271/980256

Lepine, J., & Cebon, D. (2018). *Empirical estimation of heavy goods vehicle tyre wear*, 1–11. International Forum for Heavy Vehicle Transport & Technology. https://hvttforum.org/wp-content/uploads/2019/11/Lepine-EMPIRICAL-ESTIMATION-OF-HEAVY-GOODS-VEHICLE-TYRE-WEAR.pdf

Li, Y., Zuo, S., Lei, L., Yang, X., & Wu, X. (2012). Analysis of impact factors of tire wear. *Journal of Vibration and Control*, *18*(6), 833–840. https://doi.org/10.1177/1077546311411756

Lin, SL. Research on tire crack detection using image deep learning method. *Sci Rep* 13, 8027 (2023). https://doi.org/10.1038/s41598-023-35227-z

Lupker, H., Montanaro, F., Donadio, D., Geloso, E., & Vis, M. (2002). *Truck tyre wear assessment and prediction*. 7th International Symposium on Heavy Weight Vehicles & Dimensions, Delft, The Netherlands. 275–288. https://hvttforum.org/wp-content/uploads/2019/11/Truck-Tyre-Wear-Assessment-And-Prediction-L-upker.pdf

Lyasko, M. I. (2010). How to calculate the effect of soil conditions on tractive performance. *Journal of Terramechanics*, *47*(6), 423–445. https://doi.org/10.1016/j.jterra.2010.04.003

Macmillan, R. H. (2002). *The mechanics of tractor-implement performance: Theory and worked examples: A textbook for students and engineers*, 166. https://fsantos.utad.pt/Bibliografia/65851_Macmillan.pdf

Mari, G. R., Chandio, F. A., Leghar, N., Rajper, A. G., & Shah, A. (2011). Performance evaluation of selected tillage implements under saline-sodic soil. *American-Eurasian Journal of Agricultural & Environmental Sciences, 10 (1)*. ISSN:1818-6769

Markel, A. (2016). *Reading tire wear patterns*. Babcox Media Inc. https://www.tirereview.com/reading-tire-wear-patterns/

Massola, C. P., Chaves, A. P., & Albertin, E. (2016). A discussion on the measurement of grinding media wear. *Journal of Materials Research and Technology, 5*(3), 282–288. https://doi.org/10.1016/j.jmrt.2015.12.003

Mohsenimanesh, A., Ward, S. M., Owende, P. O. M., & Javadi, A. (2009). Modelling of pneumatic tractor tyre interaction with multi-layered soil. *Biosystems Engineering*, *104*(2), 191–198. https://doi.org/10.1016/j.biosystemseng.2009.06.020

Moore, D. F. (1980). Friction and wear in rubbers and tyres. *Wear*, *61*(2), 273–282. https://doi.org/10.1016/0043-1648(80)90291-4

Naderloo, L., Alimadani, R., Akram, A., Javadikia, P., & Zeinali Khanghah, H. (2009). Tillage depth and forward speed effects on draft of three primary tillage implements in clay loam soil. *Journal of Food, Agriculture & Environment*, *7*(4), 382–385. https://www.researchgate.net/publication/255613398

Nakajima, Y., & Hidano, S. (2021). Theoretical tire model for wear progress of tires with tread pattern considering two-dimensional contact patch. *Tire and Science Technolog*y, 50 (4) 337-369. DOI: 10.2346/tire.21.20010

Nau, R. (2020). *Statistical furcating: notes on regression and time series analysis*. https://people.duke.edu/~rnau/411home.htm

Okoko, P. (2018). Draft and power requirements for some tillage implements operating in clay loam soil. *Agricultural Engineering International: CIGR Journal*, *20*(1), 95–102. https://cigrjournal.org/index.php/Ejounral/article/view/4563

Persson, B. N. J., Tartaglino, U., Albohr, O., & Tosatti, E. (2004). Sealing is at the origin of rubber slipping on wet roads. *Nature Materials*, *3*(12), 882–885. https://doi.org/10.1038/nmat1255

Persson, S. (2009). Chapter 2: Traction mechanics. Part I: Basic traction mechanics. In S. K. Upadhyaya, W.J. Chancellor, J.V. Perumpral, D. Wulfsohn, and T. R. Way (Eds.), *Advances in soil dynamics* (Vol. 3, pp. 25–58). American Society of Agricultural and Biological Engineers. https://elibrary.asabe.org/abstract.asp?aid=26871

Pohrt, R. (2019). Tire wear particle hot spots – Review of influencing factors. *Facta Universitatis. Series: Mechanical Engineering*, *17*(1), 17–27. https://doi.org/10.22190/FUME190104013P

Renius, K. T. (2020). *Fundamentals of tractor design*. Springer International Publishing. https://doi.org/10.1007/978-3-030-32804-7

Reuvekamp, L.-P. A. E. M. (2003). *Reactive mixing of silica and rubber for tyres and engine mounts: Influence of dispersion morphology on dynamic mechanical properties* [Doctoral dissertation, Twente University, Enschede, Netherlands]. https://ris.utwente.nl/ws/portalfiles/portal/255318645/thesis_L_Reuvekamp.pdf

Sabbioni, E., Negrini, S., Braghin, F., & Melzi Ing, S. (2011). A 2D model for tractor tire-soil interaction: Evaluation of the maximum traction force and comparison with experimental results. *SAE International*, Technical Paper 2011-01-0191. https://doi.org/10.4271/2011-01-0191

Shahgholi, G., & Abuali, M. (2015). Measuring soil compaction and soil behavior under the tractor tire using strain transducer. *Journal of Terramechanics*, *59*, 19–25. https://doi.org/10.1016/j.jterra.2015.02.007

Sharma, S., & Warren, J. (2024). Basics of soil bulk density. In *Oklahoma Cooperative Extension Service* (Issue PSS-2287). https://extension.okstate.edu/fact-sheets/basics-of-soil-bulk-density.html

Siemens, J. C., & Bowers, W. (1999). *Farm business management: Machinery management*. John Deere Publishing.

Singh, J., Chatha, C. H., & Sidhu, B. S. (2017). Influence of soil condition on abrasion wear behavior of tillage implements. *International Journal of Latest Trends in Engineering and Technology*, 258–263. https://www.ijltet.org/pdfviewer.php?id=925&j_id=4263

Söhne, W. (1968). Four-wheel drive or rear-wheel drive for high power farm tractors. *Journal of Terramechanics*, *5*(3), 9–28. https://doi.org/10.1016/0022-4898(68)90078-5

Srivastava A. K., Goering, C. E., Rohrbach, R. P., & Buckmaster, D. R. (2006). *Engineering Principles of Agricultural Machines* (2nd ed.). American Society of Agricultural and Biological Engineers. https://doi.org/10.13031/epam.2013

Tamada, R. & Shiraishi, M. (2017). Prediction of uneven tire wear using wear progress simulation. *Tire Science and Technology, 45,* 87–100. https://doi.org/10.2346/tire.17.450201

Tetteh, F. M., Larbi, A., Nketia, K. A., & Irmgard, H.-Z. (2016). Suitability of soils for cereal cropping in northern Ghana. *Africa Rising*. International Institute of Tropical Agriculture. https://doi.org/10.13140/RG.2.2.34455.73122

Tire Works Total Car Care. (n.d.). *Tire terminology*. https://www.tireworks.net/blog/tire-terminology

Tractor Tyre Expert. (2021a, 30 April). *Full explanations on the manufacture of agriculture tyres*. Bridgestone Europe. https://blog.bridgestone-agriculture.eu/full-explanations-on-the-manufacture-of-agricultural-tyres

Tractor Tyre Expert. (2021b, June 21). *How worn can your tractor tyres be before you need to change them*? Firestone. https://www.firestone-agriculture.eu/blog/how-worn-can-your-tractor-tyres-be-before-you-need-to-change-them.

Upadhyaya, S. K., Andrade-Sanchez, P., Sakai, K., Chancellor, W. J., & Godwin, R. J. (2009). Chapter 3: Tillage. In S. K. Upadhyaya, W. J. Chancelor, J.V. Perumpral, D. Wulfsohn, and T.R. Way (Eds.), *Advances in soil dynamics* (Vol. 3, pp. 273–395). American Society of Agricultural and Biological Engineers. https://doi.org/10.13031/2013.26876

USDA (2008). *Soil quality indicators*. USDA Natural Resources Conservation Services. https://www.nrcs.usda.gov/sites/default/files/2023-01/Soil%20Quality-Indicators-Bulk%20Density.pdf

Verdi, A., & Naseri, M. (2024). Effects of tire wear particles on the water retention of soils with different textures in the full moisture range. *Journal of Contaminant Hydrology*, *264*. https://doi.org/10.1016/j.jconhyd.2024.104345

Verma, S. R. (2006). Impact of agricultural mechanization on production, productivity, cropping Intensity income generation and employment of labour: Status of farm mechanization in India. Punjab Agricultural University, Ludhiana.

Vieira, T., Ferreira, R. P., Kuchiishi, A. K., Bernucci, L. L. B., & Sinatora, A. (2015). Evaluation of friction mechanisms and wear rates on rubber tire materials by low-cost laboratory tests. *Wear*, *328–329*, 556–562. https://doi.org/10.1016/j.wear.2015.04.001

Vignola, F., Harlan, P., Perez, R., & Kmiecik, M. (2007). Analysis of satellite derived beam and global solar radiation data. *Solar Energy, 81*(6), 768–772. https://doi.org/10.1016/j.solener.2006.10.003

Vilgis, T. A., Heinrich, G., & M, K. (2009). *Reinforcement of polymer nano-composites: Theory, experiments and applications*. Cambridge University Press.

Walters, R. (2024). Soil, draft, and traction: Technical note 21. *Dirt Hog's Companion.* https://www.mendeley.com/reference-manager/reader/5766fb00-fd97-3137-b5d6-db09b240b1ec/3bfba67e-bcc5-ffbb-0932-1ec0d6e290f4

Wang, T. (2017*). Analysis on tyre wear: Modelling and simulations* [Master's thesis]. KTH Royal Institute of Technology, Stockholm, Sweden. https://www.diva-portal.org/smash/get/diva2:1416550/FULLTEXT01.pdf

Wennekes, W. (2008). *Adhesion of RFL-treated cords to rubber* [Doctoral dissertation, University of Twente, Enschede, Netherlands]. https://ris.utwente.nl/ws/portalfiles/portal/6085993/thesis_Wennekes.pdf

Wulfsohn, D. (2009). Chapter 2: Traction mechanics. Part II: Soil-tire contact area. In S. K. Upadhyaya, W.J. Chancellor, J.V. Perumpral, D. Wulfsohn, and T. R. Way (Eds.), *Advances in soil dynamics* (Vol. 3, pp. 59–84). American Society of Agricultural and Biological Engineers. https://doi.org/10.13031/2013.26869

Yahya, Azmi Bin, *A comparative study of radial and bias R-1 drive wheel tractor tires* (1985). Retrospective Theses and Dissertations. 16352. https://lib.dr.iastate.edu/rtd/16352

Zhang, S., Liu, Y., Zhou, H., Zhang, W., Chen, Y. & Zhu, H. (2023). Analysis of the effect of wear on tire cornering characteristics based on grounding characteristics. World Electric Vehicle Journal.14, 166. https://doi.org/10.3390/wevj14070166.

APPENDICES

APPENDIX A: FIGURES RELATED TO THE FIELD OF RESEARCH

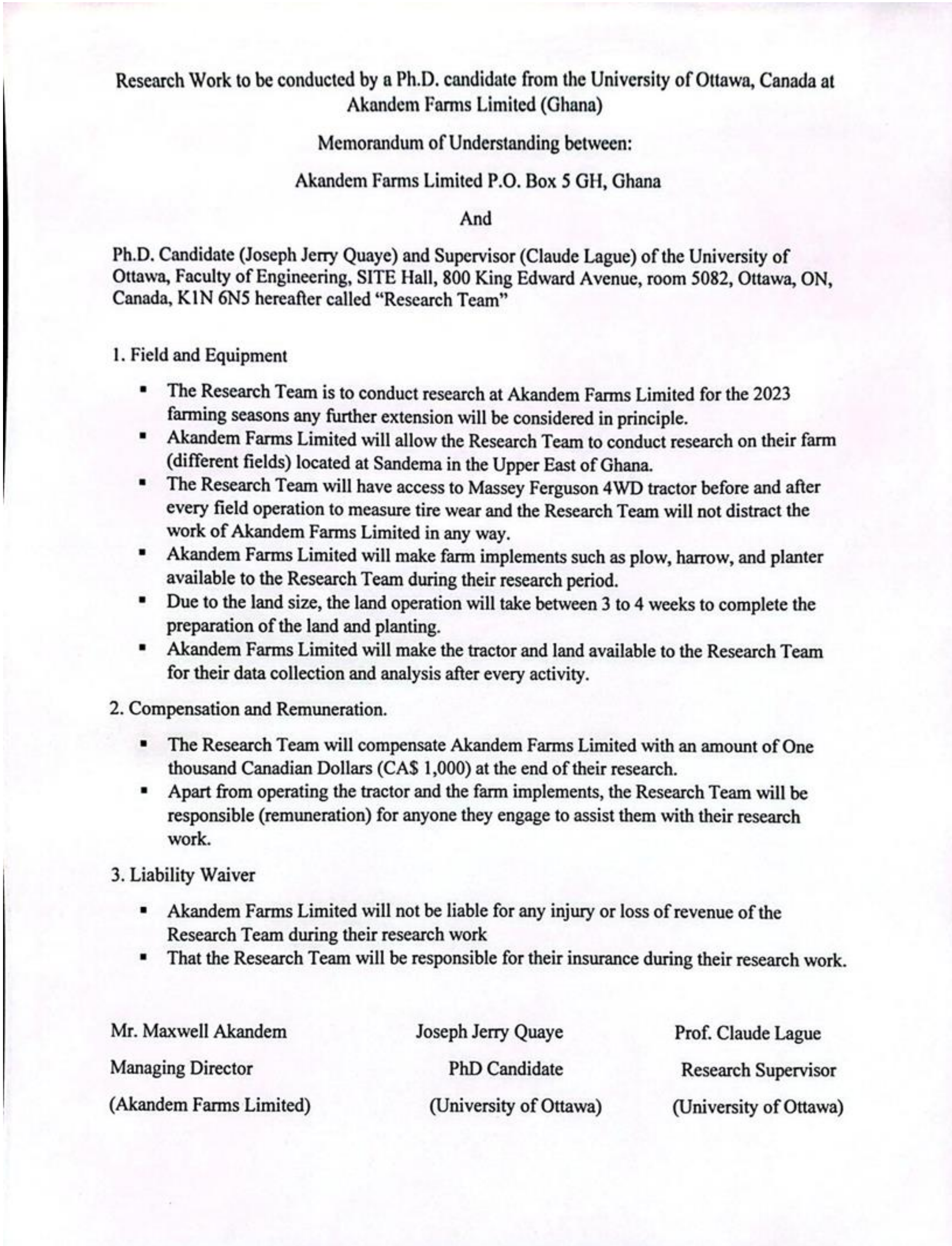

Research Work to be conducted by a Ph.D. candidate from the University of Ottawa, Canada at Akandem Farms Limited (Ghana)

Memorandum of Understanding between:

Akandem Farms Limited P.O. Box 5 GH, Ghana

And

Ph.D. Candidate (Joseph Jerry Quaye) and Supervisor (Claude Lague) of the University of Ottawa, Faculty of Engineering, SITE Hall, 800 King Edward Avenue, room 5082, Ottawa, ON, Canada, K1N 6N5 hereafter called "Research Team"

1. Field and Equipment

- The Research Team is to conduct research at Akandem Farms Limited for the 2023 farming seasons any further extension will be considered in principle.
- Akandem Farms Limited will allow the Research Team to conduct research on their farm (different fields) located at Sandema in the Upper East of Ghana.
- The Research Team will have access to Massey Ferguson 4WD tractor before and after every field operation to measure tire wear and the Research Team will not distract the work of Akandem Farms Limited in any way.
- Akandem Farms Limited will make farm implements such as plow, harrow, and planter available to the Research Team during their research period.
- Due to the land size, the land operation will take between 3 to 4 weeks to complete the preparation of the land and planting.
- Akandem Farms Limited will make the tractor and land available to the Research Team for their data collection and analysis after every activity.

2. Compensation and Remuneration.

- The Research Team will compensate Akandem Farms Limited with an amount of One thousand Canadian Dollars (CA$ 1,000) at the end of their research.
- Apart from operating the tractor and the farm implements, the Research Team will be responsible (remuneration) for anyone they engage to assist them with their research work.

3. Liability Waiver

- Akandem Farms Limited will not be liable for any injury or loss of revenue of the Research Team during their research work
- That the Research Team will be responsible for their insurance during their research work.

Mr. Maxwell Akandem	Joseph Jerry Quaye	Prof. Claude Lague
Managing Director	PhD Candidate	Research Supervisor
(Akandem Farms Limited)	(University of Ottawa)	(University of Ottawa)

Figure A1. Memorandum of understanding between Akandem Farms Limited and the University of Ottawa.

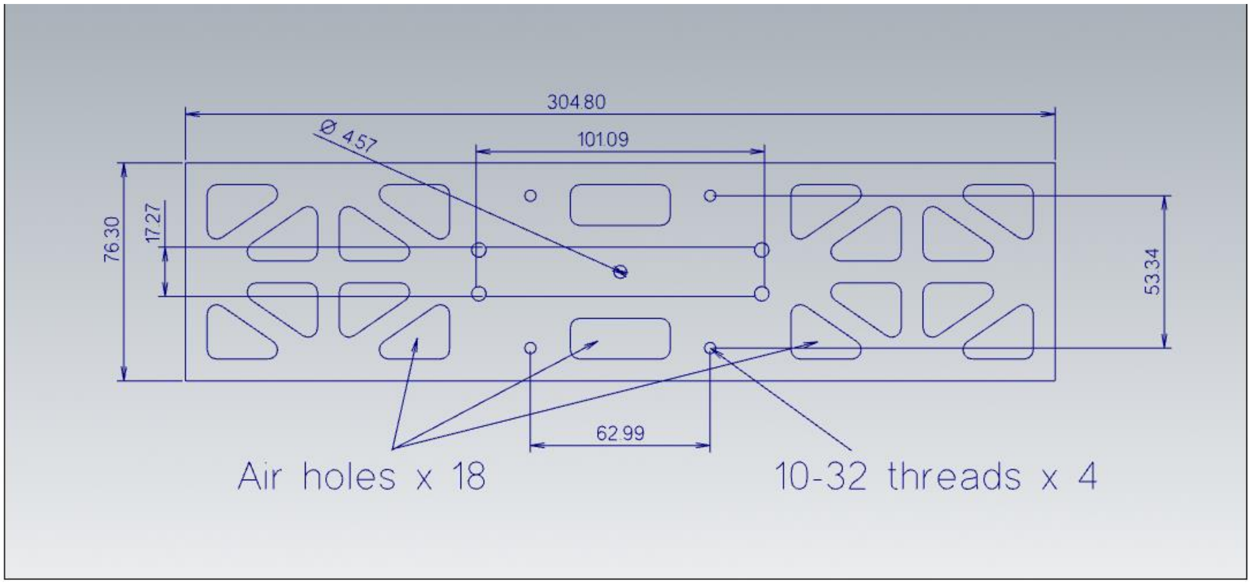

Figure A2. Detailed drawing of the fabricated base.


(a) Field 2


(b) Field 3

Figure A3. Areas of gravel on fields 2 and 3.

Note. Sections of (a) Field 2 and (b) Field 3 containing gravel.

(a)

(b)

(c)

(d)

Figure A4. Sections of the farm at various stages of operation.

Note. (a) Appearance of the field before any operation was started, (b) tractor plowing the field, (c) tractor harrowing the field, (d) image of field after planting had been done.

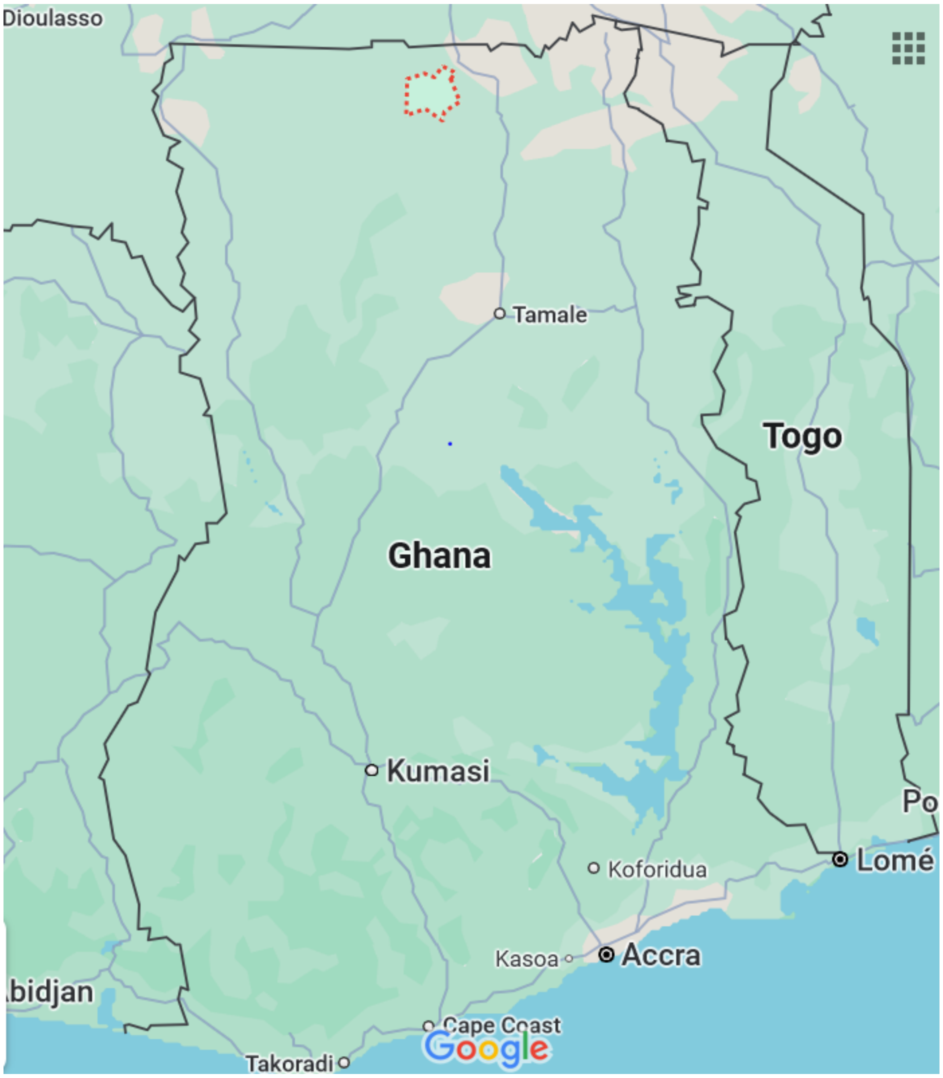

Figure A5. Location of the research site in Ghana.

Note. The red dotted area on the map shows the location of the research site in Ghana (Source: Google Maps).

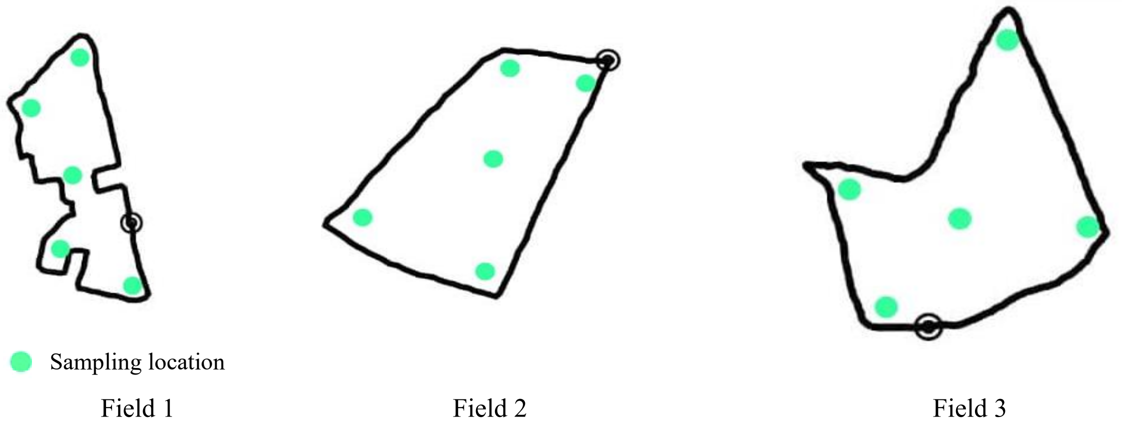

Figure A6. The five sampling locations in each field.

Note. All fields have a flat topography. Size and location: Field 1 is 9.7 ha (latitude, 10°41'54.8"N; longitude, 1°16'52.8"W), Field 2 is 15 ha (latitude, 10°47'17.5"N; longitude, 1°11'11.1"W), and Field 3 is 16.2 ha (latitude, 10°47'10.7"N; longitude, 1°11'11.1"W). The circled black dot on the edge of each figure shows where the reading of the border of each field started and ended.

Figure A7. The trajectory of how the operator plowed the land

APPENDIX B: DATA FROM THE 2023 AND 2024 FARMING SEASONS AND ANALYSES

Table B1. Draft force, slip, and tractor operating speed for each field operation on each field.

Type of operation	Draft force (kN)		Slip (%)		Operation speed (km/h)		Implement width (m or rows)	
	2023	2024	2023	2024	2023	2024	2023	2024
Field 1								
Plowing	12.82	12.61	14.20	14.95	7.20	7.00	0.51 m	0.51 m
Harrowing	7.59	6.81	8.54	8.52	9.20	9.32	1.79 m	1.79 m
Planting	11.81	11.81	9.20	9.21	7.90	7.75	4 rows	4 rows
Field 2								
Plowing	13.47	13.35	14.83	15.90	7.80	7.70	0.51	0.51
Harrowing	7.81	6.88	5.32	5.32	10.10	9.60	1.79	1.79
Planting	11.81	11.81	6.61	6.61	8.20	8.15	4 rows	4 rows
Field 3								
Plowing	13.24	13.13	14.49	14.00	7.60	7.51	0.51	0.51
Harrowing	7.74	6.86	4.95	5.90	9.80	9.50	1.79	1.79
Planting	11.81	11.81	5.90	6.22	8.00	7.65	4 rows	4 rows

Table B2. SPSS analysis results for the front left tire.

Parameter	Coefficients	Standard error	t stat	P-value	Lower 95%	Upper 95%	Lower 95.0%	Upper 95.0%
Intercept	0.000278	0.000329	0.843786	0.401705	-0.00038	0.000934	-0.00038	0.000934
Draft	2.88E-05	2.94E-05	0.980198	0.330413	-3E-05	8.75E-05	-3E-05	8.75E-05
Intercept	0.000268	0.00017	1.580783	0.118501	-7E-05	0.000607	-7E-05	0.000607
Slip	3.5E-05	1.68E-05	2.083526	0.04091	1.49E-06	6.85E-05	1.49E-06	6.85E-05
Intercept	0.002084	0.000571	3.648192	0.000509	0.000944	0.003224	0.000944	0.003224
Speed	-0.00018	6.75E-05	-2.62661	0.010616	-0.00031	-4.3E-05	-0.00031	-4.3E-05
Intercept	0.011546	0.001781	6.484358	1.13E-08	0.007994	0.015098	0.007994	0.015098
Bulk density	-0.0067	0.001089	-6.15402	4.37E-08	-0.00888	-0.00453	-0.00888	-0.00453

Note. These results were used to determine the model for predicting the tire wear rate of the front left tire.

Table B3. SPSS analysis results for the front right tire.

Parameter	Coefficients	Standard error	t stat	P-value	95% confidence intervals			
					Lower limit	Upper limit	Lower limit	Upper limit
Intercept	0.000234	0.000379	0.617278	0.539144	-0.00052	0.00099	-0.00052	0.00099
Draft	3.75E-05	3.41E-05	1.100498	0.275054	-3.1E-05	0.000105	-3.1E-05	0.000105
Intercept	0.002404	0.000671	3.582727	0.000639	0.001065	0.003744	0.001065	0.003744
Speed	-0.00021	7.9E-05	-2.64531	0.010159	-0.00037	-5.1E-05	-0.00037	-5.1E-05
Intercept	0.014107	0.002423	5.822326	1.8E-07	0.009271	0.018944	0.009271	0.018944
Bulk density	-0.00826	0.001485	-5.55994	5.07E-07	-0.01122	-0.00529	-0.01122	-0.00529

Note. These results were used to determine the model for predicting the wear rate of the front right tire.

Table B4. SPSS analysis results for the rear left tire.

Parameter	Coefficients	Standard error	t stat	P-value	95% confidence intervals			
					Lower limit	Upper limit	Lower limit	Upper limit
Intercept	0.000327	0.000387	0.845461	0.400776	-0.00045	0.0011	-0.00045	0.0011
Draft	3.39E-05	3.46E-05	0.978441	0.331275	-3.5E-05	0.000103	-3.5E-05	0.000103
Intercept	0.000316	0.0002	1.580925	0.118469	-8.3E-05	0.000714	-8.3E-05	0.000714
Slip	4.12E-05	1.98E-05	2.083354	0.040926	1.75E-06	8.06E-05	1.75E-06	8.06E-05
Intercept	0.002451	0.000672	3.646687	0.000511	0.00111	0.003792	0.00111	0.003792
Speed	-0.00021	7.94E-05	-2.62515	0.010658	-0.00037	-5E-05	-0.00037	-5E-05
Intercept	0.013583	0.002095	6.484065	1.13E-08	0.009404	0.017762	0.009404	0.017762
Bulk density	-0.00789	0.001281	-6.15373	4.37E-08	-0.01044	-0.00533	-0.01044	-0.00533

Note. These results were used to determine the model for predicting the wear rate of the rear left tire.

Table B5. SPSS analysis results for the rear right tire.

Parameter	Coefficients	Standard error	t stat	P-value	95% confidence intervals			
					Lower limit	Upper limit	Lower limit	Upper limit
Intercept	0.000275	0.000446	0.617278	0.539144	-0.00061	0.001164	-0.00061	0.001164
Draft	4.41E-05	4.01E-05	1.100498	0.275054	-3.6E-05	0.000124	-3.6E-05	0.000124
Intercept	0.002829	0.000789	3.582727	0.000639	0.001253	0.004404	0.001253	0.004404
Speed	-0.00025	9.29E-05	-2.64531	0.010159	-0.00043	-6E-05	-0.00043	-6E-05
Intercept	0.016942	0.00271	6.252482	3.21E-08	0.011534	0.02235	0.011534	0.02235
Bulk density	-0.00993	0.001662	-5.97663	9.74E-08	-0.01325	-0.00662	-0.01325	-0.00662

Note. These results were used to determine the model to predict the wear rate for the rear right tire.

Table B6. Summary output of ANOVA text for measured and predicted wear of the front left tire model.

SUMMARY OUTPUT

Regression statistics	
Multiple R	0.856315
R square	0.733276
Adjusted R square	0.729411
Standard error	0.000263
Observations	71

ANOVA

	df	SS	MS	F	Significance F
Regression	1	1.31E-05	1.31E-05	189.6945	1.76E-21
Residual	69	4.78E-06	6.92E-08		
Total	70	1.79E-05			

	Coefficients	Standard error	t stat	P-value	Lower 95%	Upper 95%	Lower 95.0%	Upper 95.0%
Intercept	0.000222	5.2E-05	4.270443	6.11E-05	0.000118	0.000326	0.000118	0.000326
Predicted wear	0.732414	0.053178	13.77296	1.76E-21	0.626327	0.8385	0.626327	0.8385

Note. ANOVA analysis used to determine Pearson's correlation and the coefficient of determination between the measured value and the predicted value of the wear rate of the front left tire model.

ANOVA = analysis of variance; df = degrees of freedom; F = F statistic; MS = mean sum of squares; SS = sum of squares. Significance F is the p-value for the F statistic.

Table B7. Summary output of ANOVA text for measured and predicted wear of the front right tire model.

SUMMARY OUTPUT

Regression statistics	
Multiple R	0.877452
R square	0.769921
Adjusted R square	0.766487
Standard error	0.000249
Observations	69

ANOVA

	df	SS	MS	F	Significance F
Regression	1	1.4E-05	1.4E-05	224.2047	4.62E-23
Residual	67	4.17E-06	6.22E-08		
Total	68	1.81E-05			

	Coefficients	Standard error	t stat	P-value	Lower 95%	Upper 95%	Lower 95.0%	Upper 95.0%
Intercept	9.74E-05	5.74E-05	1.69659	0.094416	-1.7E-05	0.000212	-1.7E-05	0.000212
Predicted wear	0.834048	0.055702	14.97347	4.62E-23	0.722867	0.945229	0.722867	0.945229

Note. ANOVA analysis used to determine Pearson's correlation and the coefficient of determination between the measured value and the predicted value of the wear rate of the front right tire model.

ANOVA = analysis of variance; df = degrees of freedom; F = F statistic; MS = mean sum of squares; SS = sum of squares. Significance F is the p-value for the F statistic.

Table B8. Summary output of ANOVA for measured and predicted wear of the rear left tire model.

SUMMARY OUTPUT

Regression statistics	
Multiple R	0.721861
R square	0.521083
Adjusted R square	0.514142
Standard error	0.000398
Observations	71

ANOVA

	df	SS	MS	F	Significance F
Regression	1	1.19E-05	1.19E-05	75.07505	1.22E-12
Residual	69	1.09E-05	1.58E-07		
Total	70	2.28E-05			

	Coefficients	Standard error	t stat	P-value	Lower 95%	Upper 95%	Lower 95.0%	Upper 95.0%
Intercept	0.000251	8.29E-05	3.028338	0.003457	8.57E-05	0.000417	8.57E-05	0.000417
Predicted wear	0.593674	0.068517	8.664586	1.22E-12	0.456986	0.730362	0.456986	0.730362

Note. ANOVA analysis used to determine Pearson's correlation and the coefficient of determination between the measured value and the predicted value of the wear rate of the rear left tire model.

ANOVA = analysis of variance; df = degrees of freedom; F = F statistic; MS = mean sum of squares; SS = sum of squares. Significance F is the p-value for the F statistic.

Table B9. Summary output of ANOVA for measured and predicted wear of the rear right tire model.

SUMMARY OUTPUT

Regression statistics	
Multiple R	0.748574
R square	0.560363
Adjusted R square	0.553801
Standard error	0.00046
Observations	69

ANOVA

	df	SS	MS	F	Significance F
Regression	1	1.81E-05	1.81E-05	85.39846	1.42E-13
Residual	67	1.42E-05	2.12E-07		
Total	68	3.22E-05			

	Coefficients	Standard error	t stat	P-value	Lower 95%	Upper 95%	Lower 95.0%	Upper 95.0%
Intercept	0.000197	0.00011	1.793058	0.077477	-2.2E-05	0.000417	-2.2E-05	0.000417
Predicted wear	0.769117	0.083228	9.241129	1.42E-13	0.602994	0.93524	0.602994	0.93524

Note. ANOVA analysis used to determine Pearson's correlation and the coefficient of determination between the measured value and the predicted value of the wear rate of the rear right tire model.

ANOVA = analysis of variance; df = degrees of freedom; F = F statistic; MS = mean sum of squares; SS = sum of squares. Significance F is the p-value for the F statistic.

Table B10. Data collected for the front left tire.

Field operation	Lug position	Tire section	Wear (mm/km)	Draft (kN)	Slip (%)	Speed (km/h)	Bulk density (g/cm^3)	Moisture (%)
FIELD 1								
Plowing	Outer	1	0.0016163	12.82	14.2	7.2	1.528	10.02
		2	0.000897	12.82	14.2	7.2	1.528	10.02
		3	0.0017186	12.82	14.2	7.2	1.528	10.02
		4	0.000919	12.82	14.2	7.2	1.528	10.02
	Inner	1	0.0031542	12.82	14.2	7.2	1.528	10.02
		2	0.002327	12.82	14.2	7.2	1.528	10.02
		3	0.0017065	12.82	14.2	7.2	1.528	10.02
		4	0.008416	12.82	14.2	7.2	1.528	10.02

Field operation	Lug position	Tire section	Wear (mm/km)	Draft (kN)	Slip (%)	Speed (km/h)	Bulk density (g/cm^3)	Moisture (%)
Harrowing	Outer	1	0.000927	7.59	8.54	9.2	1.631	7.29
		2	0.0005104	7.59	8.54	9.2	1.631	7.29
		3	0.0001841	7.59	8.54	9.2	1.631	7.29
		4	0.0005546	7.59	8.54	9.2	1.631	7.29
	Inner	1	0.0010185	7.59	8.54	9.2	1.631	7.29
		2	0.0018779	7.59	8.54	9.2	1.631	7.29
		3	0.0008208	7.59	8.54	9.2	1.631	7.29
Planting	Outer	1	0.0009575	11.81	9.2	7.9	1.623	5.48
		2	0.0006607	11.81	9.2	7.9	1.623	5.48
		3	0.0008268	11.81	9.2	7.9	1.623	5.48
		4	0.0009548	11.81	9.2	7.9	1.623	5.48
	Inner	1	0.0002473	11.81	9.2	7.9	1.623	5.48
		2	0.0001326	11.81	9.2	7.9	1.623	5.48
		3	0.0013588	11.81	9.2	7.9	1.623	5.48
		4	0.0008254	11.81	9.2	7.9	1.623	5.48
FIELD 2								
Plowing	Outer	1	0.0004632	13.47	14.83	7.8	1.623	4.83
		2	0.0004709	13.47	14.83	7.8	1.623	4.83
		3	0.0000853	13.47	14.83	7.8	1.623	4.83
		4	0.0002664	13.47	14.83	7.8	1.623	4.83
	Inner	1	0.0002585	13.47	14.83	7.8	1.623	4.83
		2	0.0000334	13.47	14.83	7.8	1.623	4.83
		3	0.0003547	13.47	14.83	7.8	1.623	4.83
		4	0.0005416	13.47	14.83	7.8	1.623	4.83
Harrowing	Outer	1	0.0009131	7.81	5.32	10.1	1.631	4.36
		2	0.0002035	7.81	5.32	10.1	1.631	4.36
		3	0.0001572	7.81	5.32	10.1	1.631	4.36
		4	0.0004212	7.81	5.32	10.1	1.631	4.36
	Inner	1	0.0005234	7.81	5.32	10.1	1.631	4.36
		2	0.0003405	7.81	5.32	10.1	1.631	4.36
		3	0.0003545	7.81	5.32	10.1	1.631	4.36
		4	0.0002093	7.81	5.32	10.1	1.631	4.36
Planting	Outer	1	0.0005133	11.81	6.11	8.2	1.638	8.13
		2	0.0004766	11.81	6.11	8.2	1.638	8.13
		3	0.0004983	11.81	6.11	8.2	1.638	8.13
		4	0.0002906	11.81	6.11	8.2	1.638	8.13
	Inner	1	0.0009008	11.81	6.11	8.2	1.638	8.13
		2	0.0012411	11.81	6.11	8.2	1.638	8.13
		3	0.0002535	11.81	6.11	8.2	1.638	8.13
		4	0.0002095	11.81	6.11	8.2	1.638	8.13

Field operation	Lug position	Tire section	Wear (mm/km)	Draft (kN)	Slip (%)	Speed (km/h)	Bulk density (g/cm^3)	Moisture (%)
FIELD 3								
Plowing	Outer	1	0.0002336	13.24	14.49	7.6	1.63	4.8
		2	0.0002427	13.24	14.49	7.6	1.63	4.8
		3	0.0002342	13.24	14.49	7.6	1.63	4.8
		4	0.0002036	13.24	14.49	7.6	1.63	4.8
	Inner	1	0.0001601	13.24	14.49	7.6	1.63	4.8
		2	0.0001706	13.24	14.49	7.6	1.63	4.8
		3	0.0001573	13.24	14.49	7.6	1.63	4.8
		4	0.0002027	13.24	14.49	7.6	1.63	4.8
Harrowing	Outer	1	0.0002283	7.74	4.95	9.8	1.667	4.33
		2	0.0002173	7.74	4.95	9.8	1.667	4.33
		3	0.0002159	7.74	4.95	9.8	1.667	4.33
		4	0.0002249	7.74	4.95	9.8	1.667	4.33
	Inner	1	0.0004201	7.74	4.95	9.8	1.667	4.33
		2	0.000156	7.74	4.95	9.8	1.667	4.33
		3	0.0003001	7.74	4.95	9.8	1.667	4.33
		4	0.0001551	7.74	4.95	9.8	1.667	4.33
Planting	Outer	1	0.0001137	11.81	5.9	8	1.734	7.9
		2	0.0001232	11.81	5.9	8	1.734	7.9
		3	0.0005625	11.81	5.9	8	1.734	7.9
		4	0.0001889	11.81	5.9	8	1.734	7.9
	Inner	1	0.0004457	11.81	5.9	8	1.734	7.9
		2	0.0004306	11.81	5.9	8	1.734	7.9
		3	0.0000685	11.81	5.9	8	1.734	7.9
		4	0.0004663	11.81	5.9	8	1.734	7.9

Table B11. Data collected for the front right tire.

Field operation	Lug position	Tire section	Wear (mm/km)	Draft (kN)	Slip (%)	Speed (km/h)	Bulk density (g/cm^3)	Moisture (%)
FIELD 1								
Plowing	Outer	1	0.0014351	12.82	14.2	7.2	1.528	10.02
		2	0.0019197	12.82	14.2	7.2	1.528	10.02
		3	0.0007086	12.82	14.2	7.2	1.528	10.02
		4	0.0025854	12.82	14.2	7.2	1.528	10.02
	Inner	1	0.0005057	12.82	14.2	7.2	1.528	10.02
		2	0.0021975	12.82	14.2	7.2	1.528	10.02
		3	0.0024121	12.82	14.2	7.2	1.58	10.02
		4	0.002778	12.82	14.2	7.2	1.528	10.02

Field operation	Lug position	Tire section	Wear (mm/km)	Draft (kN)	Slip (%)	Speed (km/h)	Bulk density (g/cm^3)	Moisture (%)
Harrowing	Outer	1	0.0002326	7.59	8.54	9.2	1.631	7.29
		2	0.000822	7.59	8.54	9.2	1.631	7.29
		3	0.0010369	7.59	8.54	9.2	1.631	7.29
		4	0.0016439	7.59	8.54	9.2	1.631	7.29
	Inner	1	0.0024356	7.59	8.54	9.2	1.631	7.29
		2	0.0000907	7.59	8.54	9.2	1.631	7.29
		3	0.0005202	7.59	8.54	9.2	1.631	7.29
		4	0.0000773	7.59	8.54	9.2	1.631	7.29
Planting	Outer	1	0.0004068	11.81	9.2	7.9	1.623	5.48
		2	0.000811	11.81	9.2	7.9	1.623	5.48
		3	0.0007955	11.81	9.2	7.9	1.623	5.48
		4	0.0009755	11.81	9.2	7.9	1.623	5.48
	Inner	1	0.0004355	11.81	9.2	7.9	1.623	5.48
		2	0.0008358	11.81	9.2	7.9	1.623	5.48
		3	0.0011303	11.81	9.2	7.9	1.623	5.48
		4	0.0017585	11.81	9.2	7.9	1.623	5.48
FIELD 2								
Plowing	Outer	1	0.0004733	13.47	14.83	7.8	1.623	4.83
		2	0.0002348	13.47	14.83	7.8	1.623	4.83
		3	0.0000659	13.47	14.83	7.8	1.623	4.83
		4	0.0000473	13.47	14.83	7.8	1.623	4.83
	Inner	1	0.0003931	13.47	14.83	7.8	1.623	4.83
		2	0.0002438	13.47	14.83	7.8	1.623	4.83
		3	0.0004525	13.47	14.83	7.8	1.623	4.83
		4	0.0005405	13.47	14.83	7.8	1.623	4.83
Harrowing	Outer	1	0.0005776	7.81	5.32	10.1	1.631	4.36
		2	0.0000212	7.81	5.32	10.1	1.631	4.36
		3	0.0000986	7.81	5.32	10.1	1.631	4.36
		4	0.0001587	7.81	5.32	10.1	1.631	4.36
	Inner	1	0.0014434	7.81	5.32	10.1	1.631	4.36
		2	0.0002208	7.81	5.32	10.1	1.631	4.36
		3	0.0000915	7.81	5.32	10.1	1.631	4.36
		4	0.000328	7.81	5.32	10.1	1.631	4.36

Field operation	Lug position	Tire section	Wear (mm/km)	Draft (kN)	Slip (%)	Speed (km/h)	Bulk density (g/cm^3)	Moisture (%)
Planting	Outer	1	0.0001046	11.81	6.11	8.2	1.64	8.13
		2	0.0003901	11.81	6.11	8.2	1.64	8.13
		3	0.0006654	11.81	6.11	8.2	1.64	8.13
		4	0.0012782	11.81	6.11	8.2	1.64	8.13
	Inner	1	0.0004274	11.81	6.11	8.2	1.64	8.13
		2	0.0006846	11.81	6.11	8.2	1.64	8.13
		3	0.0000743	11.81	6.11	8.2	1.64	8.13
		4	0.0007563	11.81	6.11	8.2	1.64	8.13
FIELD 3								
Plowing	Outer	1	0.0001955	13.24	14.49	7.6	1.63	4.8
		2	0.0003334	13.24	14.49	7.6	1.63	4.8
		3	0.0003334	13.24	14.49	7.6	1.63	4.8
		4	0.0001319	13.24	14.49	7.6	1.63	4.8
	Inner	1	0.0002193	13.24	14.49	7.6	1.63	4.8
		2	0.0002583	13.24	14.49	7.6	1.63	4.8
		3	0.0002229	13.24	14.49	7.6	1.63	4.8
		4	0.0001461	13.24	14.49	7.6	1.63	4.8
Harrowing	Outer	1	0.0001013	7.74	4.95	9.8	1.667	4.33
		2	0.0003559	7.74	4.95	9.8	1.667	4.33
		3	0.0004538	7.74	4.95	9.8	1.667	4.33
		4	0.0001768	7.74	4.95	9.8	1.667	4.33
	Inner	1	0.0002374	7.74	4.95	9.8	1.667	4.33
		2	0.0000733	7.74	4.95	9.8	1.667	4.33
		3	0.0001973	7.74	4.95	9.8	1.667	4.33
		4	0.0003945	7.74	4.95	9.8	1.667	4.33
Planting	Outer	1	0.0005353	11.81	5.9	8	1.734	7.9
		2	0.0005349	11.81	5.9	8	1.734	7.9
		3	0.0000685	11.81	5.9	8	1.734	7.9
	Inner	1	0.0001751	11.81	5.9	8	1.734	7.9
		2	0.000142	11.81	5.9	8	1.734	7.9

Table B12. Data collected for the rear left tire.

Field operation	Lug position	Tire section	Wear (mm/km)	Draft (kN)	Slip (%)	Speed (km/h)	Bulk density (g/cm^3)	Moisture (%)
FIELD 1								
Plowing	Outer	1	0.002008	12.82	14.2	7.2	1.53	10.02
		2	0.001081	12.82	14.2	7.2	1.53	10.02
		3	0.002022	12.82	14.2	7.2	1.53	10.02
		4	0.001902	12.82	14.2	7.2	1.53	10.02
	Inner	1	0.003711	12.82	14.2	7.2	1.53	10.02
		2	0.002738	12.82	14.2	7.2	1.53	10.02
		3	0.001055	12.82	14.2	7.2	1.53	10.02
		4	0.000990	12.82	14.2	7.2	1.53	10.02
Harrowing	Outer	1	0.000971	7.59	8.54	9.2	1.63	7.29
		2	0.001198	7.59	8.54	9.2	1.63	7.29
		3	0.001091	7.59	8.54	9.2	1.63	7.29
		4	0.000652	7.59	8.54	9.2	1.63	7.29
	Inner	1	0.000217	7.59	8.54	9.2	1.63	7.29
		2	0.002209	7.59	8.54	9.2	1.63	7.29
		3	0.000600	7.59	8.54	9.2	1.63	7.29
Planting	Outer	1	0.001126	11.81	9.2	7.9	1.62	5.48
		2	0.000291	11.81	9.2	7.9	1.62	5.48
		3	0.000973	11.81	9.2	7.9	1.62	5.48
		4	0.001123	11.81	9.2	7.9	1.62	5.48
	Inner	1	0.000966	11.81	9.2	7.9	1.62	5.48
		2	0.000777	11.81	9.2	7.9	1.62	5.48
		3	0.001599	11.81	9.2	7.9	1.62	5.48
		4	0.001560	11.81	9.2	7.9	1.62	5.48
FIELD 2								
Plowing	Outer	1	0.000545	13.47	14.83	7.8	1.62	4.83
		2	0.000637	13.47	14.83	7.8	1.62	4.83
		3	0.000313	13.47	14.83	7.8	1.62	4.83
		4	0.000039	13.47	14.83	7.8	1.62	4.83
	Inner	1	0.000304	13.47	14.83	7.8	1.62	4.83
		2	0.000554	13.47	14.83	7.8	1.62	4.83
		3	0.000417	13.47	14.83	7.8	1.62	4.83
		4	0.000100	13.47	14.83	7.8	1.62	4.83

Field operation	Lug position	Tire section	Wear (mm/km)	Draft (kN)	Slip (%)	Speed (km/h)	Bulk density (g/cm^3)	Moisture (%)
Harrowing	Outer	1	0.000246	7.81	5.32	10.1	1.63	4.36
		2	0.000239	7.81	5.32	10.1	1.63	4.36
		3	0.001074	7.81	5.32	10.1	1.63	4.36
		4	0.000496	7.81	5.32	10.1	1.63	4.36
	Inner	1	0.000185	7.81	5.32	10.1	1.63	4.36
		2	0.000401	7.81	5.32	10.1	1.63	4.36
		3	0.000417	7.81	5.32	10.1	1.63	4.36
		4	0.000616	7.81	5.32	10.1	1.63	4.36
Planting	Outer	1	0.000604	11.81	6.11	8.2	1.64	8.13
		2	0.000246	11.81	6.11	8.2	1.64	8.13
		3	0.000586	11.81	6.11	8.2	1.64	8.13
		4	0.000561	11.81	6.11	8.2	1.64	8.13
	Inner	1	0.001060	11.81	6.11	8.2	1.64	8.13
		2	0.001460	11.81	6.11	8.2	1.64	8.13
		3	0.000298	11.81	6.11	8.2	1.64	8.13
		4	0.000342	11.81	6.11	8.2	1.64	8.13
FIELD 3								
Plowing	Outer	1	0.000275	13.24	14.49	7.6	1.63	4.8
		2	0.000238	13.24	14.49	7.6	1.63	4.8
		3	0.000276	13.24	14.49	7.6	1.63	4.8
		4	0.000286	13.24	14.49	7.6	1.63	4.8
	Inner	1	0.000201	13.24	14.49	7.6	1.63	4.8
		2	0.000239	13.24	14.49	7.6	1.63	4.8
		3	0.000185	13.24	14.49	7.6	1.63	4.8
		4	0.000188	13.24	14.49	7.6	1.63	4.8
Harrowing	Outer	1	0.000269	7.74	4.95	9.8	1.67	4.33
		2	0.000183	7.74	4.95	9.8	1.67	4.33
		3	0.000254	7.74	4.95	9.8	1.67	4.33
		4	0.000353	7.74	4.95	9.8	1.67	4.33
	Inner	1	0.000494	7.74	4.95	9.8	1.67	4.33
		2	0.000184	7.74	4.95	9.8	1.67	4.33
		3	0.000256	7.74	4.95	9.8	1.67	4.33
		4	0.000265	7.74	4.95	9.8	1.67	4.33

Field operation	Lug position	Tire section	Wear (mm/km)	Draft (kN)	Slip (%)	Speed (km/h)	Bulk density (g/cm^3)	Moisture (%)
Planting	Outer	1	0.000222	11.81	5.9	8	1.73	7.9
		2	0.000549	11.81	5.9	8	1.73	7.9
		3	0.000662	11.81	5.9	8	1.73	7.9
		4	0.000145	11.81	5.9	8	1.73	7.9
	Inner	1	0.000524	11.81	5.9	8	1.73	7.9
		2	0.000134	11.81	5.9	8	1.73	7.9
		3	0.000081	11.81	5.9	8	1.73	7.9
		4	0.000507	11.81	5.9	8	1.73	7.9

Table B13. Data collected for the rear right tire.

Field operation	Lug position	Tire section	Wear (mm/km)	Draft (kN)	Slip (%)	Speed (km/h)	Bulk density (g/cm^3)	Moisture (%)
FIELD 1								
Plowing	Outer	1	0.002258	12.82	14.2	7.2	1.528	10.02
		2	0.001688	12.82	14.2	7.2	1.528	10.02
		3	0.000834	12.82	14.2	7.2	1.528	10.02
		4	0.003042	12.82	14.2	7.2	1.528	10.02
	Inner	1	0.000595	12.82	14.2	7.2	1.528	10.02
		2	0.002838	12.82	14.2	7.2	1.528	10.02
		3	0.002585	12.82	14.2	7.2	1.528	10.02
		4	0.003268	12.82	14.2	7.2	1.528	10.02
Harrowing	Outer	1	0.000274	7.59	8.54	9.2	1.631	7.29
		2	0.001934	7.59	8.54	9.2	1.631	7.29
		3	0.001220	7.59	8.54	9.2	1.631	7.29
		4	0.000967	7.59	8.54	9.2	1.631	7.29
	Inner	1	0.002865	7.59	8.54	9.2	1.631	7.29
		2	0.000612	7.59	8.54	9.2	1.631	7.29
		3	0.000107	7.59	8.54	9.2	1.631	7.29
		4	0.000091	7.59	8.54	9.2	1.631	7.29

Field operation	Lug position	Tire section	Wear (mm/km)	Draft (kN)	Slip (%)	Speed (km/h)	Bulk density (g/cm^3)	Moisture (%)
Planting	Outer	1	0.001148	11.81	9.2	7.9	1.623	5.48
		2	0.000936	11.81	9.2	7.9	1.623	5.48
		3	0.000954	11.81	9.2	7.9	1.623	5.48
		4	0.000479	11.81	9.2	7.9	1.623	5.48
	Inner	1	0.000512	11.81	9.2	7.9	1.623	5.48
		2	0.001330	11.81	9.2	7.9	1.623	5.48
		3	0.002069	11.81	9.2	7.9	1.623	5.48
		4	0.000983	11.81	9.2	7.9	1.623	5.48
FIELD 2								
Plowing	Outer	1	0.000557	13.47	14.83	7.8	1.623	4.83
		2	0.000532	13.47	14.83	7.8	1.623	4.83
		3	0.000078	13.47	14.83	7.8	1.623	4.83
		4	0.000636	13.47	14.83	7.8	1.623	4.83
	Inner	1	0.000463	13.47	14.83	7.8	1.623	4.83
		2	0.000556	13.47	14.83	7.8	1.623	4.83
		3	0.000287	13.47	14.83	7.8	1.623	4.83
		4	0.000276	13.47	14.83	7.8	1.623	4.83
Harrowing	Outer	1	0.000260	7.81	5.32	10.1	1.631	4.36
		2	0.000680	7.81	5.32	10.1	1.631	4.36
		3	0.001698	7.81	5.32	10.1	1.631	4.36
		4	0.000187	7.81	5.32	10.1	1.631	4.36
	Inner	1	0.000249	7.81	5.32	10.1	1.631	4.36
		2	0.000386	7.81	5.32	10.1	1.631	4.36
		3	0.000108	7.81	5.32	10.1	1.631	4.36
		4	0.000116	7.81	5.32	10.1	1.631	4.36
Planting	Outer	1	0.000123	11.81	6.11	8.2	1.638	8.13
		2	0.000459	11.81	6.11	8.2	1.638	8.13
		3	0.000890	11.81	6.11	8.2	1.638	8.13
		4	0.000087	11.81	6.11	8.2	1.638	8.13
	Inner	1	0.000783	11.81	6.11	8.2	1.638	8.13
		2	0.000805	11.81	6.11	8.2	1.638	8.13
		3	0.000503	11.81	6.11	8.2	1.638	8.13
		4	0.001504	11.81	6.11	8.2	1.638	8.13

Field operation	Lug position	Tire section	Wear (mm/km)	Draft (kN)	Slip (%)	Speed (km/h)	Bulk density (g/cm^3)	Moisture (%)
FIELD 3								
Plowing	Outer	1	0.000230	13.24	14.49	7.6	1.63	4.8
		2	0.000172	13.24	14.49	7.6	1.63	4.8
		3	0.000392	13.24	14.49	7.6	1.63	4.8
		4	0.000392	13.24	14.49	7.6	1.63	4.8
	Inner	1	0.000258	13.24	14.49	7.6	1.63	4.8
		2	0.000155	13.24	14.49	7.6	1.63	4.8
		3	0.000304	13.24	14.49	7.6	1.63	4.8
		4	0.000262	13.24	14.49	7.6	1.63	4.8
Harrowing	Outer	1	0.000232	7.74	4.95	9.8	1.667	4.33
		2	0.000208	7.74	4.95	9.8	1.667	4.33
		3	0.000534	7.74	4.95	9.8	1.667	4.33
		4	0.000119	7.74	4.95	9.8	1.667	4.33
	Inner	1	0.000419	7.74	4.95	9.8	1.667	4.33
		2	0.000086	7.74	4.95	9.8	1.667	4.33
		3	0.000279	7.74	4.95	9.8	1.667	4.33
		4	0.000464	7.74	4.95	9.8	1.667	4.33
Planting	Outer	1	0.000167	11.81	5.9	8	1.734	7.9
		2	0.000629	11.81	5.9	8	1.734	7.9
		3	0.000630	11.81	5.9	8	1.734	7.9
	Inner	1	0.000206	11.81	5.9	8	1.734	7.9
		2	0.000081	11.81	5.9	8	1.734	7.9

APPENDIX C: DATA FROM THE 2024 FARMING SEASON

Table C1. Data collected for the front left tire.

Measured wear (mm/km)	Draft (kN)	Slip (%)	Speed (km/h)	Bulk density (g/cm^3)	Moisture (%)
0.001308	12.61	14.95	7	1.55	10.02
0.001311	12.61	14.95	7	1.55	10.02
0.002022	12.61	14.95	7	1.55	10.02
0.001902	12.61	14.95	7	1.55	10.02
0.00099	12.61	14.95	7	1.55	10.02
0.002038	12.61	14.95	7	1.55	10.02
0.001055	12.61	14.95	7	1.55	10.02
0.001081	12.61	14.95	7	1.55	10.02
0.000971	6.81	8.52	9.32	1.65	7.01
0.001198	6.81	8.52	9.32	1.65	7.01
0.001091	6.81	8.52	9.32	1.65	7.01
0.000652	6.81	8.52	9.32	1.65	7.01
0.000617	6.81	8.52	9.32	1.65	7.01
0.001209	6.81	8.52	9.32	1.65	7.01
0.0006	6.81	8.52	9.32	1.65	7.01
0.001126	11.81	9.2	7.75	1.64	5.6
0.000591	11.81	9.2	7.75	1.64	5.6
0.000973	11.81	9.2	7.75	1.64	5.6
0.001123	11.81	9.2	7.75	1.64	5.6
0.000966	11.81	9.2	7.75	1.64	5.6
0.000777	11.81	9.2	7.75	1.64	5.6
0.000999	11.81	9.2	7.75	1.64	5.6
0.00096	11.81	9.2	7.75	1.64	5.6
0.000545	13.35	15.9	7.7	1.63	5.31
0.000337	13.35	15.9	7.7	1.63	5.31
0.000313	13.35	15.9	7.7	1.63	5.31
3.93E-05	13.35	15.9	7.7	1.63	5.31
0.000304	13.35	15.9	7.7	1.63	5.31
0.000354	13.35	15.9	7.7	1.63	5.31
0.000417	13.35	15.9	7.7	1.63	5.31
0.0001	13.35	15.9	7.7	1.63	5.31
0.000246	6.88	5.3	9.6	1.72	4.03
0.000239	6.88	5.3	9.6	1.72	4.03
0.000374	6.88	5.3	9.6	1.72	4.03
0.000496	6.88	5.3	9.6	1.72	4.03
0.000185	6.88	5.3	9.6	1.72	4.03
0.000401	6.88	5.3	9.6	1.72	4.03
0.000417	6.88	5.3	9.6	1.72	4.03
0.000416	6.88	5.3	9.6	1.72	4.03
0.000604	11.81	6.61	8.15	1.64	7.92

Measured wear (mm/km)	Draft (kN)	Slip (%)	Speed (km/h)	Bulk density (g/cm^3)	Moisture (%)
0.000546	11.81	6.61	8.15	1.64	7.92
0.000586	11.81	6.61	8.15	1.64	7.92
0.000561	11.81	6.61	8.15	1.64	7.92
0.00086	11.81	6.61	8.15	1.64	7.92
0.00086	11.81	6.61	8.15	1.64	7.92
0.000698	11.81	6.61	8.15	1.64	7.92
0.000442	11.81	6.61	8.15	1.64	7.92
0.000275	13.13	14	7.51	1.65	4.71
0.000238	13.13	14	7.51	1.65	4.71
0.000276	13.13	14	7.51	1.65	4.71
0.000286	13.13	14	7.51	1.65	4.71
0.000201	13.13	14	7.51	1.65	4.71
0.000299	13.13	14	7.51	1.65	4.71
0.000285	13.13	14	7.51	1.65	4.71
0.000188	13.13	14	7.51	1.65	4.71
0.000269	6.93	5.9	9.5	1.72	4.42
0.000283	6.93	5.9	9.5	1.72	4.42
0.000254	6.93	5.9	9.5	1.72	4.42
0.000353	6.93	5.9	9.5	1.72	4.42
0.000394	6.93	5.9	9.5	1.72	4.42
0.000284	6.93	5.9	9.5	1.72	4.42
0.000256	6.93	5.9	9.5	1.72	4.42
0.000265	6.93	5.9	9.5	1.72	4.42
0.000222	11.81	6.22	7.65	1.76	7.75
0.000349	11.81	6.22	7.65	1.76	7.75
0.000462	11.81	6.22	7.65	1.76	7.75
0.000145	11.81	6.22	7.65	1.76	7.75
0.000224	11.81	6.22	7.65	1.76	7.75
0.000134	11.81	6.22	7.65	1.76	7.75
0.000181	11.81	6.22	7.65	1.76	7.75
0.000507	11.81	6.22	7.65	1.76	7.75

Table C2. Data collected for the front right tire.

Measured wear (mm/km)	Draft (kN)	Slip (%)	Speed (km/h)	Bulk density (g/cm^3)	Moisture (%)
0.00163	12.61	14.95	7.00	1.55	10.65
0.00122	12.61	14.95	7.00	1.55	10.65
0.00196	12.61	14.95	7.00	1.55	10.65
0.00219	12.61	14.95	7.00	1.55	10.65
0.00154	12.61	14.95	7.00	1.55	10.65
0.00220	12.61	14.95	7.00	1.55	10.65
0.00218	12.61	14.95	7.00	1.55	10.65
0.00192	12.61	14.95	7.00	1.55	10.65

Measured wear (mm/km)	Draft (kN)	Slip (%)	Speed (km/h)	Bulk density (g/cm^3)	Moisture (%)
0.00064	6.81	8.52	9.32	1.65	7.01
0.00122	6.81	8.52	9.32	1.65	7.01
0.00098	6.81	8.52	9.32	1.65	7.01
0.00063	6.81	8.52	9.32	1.65	7.01
0.00053	6.81	8.52	9.32	1.65	7.01
0.00052	6.81	8.52	9.32	1.65	7.01
0.00086	6.81	8.52	9.32	1.65	7.01
0.00054	6.81	8.52	9.32	1.65	7.01
0.00098	11.81	9.21	7.75	1.64	5.60
0.00081	11.81	9.21	7.75	1.64	5.60
0.00106	11.81	9.21	7.75	1.64	5.60
0.00080	11.81	9.21	7.75	1.64	5.60
0.00074	11.81	9.21	7.75	1.64	5.60
0.00084	11.81	9.21	7.75	1.64	5.60
0.00099	11.81	9.21	7.75	1.64	5.60
0.00066	11.81	9.21	7.75	1.64	5.60
0.00129	13.35	15.90	7.70	1.63	5.31
0.00045	13.35	15.90	7.70	1.63	5.31
0.00097	13.35	15.90	7.70	1.63	5.31
0.00118	13.35	15.90	7.70	1.63	5.31
0.00057	13.35	15.90	7.70	1.63	5.31
0.00104	13.35	15.90	7.70	1.63	5.31
0.00115	13.35	15.90	7.70	1.63	5.31
0.00119	13.35	15.90	7.70	1.63	5.31
0.00016	6.88	5.32	9.60	1.72	4.03
0.00021	6.88	5.32	9.60	1.72	4.03
0.00080	6.88	5.32	9.60	1.72	4.03
0.00033	6.88	5.32	9.60	1.72	4.03
0.00019	6.88	5.32	9.60	1.72	4.03
0.00022	6.88	5.32	9.60	1.72	4.03
0.00028	6.88	5.32	9.60	1.72	4.03
0.00064	6.88	5.32	9.60	1.72	4.03
0.00076	11.81	6.61	8.15	1.64	7.92
0.00068	11.81	6.61	8.15	1.64	7.92
0.00067	11.81	6.61	8.15	1.64	7.92
0.00090	11.81	6.61	8.15	1.64	7.92
0.00043	11.81	6.61	8.15	1.64	7.92
0.00078	11.81	6.61	8.15	1.64	7.92
0.00067	11.81	6.61	8.15	1.64	7.92
0.00079	11.81	6.61	8.15	1.64	7.92
0.00096	13.13	14.00	7.51	1.65	4.71
0.00103	13.13	14.00	7.51	1.65	4.71
0.00133	13.13	14.00	7.51	1.65	4.71

Measured wear (mm/km)	Draft (kN)	Slip (%)	Speed (km/h)	Bulk density (g/cm^3)	Moisture (%)
0.00125	13.13	14.00	7.51	1.65	4.71
0.00118	13.13	14.00	7.51	1.65	4.71
0.00072	13.13	14.00	7.51	1.65	4.71
0.00130	13.13	14.00	7.51	1.65	4.71
0.00135	13.13	14.00	7.51	1.65	4.71
0.00040	6.93	5.90	9.50	1.72	4.42
0.00046	6.93	5.90	9.50	1.72	4.42
0.00009	6.93	5.90	9.50	1.72	4.42
0.00024	6.93	5.90	9.50	1.72	4.42
0.00060	6.93	5.90	9.50	1.72	4.42
0.00018	6.93	5.90	9.50	1.72	4.42
0.00030	6.93	5.90	9.50	1.72	4.42
0.00045	6.93	5.90	9.50	1.72	4.42
0.00014	11.81	7.30	7.65	1.76	7.75
0.00050	11.81	7.30	7.65	1.76	7.75
0.00007	11.81	7.30	7.65	1.76	7.75
0.00018	11.81	7.30	7.65	1.76	7.75
0.00061	11.81	7.30	7.65	1.76	7.75

Table C3. Data collected for the rear left tire.

Measured wear (mm/km)	Draft (kN)	Slip (%)	Speed (km/h)	Bulk density (g/cm^3)	Moisture (%)
0.00190	12.61	14.95	7.00	1.55	10.65
0.00178	12.61	14.95	7.00	1.55	10.65
0.00204	12.61	14.95	7.00	1.55	10.65
0.00156	12.61	14.95	7.00	1.55	10.65
0.00171	12.61	14.95	7.00	1.55	10.65
0.00240	12.61	14.95	7.00	1.55	10.65
0.00270	12.61	14.95	7.00	1.55	10.65
0.00140	12.61	14.95	7.00	1.55	10.65
0.00070	6.81	8.52	9.32	1.65	7.01
0.00073	6.81	8.52	9.32	1.65	7.01
0.00097	6.81	8.52	9.32	1.65	7.01
0.00085	6.81	8.52	9.32	1.65	7.01
0.00061	6.81	8.52	9.32	1.65	7.01
0.00081	6.81	8.52	9.32	1.65	7.01
0.00121	6.81	8.52	9.32	1.65	7.01
0.00156	11.81	9.21	7.75	1.64	5.60
0.00079	11.81	9.21	7.75	1.64	5.60
0.00094	11.81	9.21	7.75	1.64	5.60
0.00132	11.81	9.21	7.75	1.64	5.60
0.00130	11.81	9.21	7.75	1.64	5.60
0.00079	11.81	9.21	7.75	1.64	5.60

Measured wear (mm/km)	Draft (kN)	Slip (%)	Speed (km/h)	Bulk density (g/cm^3)	Moisture (%)
0.00143	11.81	9.21	7.75	1.64	5.60
0.00100	11.81	9.21	7.75	1.64	5.60
0.00110	13.35	15.90	7.70	1.62	5.31
0.00084	13.47	15.90	7.70	1.62	5.31
0.00045	13.47	15.90	7.70	1.62	5.31
0.00015	13.47	15.90	7.70	1.62	5.31
0.00010	13.47	15.90	7.70	1.62	5.31
0.00014	13.47	15.90	7.70	1.62	5.31
0.00042	13.47	15.90	7.70	1.62	5.31
0.00137	13.47	15.90	7.70	1.62	5.31
0.00042	6.88	5.32	9.60	1.72	4.03
0.00044	6.88	5.32	9.60	1.72	4.03
0.00080	6.88	5.32	9.60	1.72	4.03
0.00051	6.88	5.32	9.60	1.72	4.03
0.00035	6.88	5.32	9.60	1.72	4.03
0.00040	6.88	5.32	9.60	1.72	4.03
0.00117	6.88	5.32	9.60	1.72	4.03
0.00062	6.88	5.32	9.60	1.72	4.03
0.00109	11.81	6.61	8.15	1.64	7.92
0.00105	11.81	6.61	8.15	1.64	7.92
0.00074	11.81	6.61	8.15	1.64	7.92
0.00066	11.81	6.61	8.15	1.64	7.92
0.00060	11.81	6.61	8.15	1.64	7.92
0.00090	11.81	6.61	8.15	1.64	7.92
0.00080	11.81	6.61	8.15	1.64	7.92
0.00071	11.81	6.61	8.15	1.64	7.92
0.00059	13.13	14.00	7.51	1.65	4.71
0.00044	13.13	14.00	7.51	1.65	4.71
0.00044	13.13	14.00	7.51	1.65	4.71
0.00157	13.13	14.00	7.51	1.65	4.71
0.00150	13.13	14.00	7.51	1.65	4.71
0.00094	13.13	14.00	7.51	1.65	4.71
0.00104	13.13	14.00	7.51	1.65	4.71
0.00168	13.13	14.00	7.51	1.65	4.71
0.00030	6.93	5.90	9.50	1.72	4.42
0.00067	6.93	5.90	9.50	1.72	4.42
0.00050	6.93	5.90	9.50	1.72	4.42
0.00035	6.93	5.90	9.50	1.72	4.42
0.00010	6.93	5.90	9.50	1.72	4.42
0.00014	6.93	5.90	9.50	1.72	4.42
0.00027	6.93	5.90	9.50	1.72	4.42
0.00027	6.93	5.90	9.50	1.72	4.42
0.00058	11.81	7.30	7.65	1.76	7.75

Measured wear (mm/km)	Draft (kN)	Slip (%)	Speed (km/h)	Bulk density (g/cm^3)	Moisture (%)
0.00050	11.81	7.30	7.65	1.76	7.75
0.00015	11.81	7.30	7.65	1.76	7.75
0.00012	11.81	7.30	7.65	1.76	7.75
0.00052	11.81	7.30	7.65	1.76	7.75
0.00016	11.81	7.30	7.65	1.76	7.75
0.00044	11.81	7.30	7.65	1.76	7.75
0.00016	11.81	7.30	7.65	1.76	7.75

Table C4. Data collected for the rear right tire.

Measured wear (mm/km)	Draft (kN)	Slip (%)	Speed (km/h)	Bulk density (g/cm^3)	Moisture (%)
0.00164	12.61	14.95	7.00	1.55	10.65
0.00189	12.61	14.95	7.00	1.55	10.65
0.00203	12.61	14.95	7.00	1.55	10.65
0.00193	12.61	14.95	7.00	1.55	10.65
0.00197	12.61	14.95	7.00	1.55	10.65
0.00204	12.61	14.95	7.00	1.55	10.65
0.00259	12.61	14.95	7.00	1.55	10.65
0.00267	12.61	14.95	7.00	1.55	10.65
0.00097	6.81	8.52	9.32	1.65	7.01
0.00079	6.81	8.52	9.32	1.65	7.01
0.00122	6.81	8.52	9.32	1.65	7.01
0.00133	6.81	8.52	9.32	1.65	7.01
0.00157	6.81	8.52	9.32	1.65	7.01
0.00091	6.81	8.52	9.32	1.65	7.01
0.00097	6.81	8.52	9.32	1.65	7.01
0.00091	6.81	8.52	9.32	1.65	7.01
0.00158	11.81	9.21	7.75	1.64	5.60
0.00104	11.81	9.21	7.75	1.64	5.60
0.00128	11.81	9.21	7.75	1.64	5.60
0.00118	11.81	9.21	7.75	1.64	5.60
0.00195	11.81	9.21	7.75	1.64	5.60
0.00145	11.81	9.21	7.75	1.64	5.60
0.00129	11.81	9.21	7.75	1.64	5.60
0.00123	11.81	9.21	7.75	1.64	5.60
0.00029	13.35	15.90	7.70	1.63	5.31
0.00073	13.35	15.90	7.70	1.63	5.31
0.00065	13.35	15.90	7.70	1.63	5.31
0.00068	13.35	15.90	7.70	1.63	5.31
0.00067	13.35	15.90	7.70	1.63	5.31
0.00038	13.35	15.90	7.70	1.63	5.31
0.00156	13.35	15.90	7.70	1.63	5.31
0.00089	13.35	15.90	7.70	1.63	5.31

Measured wear (mm/km)	Draft (kN)	Slip (%)	Speed (km/h)	Bulk density (g/cm^3)	Moisture (%)
0.00039	6.88	5.32	9.60	1.72	4.03
0.00068	6.88	5.32	9.60	1.72	4.03
0.00071	6.88	5.32	9.60	1.72	4.03
0.00026	6.88	5.32	9.60	1.72	4.03
0.00052	6.88	5.32	9.60	1.72	4.03
0.00025	6.88	5.32	9.60	1.72	4.03
0.00061	6.88	5.32	9.60	1.72	4.03
0.00069	6.88	5.32	9.60	1.72	4.03
0.00091	11.81	6.61	8.15	1.64	7.92
0.00078	11.81	6.61	8.15	1.64	7.92
0.00079	11.81	6.61	8.15	1.64	7.92
0.00042	11.81	6.61	8.15	1.64	7.92
0.00039	11.81	6.61	8.15	1.64	7.92
0.00081	11.81	6.61	8.15	1.64	7.92
0.00100	11.81	6.61	8.15	1.64	7.92
0.00126	11.81	6.61	8.15	1.64	7.92
0.00141	13.13	14.00	7.51	1.65	4.71
0.00194	13.13	14.00	7.51	1.65	4.71
0.00226	13.13	14.00	7.51	1.65	4.71
0.00223	13.13	14.00	7.51	1.65	4.71
0.00238	13.13	14.00	7.51	1.65	4.71
0.00143	13.13	14.00	7.51	1.65	4.71
0.00240	13.13	14.00	7.51	1.65	4.71
0.00239	13.13	14.00	7.51	1.65	4.71
0.00046	6.93	5.90	9.50	1.72	4.42
0.00042	6.93	5.90	9.50	1.72	4.42
0.00053	6.93	5.90	9.50	1.72	4.42
0.00032	6.93	5.90	9.50	1.72	4.42
0.00058	6.93	5.90	9.50	1.72	4.42
0.00039	6.93	5.90	9.50	1.72	4.42
0.00073	6.93	5.90	9.50	1.72	4.42
0.00030	6.93	5.90	9.50	1.72	4.42
0.00021	11.81	7.30	7.65	1.76	7.75
0.00033	11.81	7.30	7.65	1.76	7.75
0.00030	11.81	7.30	7.65	1.76	7.75
0.00020	11.81	7.30	7.65	1.76	7.75
0.00033	11.81	7.30	7.65	1.76	7.75

Appendix D: Detailed Calculations to Predict the Maximum Area That Can Be Covered by Each Tire

Area covered by the front left tire

Equation 32 was used to predict the wear rate of the front left tire during plowing (W_{rp}), harrowing (W_{rh}), and planting (W_{rl}). This resulted in wear rates (in mm/km) of 0.00069, 0.00012, and 0.00015 mm/km, respectively. Therefore, given that 1 ha is equivalent to 0.01 km^2, the wear rate values in mm/ha for plowing, harrowing, and planting are 7.67×10^{-3}, 6.28×10^{-4}, and 6.44×10^{-4} mm/ha, respectively.

The total possible wear rate for all of three field operations is 9.6×10^{-4} mm/km (8.94×10^{-3} mm/ha). Therefore, the total possible distance for plowing (x_p), assuming a replacement lug height of 28.8 mm (the height that determines when the tire should be replaced), is determined by

$$x_p = \frac{28.8}{0.00069}$$

$$= 41{,}739.13 \text{ km.}$$

Because the tractor covers a specific amount of surface area during each operation, it is appropriate to determine the size of the total area to be covered by the tractor for each field operation.

Plowing: If the width of the plow is 0.9 m, the area plowed by the tractor is

$$Area\ covered = 41{,}739.13 \times \left(\frac{0.9}{1{,}000}\right)$$

$$= 37.57 \text{ km}^2$$

$$= 3{,}756.52 \text{ ha}$$

Harrowing: The total possible distance for harrowing (x_h), assuming a replacement lug height of 28.8 m, is

$$x_h = {}^{28.8}/_{0.00012}$$

$$= 240{,}000\ km$$

The width of the harrow is 0.00179 km. The area harrowed by the tractor is

$$Area\ covered = 240{,}000 \times 0.00179$$

$$= 429.60\ \text{km}^2$$

$$= 42{,}960\ \text{ha}$$

Planting: The distance for planting (x_l) for the replacement lug height of 28.8 mm is

$$x_l = {}^{28.8}/_{0.00015}$$

$$= 192{,}000\ \text{km}$$

The width of the planter is 0.00233 km. The area planted is

$$Area\ covered = 192{,}000 \times 0.00233$$

$$= 447.36\ \text{km}^2$$

$$= 44{,}736\ \text{ha}$$

The total possible distance traveled by the tractor's front left tire during plowing, harrowing, and planting is

$$x_t = {}^{28.8}/_{9.6 \times 10^{-4}}$$

$$= 30{,}000\ \text{km}$$

The total possible area to be covered is

$$= 28.8/8.94 \times 10^{-3}$$

$$= 3{,}221.48\ \text{ha}$$

Therefore, the front left tire will cover a total possible area of 3,221.48 ha for plowing, harrowing, and planting before needing replacement, as recommended by Firestone (BridgestoneTractor Tyre Expert, 2021b).

Using Equation 38 and the data in Table 4.14, the replacement interval for the front left tire is

$$= {}^{30,000}/_{7.00} \text{ to } {}^{30,000}/_{10.10}$$

$$= 4,285.71 \text{ to } 2,970.29 \text{ hours}$$

Hence, the front left tire will potentially travel for 2,970.29 to 4,285.71 hours before needing replacement.

Area covered by the front right tire

Using Equation 33, the wear rates of the front right tire for plowing (W_{rp}), harrowing (W_{rh}), and planting (W_{rl}) are 0.00078, 0.00019, and 0.00020 mm/km, respectively. Therefore, the wear rate values for plowing, harrowing, and planting (in mm/ha) are 8.67×10^{-3}, 1.06×10^{-3}, and 8.58×10^{-4} mm/ha, respectively. The total possible wear rate for the front right tire is 1.17×10^{-3} mm/km (10.59×10^{-3} mm/ha). The total possible travel distance for the left front tire for plowing (x_p), assuming a replacement lug height of 28.8 mm, is

$$x_p = \frac{28.8}{0.00078}$$

$$= 36,923.08 \text{ km}$$

The total possible area that has to be covered by the front right tire for plowing is

$$Area\ covered = 36,923.08 \times \left(\frac{0.9}{1,000}\right)$$

$$= 33.23 \text{ km}^2$$

$$= 3,323.08 \text{ ha}$$

The total distance for harrowing (x_h) for the wearable height of the front right tire is

$$x_h = \frac{28.8}{0.00019}$$

$$= 15{,}1578.95 \text{ km}$$

The total possible area to be covered by the tire during harrowing is

$$Area\ covered = 151{,}578.95 \times 0.00179$$

$$= 271.34 \text{ km}^2$$

$$= 27{,}132.63 \text{ ha}$$

Therefore, the front right tire will cover 27,132.63 ha during harrowing before needing replacement.

The total distance for planting (x_l) for the wearable lug height of the front right tire is

$$x_l = \frac{28.8}{0.00020}$$

$$= 144{,}000 \text{ km}$$

The area to be covered by the tire during planting for the wearable lug height is

$$Area\ covered = 144{,}000 \times 0.00233$$

$$= 335.52 \text{ km}^2$$

$$= 33{,}552 \text{ ha}$$

Therefore, the front right tire will plant an area of 33,552 ha before needing replacement.

The total distance that the front right tire for the wearable lug height will travel during all the field operations is

$$x_t = {}^{28.8}/_{1.17 \times 10^{-3}}$$

$$= 24{,}615.38 \text{ km}$$

The projected total area to be covered by the front right tire for all the field operations is

$$= {}^{28.8}/_{10.59 \times 10^{-3}}$$

$$= 2{,}719.54 \text{ ha}$$

Therefore, using Equation 38 and the data from Table 14.14, the number of hours that the front right tire will travel before needing replacement is

$$= {}^{24{,}615.38}/_{10.10} \text{ to } {}^{24{,}615.38}/_{7.00}$$

$$= 2{,}437.17 \text{ to } 3{,}516.48 \text{ to hours}$$

Hence, the projected range of hours that the front tire will travel before needing replacement is 2,437.17 to 3,516.48 hours.

Area covered by the rear left tire

Using Equation 34 to predict the wear rates of the rear left tire for plowing (W_{rp}), harrowing (W_{rh}), and planting (W_{rl}), the results are 0.00086 mm/km (9.56×10^{-3} mm/ha), 0.00019 mm/km (1.06×10^{-3} mm/ha), and 0.00023 mm/km (9.87×10^{-4} mm/ha), respectively. The wear rate for the rear left tire for all operations is 1.28×10^{-3} mm/km (11.61×10^{-3} mm/ha). The total possible distance for plowing (x_p) before the rear left tire reaches the replacement lug height of 36 mm is

$$x_p = {}^{36}/_{0.00086}$$

$$= 41{,}860.47 \text{ km}$$

The area for plowing is

$$Area\ covered = 41{,}860.47 \times \left(\frac{0.9}{1{,}000}\right)$$

$$= 37.67 \text{ km}^2$$

$$= 3{,}767.44 \text{ ha}$$

Therefore, the wearable lug height of the tire will plow 3,767.44 ha before replacement.

The distance that the wearable lug height will travel during harrowing is

$$(x_h) = {}^{36}/_{0.00019}$$

$$= 189{,}473.68 \text{ km}$$

The harrowing area for the wearable lug height is

$$Area\ covered = 189{,}473.68 \times 0.00179$$

$$= 339.15 \text{ km}^2$$

$$= 33{,}915.79 \text{ ha}$$

Hence, the wearable lug height of the rear left tire will harrow 33,915.79 ha. The possible distance for planting for the wearable lug height of the rear left tire is

$$x_l = {}^{36}/_{0.00023}$$

$$= 156{,}521.73 \text{ km}$$

The area covered for planting is

$$= 156{,}521.73 \times 0.00233$$

$$= 364.70 \text{ km}^2$$

$$= 36{,}469.56 \text{ ha}$$

The total distance traveled for planting is

$$x_t = {}^{36}/_{1.28 \times 10^{-3}}$$

$$= 28{,}125 \text{ km}$$

The estimated total area that the rear left tire will travel before replacement is

$$= {}^{36}/_{11.61 \times 10^{-3}}$$

$$= 3{,}100.78 \text{ ha}$$

The wearable lug height of the rear left tire is expected to cover a possible total area of 3,100.78 ha before replacement.

Using Equation 38 and the data from Table 14.14, the estimated number of hours needed for the rear left tire to run before replacement is

$$= {}^{28,125}/_{7.00} \text{ to } {}^{28,125}/_{10.10}$$

$$= 4,017.85 \text{ to } 2,784.65 \text{ hours}$$

Hence, the projected interval during which the front tire will travel before replacement is

$$2,784.65 \text{ to } 4,017.85 \text{ hours}$$

Area covered by the rear right tire

Equation 35 was used to predict the wear rate of the rear right tire during plowing, harrowing, and planting, which are estimated as 0.00100, 0.00023, and 0.00020 mm/km (11.11×10^{-3}, 1.28×10^{-3}, and 8.58×10^{-3} mm/ha), respectively. The total wear rate of the tire for all field operations is 1.43×10^{-3} mm/km (20.97×10^{-3} mm/ha). The possible distance that the wearable lug height of the tractor will travel is

$$x_p = {}^{36}/_{0.00100}$$

$$= 36,000 \text{ km}$$

The possible area to be covered during plowing is

$$Area\ covered\ 36,000 \times ({}^{0.9}/_{1,000})$$

$$= 32.40 \text{ km}^2$$

$$= 3,240 \text{ ha}$$

The wearable lug height of the rear right tire is expected to plow 3,510 ha before needing replacement. The possible distance for harrowing is

$$(x_h) = {}^{36}/_{0.00023}$$

$$= 156{,}521.73 \text{ km}$$

The area covered is

$$Area\ covered = 156{,}521.73\ \times 0.00179$$

$$= 280.17 \text{ km}^2$$

$$= 28{,}017.39 \text{ ha}$$

The estimated area that the rear right tire will cover during harrowing before needing replacement is 28,017.39 ha. The distance the tire will travel for planting is

$$x_l = {}^{36}/_{0.00030}$$

$$= 120{,}000 \text{ km}$$

The possible area to be covered is

$$Area\ covered = 120{,}000\ \times 0.00233$$

$$= 279.60 \text{ km}^2$$

$$= 27{,}960 \text{ ha}$$

Therefore, the rear tire is estimated to plant an area of 27,960 ha before it might be replaced. With the total wear rate of 1.43×10^{-3} mm/km for all the field operations, the rear right tire is expected to travel an estimated distance of

$$^{36}/_{1.43\ \times 10^{-3}}$$

$$= 25{,}174.82 \text{ km}$$

The total area estimated to be covered by the rear right tire before replacement is

$$= {}^{36}/_{20.97 \times 10^{-3}}$$

$$= 1{,}716.74 \text{ ha}$$

The wearable lug height of the rear right tire is expected to cover a total area of 1,716.74 ha before replacement.

Using Equation 38 and the data from Table 14.14, the estimated number of hours needed for the front right tire to run before needing replacement is

$$= {}^{25{,}174.82}/_{10.10} \text{ to } {}^{25{,}174.82}/_{7.00}$$

$$= 2{,}492.56 \text{ to } 3{,}596.40 \text{ hours}$$

Hence, the projected interval during which the front tire will travel before needing replacement is 2,492.56 to 3,596.40 hours.